The Journal of The Royal Astronomical Society of Canada

Journal

Le Journal de la Société royale d'astronomie du Canada

PROMOTING ASTRONOMY IN CANADA

June/juin 2017
Volume/volume 111
Number/numéro 3 [784]

Inside this issue:

Southern Annular Eclipse at Third Contact

The Best of Monochrome.

Drawings, images in black and white, or narrow-band photography.

Michael Watson photographed the waning gibbous moon from mid-town Toronto on 2016 July 23 using a Nikon D810 camera body on Explore Scientific 152-mm (6") apochromatic refracting telescope, mounted on a Sky-Watcher AZ-EQ6 SynScan mount and 1200 mm focal length, ƒ/8. The image is a stack of eight images.

Journal
June/juin 2017 | Vol. 111, No. 3 | Whole Number 784

Royal Astronomical Society of Canada
Société Royale d'Astronomie du Canada

contents / table des matières

Research Articles / Articles de recherche

Columns / Rubriques

Departments / Départements

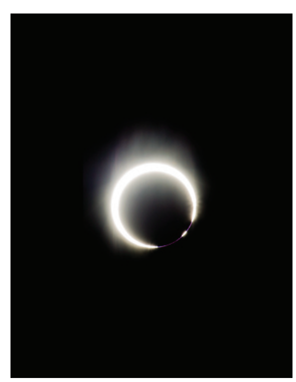

This photograph, taken in the arid environment of the Patagonian plains of Argentina, shows the annular solar eclipse of 2017 February 26 at third contact, the moment when annularity ends and the Moon's edge is observed as it begins to move through the limb of the Sun. A 60° arc of magenta chromosphere spans between the cusps of the eclipsed Sun. A bright Bailey's Bead (the Sun's photosphere shining through a valley on the lunar edge) appears near the four o'clock position. Stephen Beddingfield photographed this beautiful sight using a Canon 5Dm3, 100–400-mm lens @ 400 mm, ISO 100, ƒ/11, 1/5000 sec, unfiltered.

Journal

The *Journal* is a bi-monthly publication of The Royal Astronomical Society of Canada and is devoted to the advancement of astronomy and allied sciences. It contains articles on Canadian astronomers and current activities of the RASC and its Centres, research and review papers by professional and amateur astronomers, and articles of a historical, biographical, or educational nature of general interest to the astronomical community. All contributions are welcome, but the editors reserve the right to edit material prior to publication. Research papers are reviewed prior to publication, and professional astronomers with institutional affiliations are asked to pay publication charges of $100 per page. Such charges are waived for RASC members who do not have access to professional funds as well as for solicited articles. Manuscripts and other submitted material may be in English or French, and should be sent to the Editor-in-Chief.

His Excellency the Right Honourable **David Johnston**, C.C., C.M.M., C.O.M., C.D., Governor General of Canada, is the Viceregal Patron of the RASC.

The *Journal* of The Royal Astronomical Society of Canada is published at an annual subscription rate of $93.45 (including tax) by The Royal Astronomical Society of Canada. Membership, which includes the publications (for personal use), is open to anyone interested in astronomy. Applications for subscriptions to the *Journal* or membership in the RASC and information on how to acquire back issues of the *Journal* can be obtained from:

The Royal Astronomical Society of Canada
203 – 4920 Dundas St W
Toronto ON M9A 1B7, Canada

Email: nationaloffice@rasc.ca
Web site: www.rasc.ca
Telephone: 416-924-7973
Fax: 416-924-2911

Canadian Publications Mail Registration No. 09818
Canada Post: Send address changes to 203 – 4920 Dundas St W, Toronto ON M9A 1B7

Canada Post Publication Agreement No. 40069313
We acknowledge the financial support of the Government of Canada through the Canada Periodical Fund (CPF) for our publishing activities.

President's Corner

by Craig Levine, London Centre
(craigslevine@gmail.com)

The year 1868 was an important year in Canada. Our nascent country celebrated its first birthday that year. Queen Victoria was our monarch, and the storied Sir John A. Macdonald was our Prime Minister. Father of Confederation Thomas D'Arcy McGee was assassinated; the Militia Act was proclaimed into law, creating a Canadian army; and Emily Murphy was born. She was a jurist and the first female magistrate in the British Empire (and the first in Canada). We can also claim the first woman sworn into a legislative assembly in the Empire as well: Louise McKinney from Alberta was born that year too.

Also in December of 1868, Andrew Evans met with several like-minded friends from the Canadian Institute to form a group devoted to astronomy, the Toronto Astronomy Club. They changed the word "Club" to "Society" the following year. Several more names followed: The Astronomical and Physical Society of Toronto, the Toronto Astronomical Society, and in 1903 it was granted its royal charter by King Edward VII, and became The Royal Astronomical Society of Canada. This name change was auspicious. No longer confined to Toronto, the Society and its leadership had designs on being national in its scope and reach. In 1906, the second Centre of the RASC was founded in the same city as the Dominion Observatory: our capital city, Ottawa.

And how we have grown over the past 150 years! We have over 5000 members across the country and in 29 Centres, including our newest, the Yukon Centre. Our publications are sold and subscribed to, and read, around the globe. Our centres provide diverse and frankly amazing outreach to the public and to schools. Our brand is recognized as one of the premier organizations in Canada and the world for astronomers of all interests and skills, and if I may say, deservedly so. I've met members from all corners of the country who are doing simply extraordinary things in terms of volunteerism, outreach, pro-am research, astrophotography, education, and so much more. It's sincerely thrilling for me to hear their stories, and I'm proud of the passion that they exude for their activities and the RASC. We truly have so much to celebrate on our 150th solar orbit. For 2018 and the RASC's own 150th birthday, Calgary will be our host city for our annual General Assembly as we pause to celebrate our past, who we are now, and look forward to our next 150 years of fellowship, education, and outreach.

This brings me back to RASC Centre #2 and another significant 150th celebration. The Ottawa Centre is hosting our annual General Assembly this year from June 30 to July 3. This gathering of RASCals and friends will coincide with Canada's 150th birthday party. This GA will be an amazing event unto itself, with the backdrop of our national birthday celebrations occurring simultaneously and woven into the schedule. If you have never been to one of our GAs, this one simply must not be missed.

I hope to see many of you in Ottawa over the July long weekend, as we celebrate with our sisters and brothers in the RASC, and with our country. ✶

News Notes / En Manchette

Compiled by Jay Anderson

Missing: Dark Matter.

New observations by astronomers using facilities at the European Southern Observatory seem to show that massive galaxies in the early Universe were dominated by "normal" matter rather than the mysterious "dark matter" haloes found in present-day galaxies.

The international team led by Reinhard Genzel at the Max Planck Institute for Extraterrestrial Physics in Garching, Germany, have used the K-band Multi-Object Spectrograph (KMOS) and the Spectrograph for INtegral Field Observations in the Near Infrared (SINFONI) instruments at ESO's 8.2-m Very Large Telescope (VLT) in Chile to measure the rotation of six massive, star-forming galaxies in the distant Universe, at the peak of galaxy formation 10 billion years ago. Unlike spiral galaxies in the modern Universe, the outer regions of these distant galaxies seem to be rotating more slowly than regions closer to the core—suggesting there is less dark matter present than expected.

Spiral galaxy cores have high concentrations of stars, but the density of bright matter decreases toward their outskirts. If a galaxy's mass consisted entirely of normal matter, then the sparser outer regions should rotate more slowly than the dense regions at the centre. But observations of nearby spiral galaxies show that their inner and outer parts actually rotate at approximately the same speed. These "flat rotation curves" indicate that spiral galaxies must contain large amounts of non-luminous matter in a halo surrounding the galactic disk in order to maintain the constant rotation speed.

> *"Surprisingly, the rotation velocities are not constant, but decrease further out in the galaxies," comments Genzel, lead author of the* Nature *paper. "There are probably two causes for this. Firstly, most of these early massive galaxies are strongly dominated by normal matter, with dark matter playing a much smaller role than in the Local Universe. Secondly, these early disks were much more turbulent than the spiral galaxies we see in our cosmic neighbourhood." That turbulence adds a pressure to the gravitational balance that also slows the rotation rate.*

Both effects seem to become more marked as astronomers look further and further back in time. This suggests that three to four billion years after the Big Bang, the gas in galaxies had already efficiently condensed into flat, rotating disks, while the dark-matter halos surrounding them were much larger and diffuse. Apparently it took billions of years longer for dark matter to condense, so its dominating effect is only seen on the rotation velocities of more recent galaxy disks. This explanation is consistent with observations showing that early galaxies were much more gas-rich and compact than today's galaxies.

The six galaxies mapped in this study were among a larger sample of 100 distant, star-forming disks imaged with the KMOS and SINFONI instruments at the Paranal

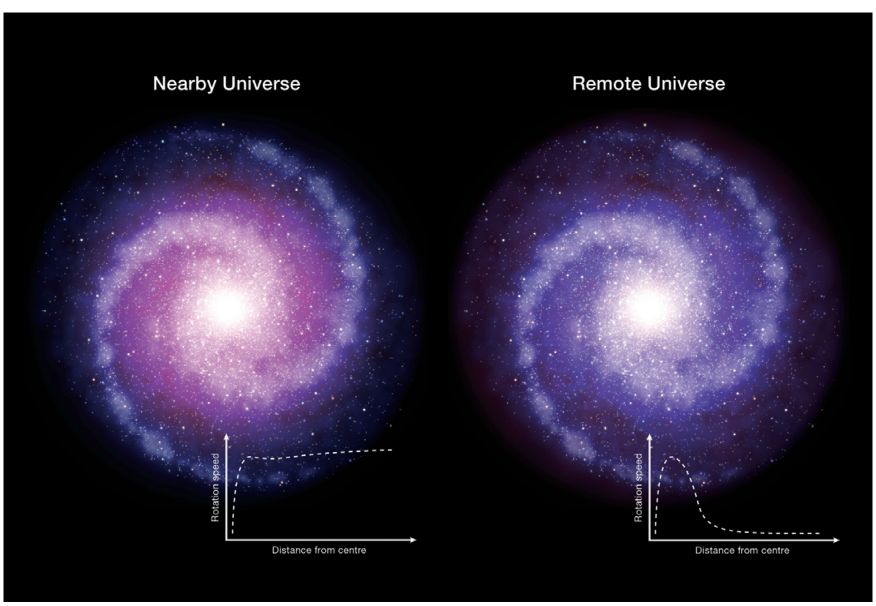

Figure 1 — Schematic representation of rotating disk galaxies in the distant Universe and the present day. Observations with ESO's Very Large Telescope suggest that such massive star-forming disk galaxies in the early Universe were less influenced by dark matter. As a result, the outer parts of distant galaxies rotate more slowly than comparable regions of galaxies in the local Universe. Their rotation curves, rather than being flat, drop with increasing radius. Image: ESO

Observatory in Chile. In addition to the individual galaxy measurements described above, an average rotation curve was created by combining the weaker signals from the other galaxies. This composite curve also showed the same decreasing velocity trend away from the centres of the galaxies. In addition, two further studies of 240 star-forming disks also support these findings.

Detailed modelling shows that while normal matter typically accounts for about half of the total mass of all galaxies on average, it completely dominates the dynamics of galaxies at the highest redshifts. This new result does not call into question the need for dark matter as a fundamental component of the Universe or the total amount, but instead suggests that dark matter was differently distributed in and around disk galaxies at early times compared to the present day.

Complied with material provided by the European Space Agency.

A ring for Mars?

Figure 2 — New modelling indicates that the grooves on Mars's moon Phobos could be produced by tidal forces—the mutual gravitational pull of the planet and the moon. Image: NASA/JPL-Caltech/University of Arizona.

Our dusty Solar System neighbour orbits the Sun in the company of two battered and very different moons: Phobos and Deimos. It may not always have been that way, as, according to two astronomers at Purdue University, Phobos may in fact be Phobos 7.0—the seventh iteration of a cycle that takes it from moon to ring and back to moon again.

David Minton, assistant professor of Earth, atmospheric and planetary sciences, and Andrew Hesselbrock, a doctoral student in physics and astronomy, developed a model that postulates that Phobos's history began when a 2000-km object collided with Mars around 4.3 billion years ago. That collision may have formed the Borealis Basin, an impact structure that covers about 40% of the northern hemisphere of the planet, while at the same time ejecting a large amount of material into space. "That large impact would have blasted enough material off the surface of Mars to form a ring," Hesselbrock said.

Accretion of ring material could have formed a number of satellites, but those within about 3 Mars radii would have gradually drifted to lower orbits and be disrupted again when they reached the Roche limit at around 1.6 Mars radii. At the Roche limit, the gravity gradient of Mars would be able to tear the primordial moons apart, depositing most of their material onto the planet's surface, particularly in equatorial regions.

About 20% of the debris was flung far enough from Mars to clump into more sustainable Martian moons, but once the inner debris ring was cleared, tidal torques would cause the orbits of these new moons to evolve inward toward the planet, likely accreting into one body during the descent. At the Roche limit, the satellite would be disrupted again, forming a second-generation ring with most of the material falling onto Mars's surface and a small portion being ejected to coalesce into a second generation of satellites.

Because much of the debris created by the disruption of the moon at the Roche limit is dropped onto the planet's surface, the second generation of satellites will be much smaller than the previous. After several ring-satellite-ring cycles—anywhere from three to seven in the model—a single Phobos-sized moon would be left. It is estimated that in about 70 million years, Phobos will reach the Roche limit (once again?) and be torn apart to undergo yet another cycle of destruction and rebirth.

While the model described by Minto and Hesselbrock is capable of describing the evolution of Phobos, it is not so successful with Deimos. Instead, Deimos is thought to have formed at a point where it is in synchronous orbit with Mars, and so has no particular torque to draw it in closer to the planet.

One way to test the model is to look for evidence of material that has been dropped onto the surface over the 4.3 billion years that Mars has existed. It may be there. "You could have had kilometre-thick piles of moon sediment raining down on Mars in the early parts of the planet's history, and there are enigmatic sedimentary deposits on Mars with no explanation as to how they got there," Minton said. "And now it's possible to study that material."

While the idea is compelling, it's not the only proposal for the origin of Mars's moons. It does, however, offer something concrete for researchers to look for on the surface of Mars: piles or layers of moon rocks from past moon explosions. Minton and Hesselbrock will now focus their work on either the dynamics of the first set of rings that formed or the materials that have rained down on Mars from disintegration of moons.

Complied in part from material provided by Purdue University.

Wind circulation on Venus gets a critical update

Venus, for all its simplicity, has a few mysteries that have baffled scientists and kept modellers busy. The most pressing is the question of the planet's upper-level winds, which circle the planet with speeds as much as 400 km/h. This super-rotation is over 60 times Venus's rotation; Earth's fastest winds circulate at 10 to 20% of our rotation rate. At the surface, in contrast, Venusian winds are very light, barely 10 km/h.

Theory suggests that the circulation on Venus should be simple: air rises on the hot sunward side and descends on the cool dark side. This implies a north-to-south (meridional) wind flow to go along with the east-to-west (zonal) flow of the upper winds, but that meridional circulation has been difficult or impossible to detect up to now, even from a satellite. That conundrum was at least partly solved by an announcement, in March this year, that observers using the Canada-France-Hawaii Telescope (CFHT) and observations from the *Venus Express* spacecraft had finally measured the missing circulation. The observation was gathered by an international team led by Pedro Machado, of the Instituto de Astrofísica e Ciências do

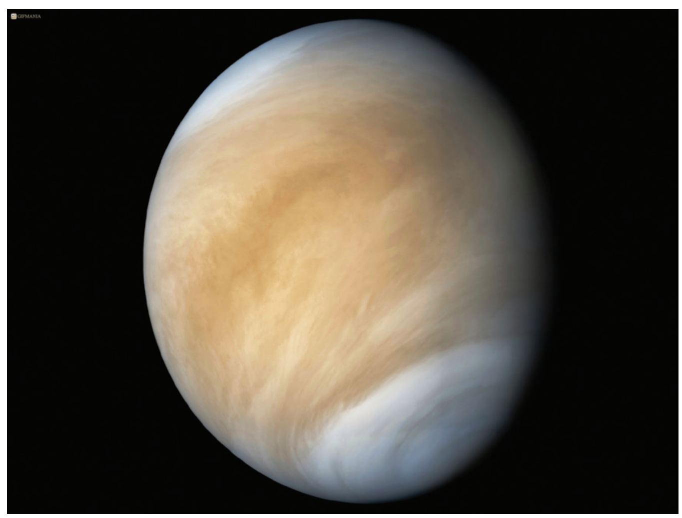

Figure 3 — Venus's cloud tops. The chevron-shaped pattern is due to the strong zonal wind flow at upper levels in the atmosphere. Image: ESA/MPS/DLR/IDA.

Espaço (IA) and Faculdade de Ciências da Universidade de Lisboa (FCUL).

Analyzing the Doppler signal from light reflected from the top of the clouds on Venus, Pedro Machado and his team identified, in both hemispheres, a wind component perpendicular to the equator consistent with the characteristic atmospheric circulation of an Hadley cell and with an average velocity of

81 km/h. Pedro Machado says that "this detection is crucial to understand the transfer of energy between the equatorial region and the high latitudes, shedding light on a phenomenon that for decades has remained unexplained and which is the super-rotation of the Venus atmosphere." The team was also able to measure spatial and temporal variability of the zonal flow with latitude and local time, with a significant increase of wind amplitude near the morning terminator.

"It is amazingly hard to make these kinds of measurements," says Glyn Collinson at NASA's Goddard Space Flight Center in Greenbelt, Maryland. "I just read the paper and thought, holy smoke, you measured *that*?"

Presently, the scientific community is searching for a physical model capable of explaining this phenomenon of super-rotation. In their observation, the team is adding additional components to the model of the zonal wind, and how it changes with time and with the latitude. One of the next steps is to detect the branch of meridional wind at lower altitude along which the air returns to the equator.

"This is very important, because we don't know how the atmosphere of Venus works," says Ricardo Hueso at the University of the Basque Country in Bilbao, Spain. "Understanding meridional circulation is one of the key elements to solving this problem." Machado and his team have also designed the only method today that uses visible light to measure the instantaneous speed of the wind in the atmosphere of another planet from telescopes on Earth.

Compiled in part using material from CFHT, Icarus, *and the Instituto de Astrofísica e Ciências do Espaço.*

Beta Pictoris b exposed as brown dwarf

Beta Pictoris is a young, nearby, 4th-magnitude, main-sequence star that sports a large dusty debris disk organized into a number of belts. It also is the parent star to β Pictoris b, a massive planet orbiting at a distance of about 9.2 AU (Saturn's distance) with an orbital period of 20–21 years. The planet was discovered in 2003 by direct imaging with the Very Large Telescope in Chile. Because of its proximity to the host star, β Pictoris b is difficult to observe, but over the years, its physical characteristics have gradually been revealed.

Most recently, a team of astronomers led by Jeffrey Chilcote (University of Toronto), using the Gemini Planetary Imager (GPI) found that β Pictoris b is about 13 times more massive than Jupiter, has a surface temperature of about 1724 K and a radius 1.46 times that of Jupiter. While these parameters are in good agreement with the earlier observations, they allow better comparisons with planetary-evolution models. The Gemini data indicate that β Pictoris b best matches an exoplanet with an atmosphere like that of a low-surface-gravity (L2) brown dwarf.

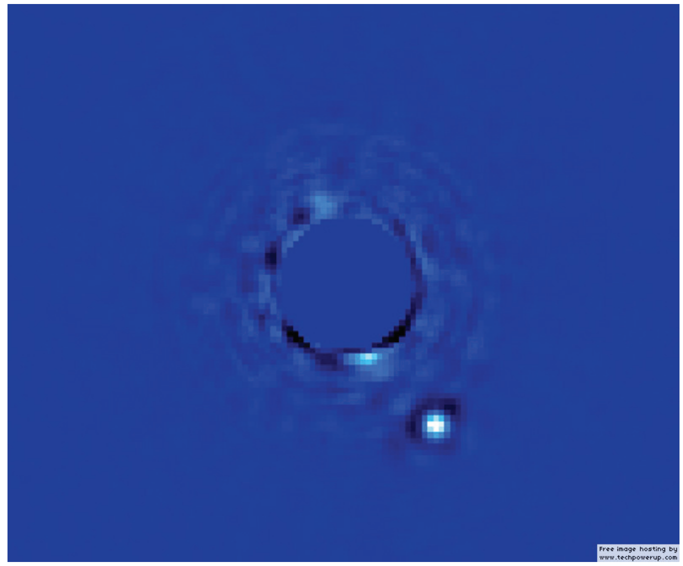

Figure 4 — Gemini Planet Imager's first-light image of β Pictoris b, a planet orbiting the star β Pictoris. This near-infrared image (1.5–1.8 microns) shows the planet glowing in infrared light from the heat released in its formation. The star is blocked in this image by a mask so its light doesn't interfere with the light of the planet. In addition to the image, GPI obtains a spectrum from every pixel element in the field of view to allow scientists to study the planet in great detail. Image: Processing by Christian Marois, NRC Canada.

β Pictoris b is at the mass boundary sometimes used to distinguish between an exoplanet and a brown dwarf. Brown dwarfs are objects that are not massive enough for sustained nuclear reactions. Brown dwarfs less massive than 13 Jupiters cannot even start a nuclear reaction. Based on the GPI data, combined with planetary evolution and atmospheric models, Chilcote suggests a "hot-start" planet-formation scenario for β Pictoris b. He adds, "This is consistent with the disk instability formation mechanism for wide-orbit giant exoplanets." However, the characteristics for the atmosphere of β Pictoris b found in this work best match those of low-surface-gravity brown dwarfs, not planets.

Other research with the GPI predicts that there is a small chance that the planet will transit β Pictoris in late 2017, allowing a very precise measurement of the planet's size.

Since the first detection of an exoplanet in 1995 (51 Pegasi b), the discovery and characterization of extrasolar planets has changed the understanding of planetary systems and their formation. Over the past two decades, more than 3400 planetary systems with stars of various masses and at different stages of evolution have been detected. Some of these planetary systems present features very similar to our Solar System. The current challenge for astronomers is to better characterize these planets, especially the exoplanet atmospheres that can give us information about the history of formation of the planets.

Compiled in part with material provided by Gemini Observatory.

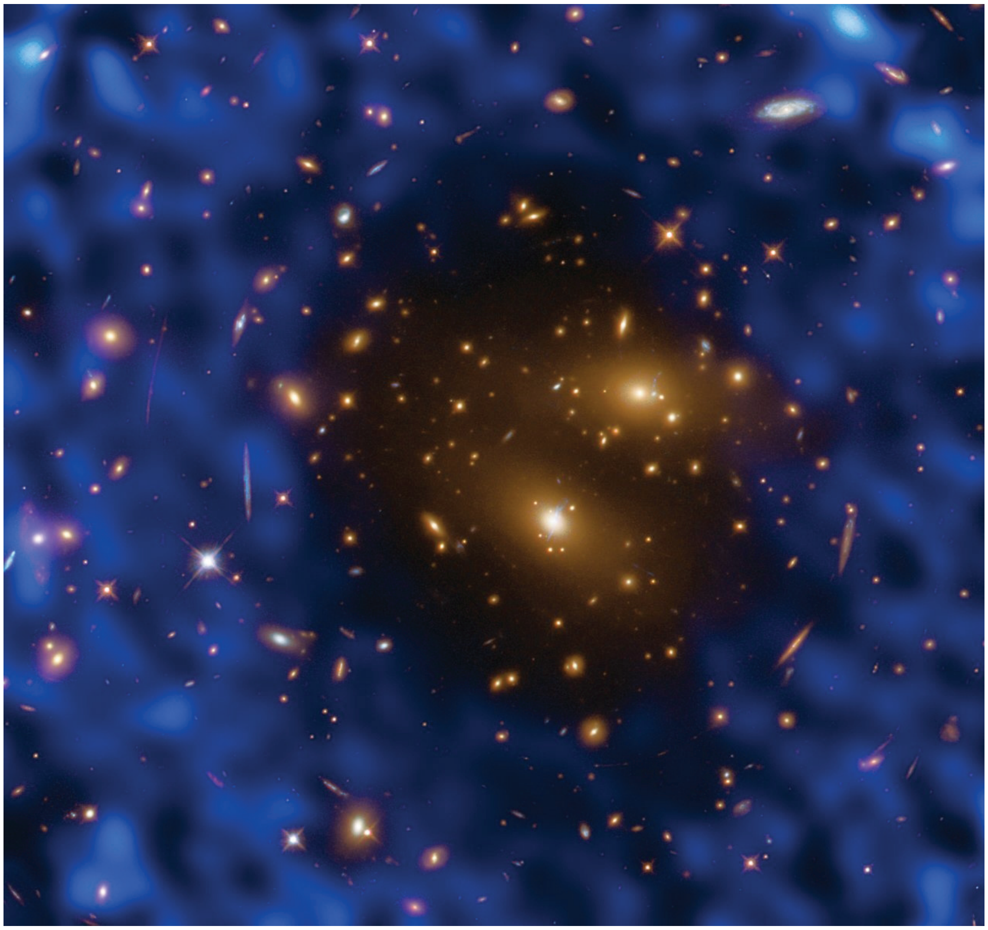

Figure 5 — This image shows the first measurements of the thermal Sunyaev-Zel'dovich effect from the Atacama Large Millimetre/submillimetre Array (ALMA) in Chile (in blue). Astronomers combined data from ALMA's 7- and 12-metre antennae to produce the sharpest possible image. The target was one of the most massive known galaxy clusters, RX J1347.5-1145, the centre of which shows up here in the dark "hole" in the ALMA observations. The energy distribution of the CMB photons shifts and appears as a temperature decrease at the wavelength observed by ALMA, hence a dark patch is observed in this image at the location of the cluster. Image: ESA/Hubble & NASA, T. Kitayama (Toho University, Japan)/ESA/Hubble & NASA

A radio "hole" in a galaxy cluster

The events surrounding the Big Bang left an indelible imprint on the fabric of the cosmos—an imprint that can be detected today by observing the oldest light in the Universe. This light is the cosmic microwave background (CMB), which has expanded over the past 13 billion years to permeate the entire cosmos, filling it with detectable photons. On their journey toward us, CMB microwaves pass through galaxy clusters that contain high-energy electrons. Scattering from these electrons give the microwave photons a tiny boost of energy, changing their wavelengths to shorter values and creating a scarcity of the original lower-energy photons in the direction of the galaxy cluster. The result is known as the Sunyaev-Zel'dovich (S-Z) effect after Rashid Sunyaev and Yakov Zel'dovich who predicted the effect in 1969. It appears as a "hole" surrounding a cluster of galaxies when observed in appropriate wavelengths.

A research team led by Tetsu Kitayama, a professor at Toho University, Japan, used the Atacama Large Millimetre/submillimetre Array (ALMA) to investigate the hot gas in the galaxy cluster RX J1347.5-1145 and successfully imaged this radio hole. RX J1347.5-1145, lying 4.8 billion light-years away, is known among astronomers for its strong S-Z effect and has been observed many times with radio telescopes. One of these, the Nobeyama 45-m radio telescope operated by the National Astronomical Observatory of Japan, had previously revealed an uneven distribution of the hot gas in this galaxy cluster that was not seen in X-ray observations. To better understand the unevenness, astronomers need higher-resolution observations. But relatively smooth and widely-distributed objects, such as the hot gas in galaxy clusters, are difficult to image with high-resolution radio interferometers that can only observe a limited area of the sky.

To overcome this difficulty, ALMA utilized the Atacama Compact Array, also known as the Morita Array, the major Japanese contribution to the project. The Morita Array's smaller-diameter antennae and the close-packed antenna configuration provide a wider field of view. By using the data from the Morita Array, astronomers can precisely measure the radio waves from objects subtending a large angle on the sky.

With ALMA, the team obtained an S-Z-effect image of RX J1347.5-1145, with twice the resolution and ten times better sensitivity than previous observations. This is the first image of the S-Z effect with ALMA. The ALMA S-Z image is consistent with the previous observations and better illustrates the pressure distribution of hot gas. It proves that ALMA is highly capable of observing the S-Z effect and clearly shows that a gigantic collision is ongoing in this galaxy cluster.

"It was nearly 50 years ago that the S-Z effect was proposed for the first time," explains Kitayama. "The effect is pretty weak, and it has been tough to image the effect with high resolution. Thanks to ALMA, this time we made a long-awaited breakthrough to pave a new path to probe the cosmic evolution." ✶

Compiled with material provided by ALMA.

Research Articles / Articles de recherche

Milky Way Globular Clusters and the Astronomical Literature

by Graeme H. Smith, University of California Observatories, University of California, Santa Cruz CA 95064 U.S.A. (graeme@ucolick.org)

Abstract

Globular clusters of the Milky Way have been the subject of many publications in the astronomical literature. However, there is quite a large dispersion in the level of scrutiny that individual clusters have received from the astronomy research community. The goal of this paper is to address the question: what makes some clusters more popular than others? Several metrics are used to compare the numbers of papers written about each globular cluster of the galaxy prior to 2015. The extent to which the metrics correlate with various intrinsic and extrinsic cluster properties is explored. The metrics are used to highlight the ten most-studied globular clusters, as well as to delineate certain types of clusters that have been least covered by research to date. As a guide to objects that might potentially reward increased study, a list is given of the highest-mass globular clusters that have received relatively little attention to date.

Introduction

Since the pioneering work of Shapley (1917, 1919a,b), studies of globular clusters (GCs) of the Milky Way (MW) have made numerous contributions to fields of astrophysics as diverse as variable stars, stellar abundances, stellar structure and evolution, stellar dynamics, and galactic evolution (e.g.[1] ten Bruggencate 1927; Shapley 1930; Sawyer Hogg 1973a,b; Hanes & Madore 1980; Grindlay & Davis Philip 1988; Spitzer 1988; Ashman & Zepf 1998; Djorgovski & Meylan 1993; Martinez Roger, Perez Fournon, & Sanchez 1999; Carney & Harris 2001). Investigations of globular clusters constitute a significant component of the published research in astronomical journals, and Canadian astronomers have contributed much to this literature. With over 150 known GCs in the galaxy having a wide range of properties and characteristics, it is inevitable that different clusters have received different degrees of scrutiny, not only because of observational accessibility but also due to differences in perception among astronomers of what makes a globular cluster intrinsically interesting. This article investigates whether the amount of research directed at individual GCs of the Milky Way can be correlated with various cluster properties. Ten systems are highlighted as having received the greatest attention in print to date, and reasons for their "popularity" are summarized. Some of the lesser-studied types of GCs are identified as a potential guide for further research.

Three Metrics

Three approaches were chosen in an effort to obtain metrics that quantify the degree to which a given globular cluster of the Milky Way has been the focus of refereed papers published in the astronomical literature. Two of the metrics employ information derived from the titles and abstracts of papers written about a cluster. The tool that was used here is the SAO/NASA Astrophysics Data System (ADS)[2] (Kurtz et al. 2000). Refereed papers in the ADS database for the years 2014 and earlier were considered. The two metrics counted were: (A) the number of papers $N_{\mathrm{A},titles}$ for which the name of a cluster appears in the title, and (B) the number of papers $N_{\mathrm{B},abstracts}$ wherein a cluster name appears either in the Abstract or as a keyword. The second metric is an attempt to count papers dealing with more than one cluster, or for which individual object names are not given in the title.[3] Even based on metric B some multi-cluster papers will still not have been included in a search. The comparative study of GC colour-magnitude diagrams by Arp (1955) is one notable example. A valuable source of astronomical data on individual globular clusters is the SIMBAD Astronomical Database (Wenger et al. 2000) maintained by the University of Strasbourg in France. Consequently, another metric has been compiled that is based on the number of references (sources of literature) returned by SIMBAD for a given cluster. This third metric, denoted $N_{\mathrm{C},simbad}$, is defined as the number of references to a cluster returned by SIMBAD for years up through and including 2015. Metric C includes sources additional to refereed papers, such as published proceedings of Symposia of the International Astronomical Union. Furthermore, a SIMBAD search is not limited to papers in which the name of a particular GC is required in either the title or the abstract, but it also includes sources wherein a cluster is referenced only within the main text of the publication.

Relations Between Metrics

The number of papers $N_{\mathrm{B},abstracts}$ for metric B is plotted versus $N_{\mathrm{A},titles}$ for metric A in Figure 1. A solid line corresponding to the relation $N_{\mathrm{B},abstracts} = 2N_{\mathrm{A},titles}$ is included, and appears to give a close approximation to the counts. The correlation in Figure 1 suggests that metric A provides a useful measure of the amount of research effort that has been spent upon a given cluster.

A comparison between the counts for metrics A and C is shown in Figure 2. Filled circles depict clusters that are members of the *New General Catalogue of Nebulae and Clusters* *of Stars* (Dreyer 1888; NGC). Open circles depict clusters that are not in the NGC, having been mostly discovered since that catalogue was compiled. The solid line in Figure 2 has the equation $N_{C,simbad} = 10N_{A,titles}$, and was chosen for illustrative purposes, although it approximates a lower limit to the data points. There is a reasonable correlation between metrics A and C for globular clusters from the New General Catalogue.

A "Top Ten" of Globular Clusters

The distribution of clusters with respect to metric A is given in Table 1. There are ten systems for which $N_{A,titles} > 100$, so this parameter provides one means for distinguishing a "top ten" among Milky Way globular clusters. These clusters are listed in Table 2 in order of rank according to the value of $N_{A,titles}$. Included in the table are also the metallicity[4] [Fe/H] for each cluster, and integrated absolute visual magnitude M_V (a measure of the total brightness of a cluster, and hence the total mass), as taken from the 2010 version of the catalogue by Harris (1996). Five of the clusters in Table 2 are in the northern sky, five in the southern. The top ten GCs are all Messier or NGC objects. Messier 22 (NGC 6656) falls just outside the top ten with $N_{A,titles} = 95$.

Metric B was not counted for the clusters ω Cen, M3, M4, and M5 because of the time that would be required to sort cluster from non-cluster papers. For the remaining six clusters, metric B ranks the objects in the same order as metric A. The relative ranking of each cluster according to $N_{C,simbad}$ is also listed in Table 2. Metric C returns the same top ten GCs as metric A, although the rankings are somewhat different.

The cluster that has gleaned the highest value of $N_{A,titles}$ is ω Centauri. It has received considerable attention in part because it is the most massive globular cluster in the Milky Way, and it is inhomogeneous with respect to many chemical elements (Norris, Freeman, & Mighell 1996; Suntzeff & Kraft 1996; Smith et al. 2000). The suggestion that the chemically evolved ω Cen (Sollima et al. 2005) is the stripped nucleus of a dwarf galaxy (Bekki & Freeman 2003) has heightened interest in the system.

Ranked equal second on the basis of $N_{A,titles}$ is the contrasting pair of clusters, M15 and 47 Tuc. The former of these two is an archetypal cluster of the galactic halo with [Fe/H] = −2.4 (Sneden et al. 1997), which makes it one of the most metal-poor globular clusters of the Milky Way. By contrast, 47 Tuc has a metallicity of [Fe/H] = −0.8 (Brown & Wallerstein 1992), which is near the low-abundance limit for globular clusters belonging to the bulge or thick disk population. The high mass, near proximity, low reddening, and interesting metallicities of these two clusters have combined to make them both observationally accessible and popular represen-

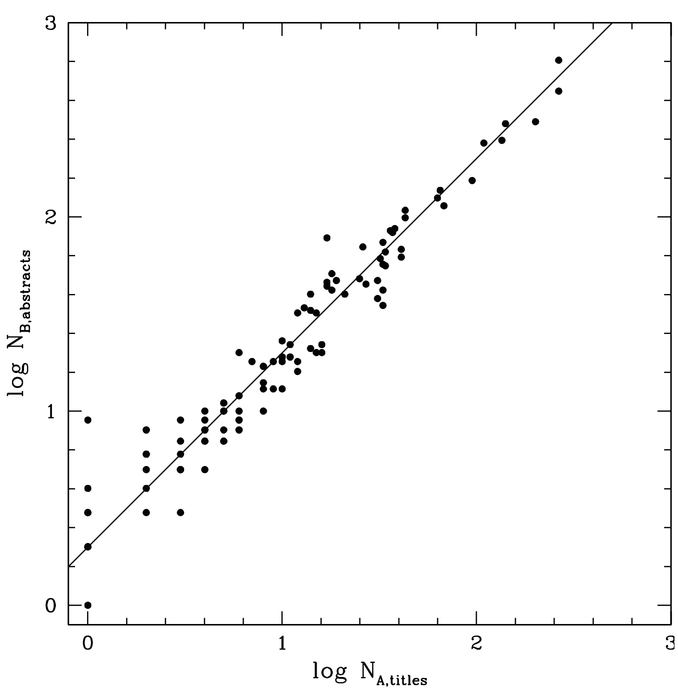

Figure 1 — Number of papers per cluster N_B, abstracts counted according to metric B (i.e. a cluster is named in either the Abstract of a paper or as a keyword) vs. the number of papers $N_{A,titles}$ according to metric A (i.e. the name of a cluster appears in a paper title). The plot is on a decimal logarithmic scale, with the solid line corresponding to $\log N_{B,abstracts} = \log N_{A,titles} + 0.30$.

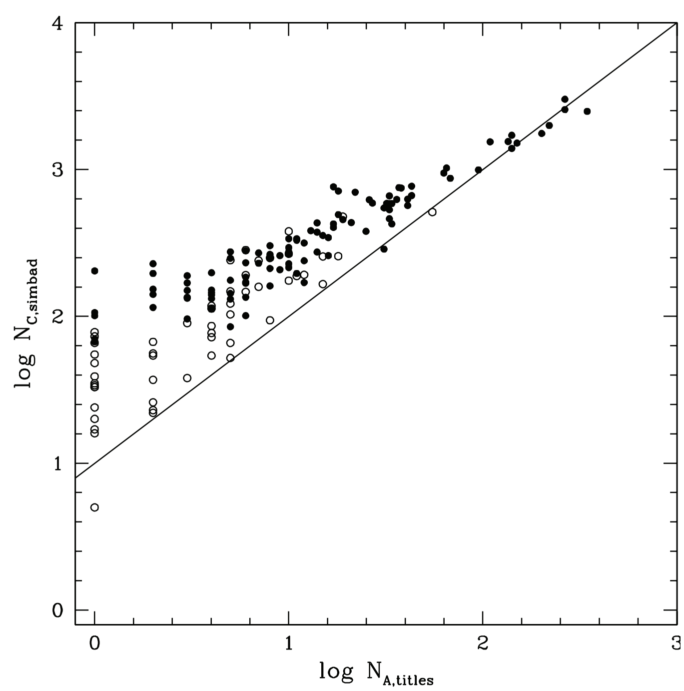

Figure 2 — The number of papers listed by SIMBAD that contain a reference to a globular cluster vs. the number of refereed papers found on the basis of metric A ($N_{A,titles}$). A log-log scale is used. The solid line has the equation $N_{C,simbad} = 10N_{A,titles}$, and appears to provide a reasonable lower envelope to the data. Filled (open) circles correspond to clusters that do (do not) appear in the New General Catalogue.

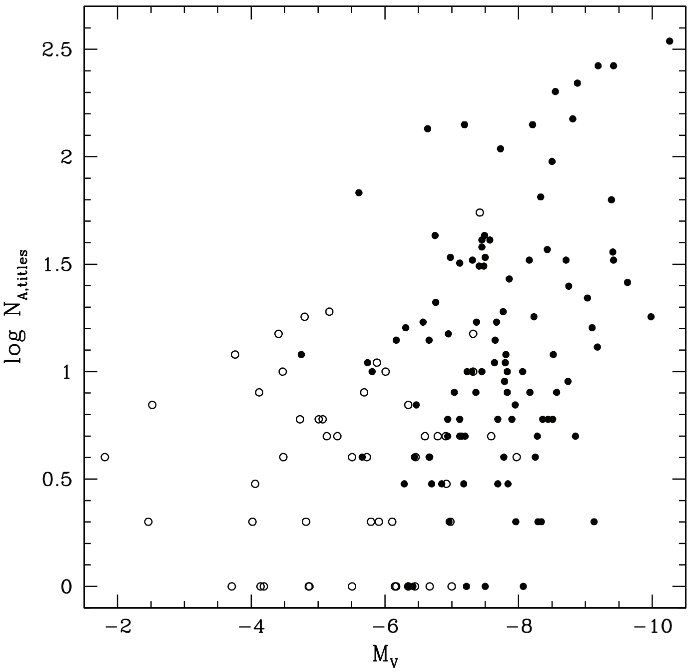

Figure 3 — The number of papers per cluster counted according to metric A vs. cluster absolute integrated magnitude in the V band. The more negative the value of M_V the brighter the cluster. Filled (open) circles correspond to clusters that do (do not) appear in the New General Catalogue.

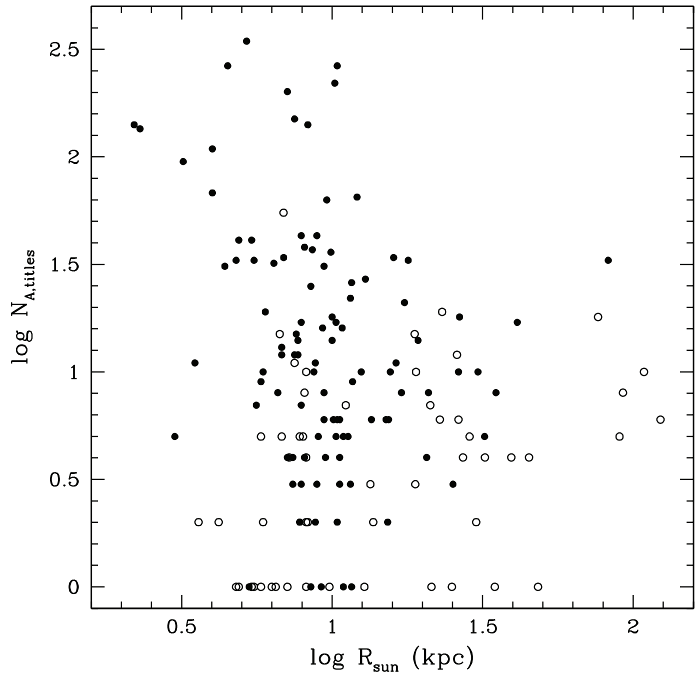

Figure 4 — Number of papers per cluster counted according to metric A vs. heliocentric distance R_{sun} in kpc. Filled (open) circles correspond to clusters that do (do not) appear in the New General Catalogue.

tatives of the two major sub-populations within the overall Milky Way globular cluster system.

Five well-known northern Messier clusters make the top ten: M15, M92, M3, M13, and M5. These clusters played a significant role in measurements of early GC colour-magnitude diagrams (ten Bruggencate 1927). They were at the centre of efforts to reach the faint dwarf stars thought to be present within globular clusters (Arp, Baum, & Sandage 1952, 1953; Baum et al. 1959), and to delineate the properties of red-giant stars (Shapley 1919a; Sandage, Katem, & Kristian 1968). Consequently, their Hertzsprung–Russell diagrams became early keys to understanding the evolution of low-mass stars from the main sequence to the red-giant branch, as well as through more advanced stages of stellar evolution involving helium fusion (Hoyle & Schwarzschild 1955; Faulkner & Iben 1966).

Eight of the globular clusters in the "top ten" are members of the metal-poor Milky Way halo, having [Fe/H] < −0.9, while 47 Tuc is the closest GC having kinematics and metallicity consistent with membership of the galactic thick disk (Cudworth & Hanson 1993). One cluster in the "top ten" is somewhat ambiguous; M4 has a [Fe/H] consistent with the high-end of the halo-GC metallicity distribution, but a rather thick-disk-like space motion (Cudworth & Hanson 1993). Both M4 and NGC 6397 are of intermediate mass, but the fact that they are the two closest globular clusters to the Sun has contributed to their observational accessibility, although the field of M4 is complicated by differential reddening (Hendricks et al. 2012).

Metric A and Globular Cluster Properties

Several factors that might be expected to influence whether a given globular cluster is conducive to observational study include mass (the number of stars available for observation), distance from the Sun, interstellar reddening, and galactic latitude. Plots of $N_{A,titles}$ versus three of these parameters are shown in Figures 3–5. In this set of figures, filled and open circles correspond to clusters that are listed, or not listed, within the *New General Catalogue*.

The largest number of metric-A papers are found among the highest mass clusters, and GCs to which more than 20 metric-A papers have been devoted are typically brighter than $M_V = -6.5$ (Figure 3). This can be compared with a mean absolute magnitude of $M_V \sim -7.5$ for both halo and disk globular clusters (Armandroff 1989). However, not all high-mass clusters have been equally well studied, and there are a few relatively massive clusters with $M_V < -8.0$ for which fewer than 10 metric-A papers have been published in the refereed literature. The data in Figure 3 are characterized by an upper limit to $N_{A,titles}$ that increases with cluster brightness (mass), but there is no clear correlation. Notable from the figure is that, with only a few exceptions, low-mass globular clusters with $M_V > -5.5$ are largely absent from the *New General Catalogue*. Evidently such faint clusters required

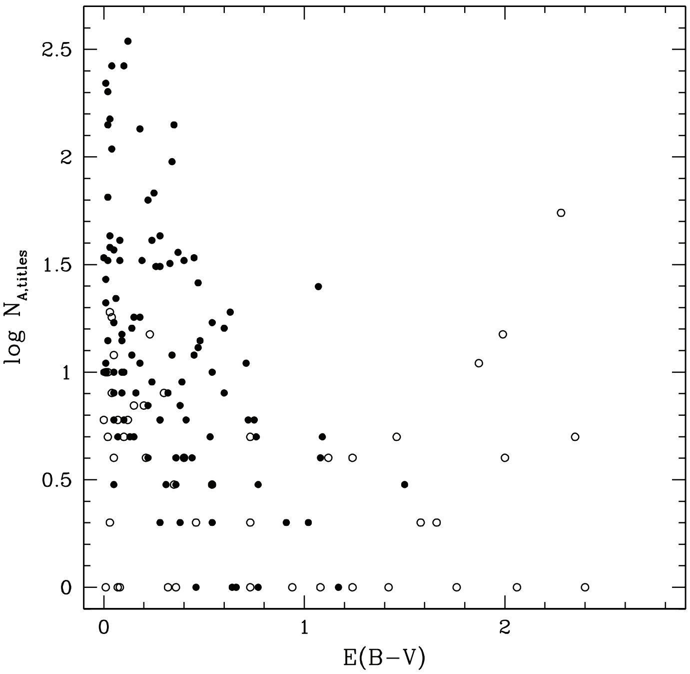

Figure 5 — Number of papers per cluster counted according to metric A vs. interstellar reddening E(B – V). Filled (open) circles correspond to clusters that do (do not) appear in the New General Catalogue.

more than just visual searches to enable their discovery. For example, the so-called Palomar clusters were discovered by Abell (1955) on photographic plates obtained as part of the National Geographic Society-Palomar Observatory Sky Survey (Minkowski & Abell 1963).

Clusters for which more than 20 metric-A papers have been published are within 20 kpc of the Sun, while clusters receiving more than 50 papers are typically within 12 kpc of the Sun (Figure 4). Clearly the apparent magnitude of the member stars is one influence on the popularity of a cluster. Nonetheless, there are GCs within 6 kpc of the Sun that have yet to receive the attention that might be expected on the basis of their relative proximity. These include the relatively metal-rich clusters NGC 6304, NGC 6352, and NGC 6366, as well as NGC 6540 and NGC 6544 with [Fe/H] ~ –1.4, studies of which are hindered by low galactic latitude and/or high reddening.

With one exception, GCs for which $N_{A,titles} > 40$ have a reddening of $E(B-V) < 0.40$. Many fewer metric-A papers have been written about clusters for which $E(B-V) > 0.50$. Nonetheless, Figure 5 shows that there is a significant number of low-reddening GCs with $E(B-V) < 0.10$ that have received less than 10-20 metric-A papers. By contrast, Terzan 5 is one highly reddened cluster that had been the subject of 55 metric-A papers prior to 2015, despite a problematic reddening of $E(B-V) = 2.3$. Several discoveries have led to the popularity of this cluster, among the earliest of which included relatively large numbers of millisecond pulsars (Lyne et al. 1990, 2000) and low-mass X-ray sources (Johnston, Verbunt, & Hasinger 1995; Heinke et al. 2006). In addition, it is a bulge globular cluster with [Fe/H] ≥ –0.3, and an internal dispersion in metallicity of approximately 0.5 dex (Origlia et al. 2011), a discovery that has led to the suggestion that it is a left-over building block of the galactic bulge (Ferraro et al. 2009).

Crowded fields and high reddenings have caused difficulties for the study of many globular clusters at low galactic latitude, particularly in directions toward the galactic centre. For example, a large number of less-well-studied GCs for which $N_{A,titles} < 20$ are located at $|b| \leq 10°$, i.e. within 10 degrees of the galactic plane as projected on the sky.

While strict correlations are not seen in Figures 3–5 between $N_{A,titles}$ and the various cluster parameters depicted therein, might it be possible to formulate a mathematical combination of these parameters that more nearly correlates with metric A? As one example, we considered the function

$$T = (18.75 + 1.875M_V) + 10\log(R_{SUN} - 1) + 5.0E(B-V) + 15(1 - \sin|b|). \quad (1)$$

The right-hand side of equation (1) is the sum of four terms, where $T = (18.75 + 1.875M_V)$ is a function of cluster absolute magnitude, while other terms are functions of the heliocentric distance R_{SUN} (kpc), $E(B-V)$ reddening, and galactic

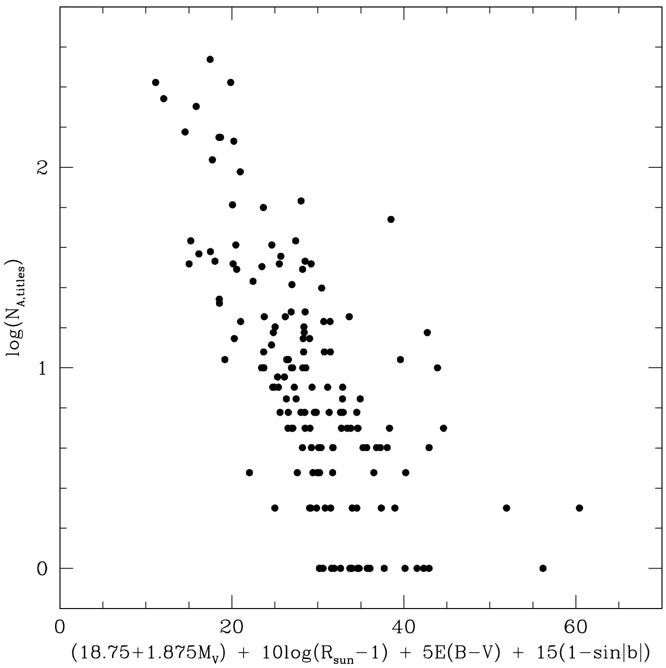

Figure 6 — The metric log $N_{A,titles}$ vs. the parameter T given by equation (1) of the text.

latitude *b*. Each of the four terms was arbitrarily chosen so as to vary in value from ≈ 0 to 16 as M_V, R_{SUN}, $E(B-V)$, and $|b|$ range over the parameter space occupied by the majority of GCs in the Milky Way. For example, as R_{SUN} varies from 2 kpc to 40 kpc, the second term 10 log(R_{SUN} – 1) varies mainly within the range 0 to 16. The form of equation (1) was chosen such that as *T* increases we might expect a cluster to become more challenging for observational study. In Figure 6, the metric $N_{A,titles}$ is plotted against the value of *T*. The fact that a correlation is revealed implies that observational accessibility has indeed had a significant effect on the extent to which individual globular clusters have been studied.[5]

What Types of Clusters are Poorly Represented in the Literature?

The globular cluster population of the Milky Way exhibits broad distributions in properties such as cluster mass, metallicity, and distance from the galactic centre. Metric A has been used to investigate how uniformly GCs have been sampled by studies to date with respect to six different parameters. Clusters were compiled into 5-6 subdivisions (bins) with respect to each of the following properties: metallicity [Fe/H], central concentration *c*,[6] galactic latitude, integrated magnitude M_V, galactocentric distance R_{gc}, and distance from the Sun R_{SUN}. Table 3 contains a list of the bins employed. The number of GCs in each parameter bin was counted along with the number of metric-A papers for these clusters, thereby allowing the average number of papers per cluster to be determined for each parameter bin. Results are listed in Table 3.

Heliocentric distance, galactic latitude, and galactocentric distance are extrinsic properties determined by the location of a cluster within the Milky Way. The data in Table 3 reveal that the average number of metric-A papers per cluster tends to decrease with increasing heliocentric distance. With respect to R_{SUN}, GCs within 4 kpc of the Sun have been the subject of the most metric-A papers. There is a systematic falloff in metric A when comparing the bins of increasing heliocentric distance in Table 3.

This comparison reinforces a conclusion from the previous section that heliocentric distance is one extrinsic parameter that has influenced cluster popularity.

Table 3 illustrates that GC studies have preferred to avoid the galactic plane, with the average number of metric-A papers per cluster increasing systematically with galactic latitude. As a consequence, GCs of the bulge population have been less well studied than halo clusters. Low galactic latitude has played a role in limiting globular cluster studies because it is often associated with high stellar crowding and interstellar reddening.

As a function of galactocentric distance, GCs in the range R_{gc} = 6–12 kpc have received notably greater attention than clusters either closer to the galactic centre or in the remote halo. This is partially a reflection of several of the factors that appear in equation (1). Clusters in the remote halo are at great distances from the Sun, whereas study of GCs near the galactic centre are hindered not only by distance, but high reddening and interstellar obscuration, and field crowding. By contrast, nearby unobscured clusters have galactocentric distances not too dissimilar from the Sun.

Turning to intrinsic cluster properties, total mass as one determinant of popularity was considered in the preceding section. As revealed in Table 3, there is an increase in the average number of metric-A papers per cluster as the integrated magnitude becomes brighter. The higher the mass the more attention is a GC likely to have received, even though there is not a strict cluster-by-cluster correlation between M_V and the number of metric A papers (Figure 3).

There is some trend in the number of metric-A papers per cluster across the various bins in central concentration *c* listed in Table 3. The most compact clusters with $c > 2.0$ owe part of their popularity to studies of dynamical evolution that have focused on the phenomenon of core collapse. There is a paucity of literature on the lowest concentration GCs of the galaxy, and systems with $c < 1.0$ have on average received notably fewer papers than more centrally concentrated systems. Globular clusters with $c < 1$ tend to have absolute M_V magnitudes fainter than −8.0, and among non-core-collapse clusters there is a correlation between M_V and *c*, albeit with scatter (van den Bergh 2003; Djorgovski & Meylan 1994). As such, the trend in publications with respect to central concentration may mirror to an extent the trend with cluster mass.

As noted above, several factors have hindered the study of globular clusters near the galactic centre and plane. One consequence is that the metal-richer GCs of the disk and bulge population have received less attention than many metal-poorer halo clusters (Table 3). Even within the galactic halo, not all metallicity ranges have received equal attention. Clusters with [Fe/H] < −2.0 have been more popular in terms of their average number of papers than those of metallicity −2.0 < [Fe/H] < −1.5. Astronomers have had a long-standing interest in the most metal-poor stars of the Milky Way.

Among the lesser-studied GCs for which $N_{A,titles} < 10$ there are quite a few objects from the *New General Catalogue*, whereas other such objects have only been discovered since 1950. One particular subset of clusters for which $N_{A,titles} < 10$ and $M_V \leq -8.0$ is summarized in Table 4, which comprises a list of the highest-mass "neglected" GCs. Various cluster parameters are listed in the table: declination, heliocentric distance R_{SUN}, [Fe/H] abundance, absolute value of galactic latitude $|b|$, distance from the galactic centre R_{gc}, absolute value of the vertical distance of a cluster $|Z|$ from the midplane of the galactic disk, interstellar reddening $E(B-V)$, and integrated absolute magnitude M_V, the source again being various editions of the Harris (1996) catalogue. Since all of these clusters are NGC objects they may appeal to amateur astronomers for observation, particularly with the thought that they have been rather avoided by the professional astronomy community. Several have very high reddenings, but the few with $E(B-V) < 0.3$, i.e. extinctions in V of less than 1 mag., may be the more visually enticing objects. The inconvenience for Canadian astronomers is that all of these clusters are south of the celestial equator.

Nine of the clusters in Table 4 have metallicities of [Fe/H < −1.0, which suggests that they are members of the halo GC population. Nonetheless, most of these metal-poor systems are less than 3 kpc above or below the galactic plane. They may constitute a group of relatively massive halo clusters that are currently in moderate proximity to the galactic disk or bulge.

Acknowledgments

This work has made use of the NASA/SAO Astrophysics Data System, as well as the SIMBAD Astronomical Database, operated at CDS, Strasbourg, France. ✶

Endnotes

1 This *Journal* provides many illustrations via the abstracts of papers presented at annual meetings of the Canadian Astronomical Society, e.g. volumes 85-93 of the *JRASC* for years 1991-1999, as well as previous volumes for earlier meetings. See also the Proceedings of the Kingston Conference held at the Dominion Astrophysical Observatory in 1989, published in the *JRASC* (Tatum 1990).

2 The NASA ADS system is accessible at http://adswww.harvard.edu

3 An ADS search for abstracts in which clusters are denoted by a Messier nomenclature such as M3 and M4 will also turn up papers devoted to stars of M spectral type. Hence $N_{B,abstracts}$ was not counted for some clusters where such a potential for confusion occurs.

4 The "metallicity" of a GC typically refers to the iron abundance of the member stars within that cluster. Conventionally the Fe abundance of any star is referenced to the Sun (⊙), and defined according to the notation

$$[Fe/H] = \log_{10} \frac{(N_{Fe}/N_H)_{star}}{(N_{Fe}/N_H)_{\odot}} ,$$

where N_{Fe} and N_H are the number of atoms per cubic centimeter of iron and hydrogen in the atmosphere of a star. Most, but not all, globular clusters of the Milky Way are homogeneous with respect to [Fe/H] of the member stars, but this metallicity differs considerably from cluster to cluster.

5 Different factors seem to have been in play for different clusters. For example, among the top ten clusters of Table 2, proximity to the Sun has facilitated the study of M4 and NGC 6397, despite these clusters having the lowest masses of the top ten. In the cases of M15 and 47 Tuc, both proximity and relatively high mass, as well as [Fe/H] metallicities near the lower limit for the halo and disk populations of GCs respectively, have all likely been contributing factors.

6 This parameter pertains to the spatial distribution of stars within a cluster (King 1962, 1966; Peterson & King 1975). Formally $c = \log(rt/rc)$, where rt and rc are known as the tidal radius and core radius respectively. These radii are derived by fitting mathematical functions or models to measurements of the surface density of stars as projected on the sky (for example, the number of stars $f(r)$ per square arcminute versus projected radius r from cluster centre in arcminutes). The tidal radius is the projected radius at which the number of cluster stars drops to zero. This radius is set by the gravitational tidal field of the galaxy. The core radius refers to how centrally concentrated the stars are within a cluster. It can be defined via mathematical fits to measurements of $f(r)$ versus r for a cluster. For example, the core radius appears as a scaling factor in the equation

$$f(r) = \frac{f(r=0)}{1 + (r/r_c)^2} ,$$

that was found by King (1962) to be a useful approximation to observed data for the inner region of 47 Tucanae.

Table 1 – Distribution of Globular Clusters with Respect to Metric A

Range in value of $N_{A,titles}$	Number of GCs
1-5	64
6-10	32
11-19	25
20-39	17
40-99	9
> 100	10

Table 2 – Rankings of the "Top Ten" Globular Clusters

Rank by Metric A	Cluster	$N_{A,titles}$	Rank by Metric *c*	[Fe/H]	M_V (mag)
1	ω Cen	345	(3)	–1.5	–10.3
2	47 Tuc/M15	265	(1)/(2)	–0.7/–2.4	–9.4/–9.2
3	M3	220	(4)	–1.5	–8.9
4	M13	201	(5)	–1.5	–8.6
5	M5	150	(9)	–1.3	–8.8
6	M4/M92	141	(10)/(6)	–1.2/–2.3	–7.2/–8.2
7	NGC 6397	135	(7)	–2.0	–6.6
8	NGC 6752	109	(8)	–1.5	–7.7

Table 3 – Statistics of Papers Versus Globular Cluster Parameters

R_{SUN} (kpc)	≤ 4.0	> 4.0	> 6.0	> 8.0	> 12	> 30
heliocentric distance		≤ 6.0	≤ 8.0	≤ 12	≤ 30	
number of metric-A papers per cluster	70.8	42.5	23.0	24.0	11.5	8.5
$\|b\|$(º)	≤ 5	> 5	> 10	> 20	> 40	
absolute value of galactic latitude		≤ 10	≤ 20	≤ 40		
number of metric-A papers per cluster	9.1	12.8	26.1	37.3	47.2	
R_{gc}kpc)		> 2.0	> 4.0	> 6.0	> 8.0	> 12.0
galactocentric distance	≤ 2.0	≤ 4.0	≤ 6.0	≤ 8.0	≤ 12	
number of metric-A papers per cluster	10.0	10.3	28.5	75.8	73.8	11.7
M_V (mag)	≥ –4.0	< –4.0	< –6.0	< –8.0	unknown	
integrated magnitude		≥ –6	≥ –8			
number of metric-A papers per cluster	4.0	8.3	16.1	59.6	1.0	
c	≤ 1.0	> 1.0	> 1.5	> 2.0	unknown	
central concentration		≤ 1.5	≤ 2.0			
number of metric-A papers per cluster	7.8	24.2	33.1	33.0	4.0	
[Fe/H]	≤ –2.0	> –2.0	> –1.5	> –1.0	> –0.5	unknown
metallicity		≤ –1.5	≤ –1.0	≤ –0.5	≤ 0.0	
number of metric-A papers per cluster	54.9	31.2	18.5	19.3	13.1	1.4

Table 4 – Clusters with $N_{A,titles}$ < 10 and M_V ≤ –8.0

Cluster	Dec (2000)	R_{sun} (kpc)	[Fe/H]	$\|b\|$ (°)	R_{gc} (kpc)	$\|Z\|$ (kpc)	$E(B-V)$ (mag)	M_V (mag)
NGC 4833	–70:52.5	6.6	–1.85	8.02	7.0	0.9	0.32	–8.17
NGC 5286	–51:22.4	11.7	–1.69	10.57	8.9	2.1	0.24	–8.74
NGC 5824	–33:04.1	32.1	–1.91	22.07	25.9	12.1	0.13	–8.85
NGC 5986	–37:47.2	10.4	–1.59	13.27	4.8	2.4	0.28	–8.44
NGC 6139	–38:50.9	10.1	–1.65	6.94	3.6	1.2	0.75	–8.36
NGC 6273	–26:16.1	8.8	–1.74	9.38	1.7	1.4	0.38	–9.13
NGC 6316	–28:08.4	10.4	–0.45	5.76	2.6	1.0	0.54	–8.34
NGC 6355	–26:21.2	9.2	–1.37	5.43	1.4	0.9	0.77	–8.07
NGC 6356	–17:48.8	15.1	–0.40	10.22	7.5	2.7	0.28	–8.51
NGC 6517	–08:57.5	10.6	–1.23	6.76	4.2	1.3	1.08	–8.25
NGC 6539	–07:35.1	7.8	–0.63	6.78	3.0	0.9	1.02	–8.29
NGC 6569	–31:49.6	10.9	–0.76	6.68	3.1	1.3	0.53	–8.28
NGC 6864	–21:55.3	20.9	–1.29	25.75	14.7	9.1	0.16	–8.57

References

Abell, G.O. (1955). Globular clusters and planetary nebulae discovered on the National Geographic Society-Palomar Observatory Sky Survey. *PASP, 67*, 258.

Armandroff, T.E. (1989). The properties of the disk system of globular clusters. *AJ, 97*, 375.

Arp, H.C. (1955). Color-magnitude diagrams for seven globular clusters. *AJ, 60*, 317.

Arp, H.C., Baum, W.A., & Sandage, A.R. (1952). The HR diagrams for the globular clusters M92 and M3. *AJ, 57*, 4.

Arp, H.C., Baum, W.A., & Sandage, A.R. (1953). The color-magnitude diagram of the globular cluster M 92. *AJ, 58*, 4.

Ashman, K.M. & Zepf, S.E. (1998). Globular Cluster Systems. Cambridge University Press: Cambridge.

Baum, W.A., Hiltner, W.A., Johnson, H.L., & Sandage, A.R. (1959). The main sequence of the globular cluster M13. *ApJ, 130*, 749.

Bekki, K., & Freeman, K.C. (2003). Formation of ω Centauri from an ancient nucleated dwarf galaxy in the young galactic disc. *MNRAS, 346*, L11.

Brown, J.A. & Wallerstein, G. (1992). High-resolution CCD spectra of stars in globular clusters. VII. Abundances of 16 elements in 47 Tuc, M4, and M22. *AJ, 104*, 1818.

Carney, B.W. & Harris, W.E. (2001). Star Clusters. *Saas-Fee Advanced Course 28*. Springer-Verlag: Berlin.

Cudworth, K.M. & Hanson, R.B. (1993). Space velocities of 14 globular clusters. *AJ, 105*, 168.

Dreyer, J.L.E. (1888). New general catalogue of nebulae and clusters of stars. *Memoirs of the Royal Astronomical Society, 49*, 1.

Djorgovski, S.E. & Meylan, G. (1993). Structure and dynamics of globular clusters. *Astronomical Society of the Pacific Conference Series No. 50*. Astronomical Society of the Pacific: San Francisco.

Djorgovski, S. & Meylan, G. (1994). The galactic globular cluster system. *AJ, 108*, 1292.

Faulkner, J. & Iben, I. Jr. (1966). The evolution of Population II stars. *ApJ, 144*, 995.

Ferraro, F.R., et al. (2009). The cluster Terzan 5 as a remnant of a primordial building block of the Galactic bulge. *Nature, 462*, 483.

Grindlay, J.E. & Davis Philip, A.G. (1988). The Harlow-Shapley symposium on globular cluster systems in galaxies. *Proceedings of IAU Symposium 126*. Kluwer Academic Publishers: Dordrecht.

Hanes, D. & Madore, B. (1980). Globular Clusters. *Based on the Proceedings of NATO Advanced Study Institute* held at the Institute of Astronomy University of Cambridge, August 1978. Cambridge University Press; Cambridge.

Harris, W.E. (1996). A catalog of parameters for globular clusters in the Milky Way. *AJ, 112*, 1487.

Heinke, C.O., Wijnands, R., Cohn, H.N., Lugger, P.M., Grindlay, J.E., Pooley, D., & Lewin, W.H.G. (2006). Faint x-Ray sources in the globular cluster Terzan 5. *ApJ, 651*, 1098.

Hendricks, B., Stetson, P.B., Vandenberg, D.A., & Dall'Ora, M. (2012). A new reddening law for M4. *AJ, 144*, 25.

Hoyle, F. & Schwarzschild, M. (1955). On the evolution of Type II stars. *ApJS, 2*, 1.

Johnston, H.M., Verbunt, F., & Hasinger, G. (1995). The position of the x-ray sources in the globular clusters Terzan 1, Terzan 5 and NGC 6440. *A&A, 298*, L21.

King, I.R. (1962). The structure of star clusters. I. An empirical density law. *AJ, 67*, 471.

King, I. R. (1966). The structure of star clusters. III. Some simple dynamical models. *AJ, 71*, 64.

Kurtz, M.J., Eichhorn, G., Accomazzi, A., Grant, G.S., Murray, S.S., & Watson, J.M. (2000). The NASA astrophysics data system: overview. *A&AS, 143*, 41.

Lyne, A.G., Johnston, S., Manchester, R.N., Stavely-Smith, L., D'Amico, M. (1990). An eclipsing millisecond pulsar in the globular cluster Terzan 5. *Nature, 347*, 650.

Lyne, A.G., Mankelow, S.H., Bell, J.F., & Manchester, R.N. (2000). Radio pulsars in Terzan 5. *MNRAS, 316*, 491.

Martinez Roger, C., Perez Fournon, I., & Sanchez, F. (1999). *Globular Clusters: X Canary Islands Winter School of Astrophysics*, Cambridge University Press: Cambridge.

Minkowski, R.L. & Abell, G.O. (1963). The National Geographic Society-Palomar Observatory Sky Survey. *Basic Astronomical Data: Stars and Stellar Systems*. ed. K. A. Strand, University Chicago Press: Chicago.

Norris, J.E., Freeman, K.C., & Mighell, K.J. (1996). The giant branch of ω Centauri. V. The calcium abundance distribution *ApJ, 462*, 241.

Origlia, L., Rich, R.M., Ferraro, F.R., Lanzoni, B., Bellazini, M., Dalessandro, E., Mucciarelli, A., Valenti, E., & Beccari, G. (2011). Spectroscopy unveils the complex nature of Terzan 5. *ApJ, 726*, L20.

Peterson, C.J. & King, I.R. (1975). The structure of star clusters. VI. Observed radii and structural parameters in globular clusters. *AJ, 80*, 427.

Sandage, A., Katem, B., & Kristian, J. (1968). An indication of gaps in the giant branch of the globular cluster M15. *ApJ, 153*, L129.

Sawyer Hogg, H. (1973a). Variable stars in globular clusters. *JRASC, 67*, 8.

Sawyer Hogg, H. (1973b). A third catalogue of variable stars in globular clusters comprising 2119 entries. *Publications of the David Dunlap Observatory Vol. 3*. University of Toronto Press: Toronto.

Shapley, H. (1917). Studies based on the colors and magnitudes in stellar clusters. I. II. III. *ApJ, 45*, 118.

Shapley, H. (1919a). Studies based on the colors and magnitudes in stellar clusters. X. A critical magnitude in the sequence of stellar luminosities. *ApJ, 49*, 96.

Shapley, H. (1919b). Studies based on the colors and magnitudes in stellar clusters. XII. Remarks on the arrangement of the sidereal universe. *ApJ, 49*, 311.

Shapley, H. (1930). *Star Clusters.* McGraw-Hill Book Company: New York.

Smith, V.V., Suntzeff, N.B., Cunha, K., Gallino, R., Busso, M., Lambert, D.L., & Straniero, O. (2000). The chemical evolution of the globular cluster ω Centauri (NGC 5139). *AJ, 119*, 1239.

Sneden, C., Kraft, R.P., Shetrone, M.D., Smith, G.H., Langer, G.E., & Prosser, C.F. (1997). Star-to-star abundance variations among bright giants in the metal-poor globular cluster M15. *AJ, 114*, 1964.

Sollima, A., Pancino, E., Ferraro, F.R., Bellazini, M., Straniero, O., & Pasquini, L. (2005). Metallicities, relative ages, and kinematics of stellar populations in ω Centauri. *ApJ, 634*, 332.

Spitzer, L. Jr. (1988). *Dynamical Evolution of Globular Clusters*. Princeton University Press: Princeton.

Suntzeff, N.B. & Kraft, R.P. (1996). The abundance spread among giants and subgiants in the globular cluster ω Centauri. *AJ, 111*, 1913.

Tatum, J.B. (1990). Editorial. *JRASC, 84*, 57.

ten Bruggencate, P. (1927). *Sternhaufen*, Springer: Berlin.

van den Bergh, S. (2003). Some global characteristics of the galactic globular cluster system. *ApJ, 590*, 797.

Wenger, M., et al. (2000). The SIMBAD astronomical database. The CDS reference database for astronomical objects. *A&AS, 143*, 9.

Near-infrared Photometry of Venus

Richard W. Schmude, Jr.; Kingston Centre
Gordon State College, 419 College Dr, Barnesville, GA 30204
Schmude@gordonstate.edu

Abstract

Several dozen J and H filter brightness measurements of Venus are reported covering the period May 2014 to February 2016. Optec (2005) reports that their J filter is sensitive to wavelengths of between 1.25 and 1.45 micrometres (μm) and their H filter is sensitive to wavelengths of between 1.5 and 1.8 μm. Photometric constants of Venus for the J and H filters are presented. It is concluded that at the 90% confidence level, Venus has the same normalized magnitude for a given phase angle at waxing and waning phases to within experimental uncertainty. Cubic equations, with respect to the solar phase angle (α), are selected to describe the normalized magnitude as a function of a for the J and H filters.

Introduction

Harris (1961) reviewed early brightness measurements of Venus. He cites (Kuiper, 1952) and reports that Venus reflects about 60% more 2-μm than 1-μm light. Pollack et al. (1974) reported near-infrared spectra of Venus using a telescope onboard a NASA – Ames operated Learjet. This group reported the reflectivity of Venus over the wavelength range of 1.2 to 2.4 μm and 2.7 to 4.4 μm. They reported that Venus had a phase angle of ~120° when the spectra were recorded. In 1983, near-infrared images of Venus's dark side were made with wavelengths near 1.74 μm and 2.3 μm (Allen & Crawford, 1984). These two reported that this radiation was 0.03 to 1.0% that of peak intensity. They reported images showing albedo features on the dark side of Venus having a rotation period of 5.4 ±0.1 days retrograde. The brightness temperature of the features imaged at 1.74 μm was 450 K. A second group reported blackbody temperatures of 380 K for features imaged near 2.3 μm and 485 K for those imaged at 1.74 μm (Bézard, de Bergh, Crisp, & Mallard, 1990). These results are consistent with the 1.74-μm radiation reaching deeper into the atmosphere. Near-infrared thermal images recorded by the *Galileo* spacecraft, at a wavelength of 1.18 μm, are consistent with a surface temperature gradient of 8 K per kilometre (Carlson et al., 1993). This group reported that the surface has about a 100 K temperature range between Maxwell Montes (elevation 12 km) and Sedna Planitia (elevation −1 km). One group used images recorded of Venus's night side at a wavelength of 1.02 μm to image surface features (Mueller, Helbert, Erard, Piccioni, & Drossart, 2012). They reported that the brightness is anticorrelated with elevation. This group also utilized these images along with data from *Magellan* to

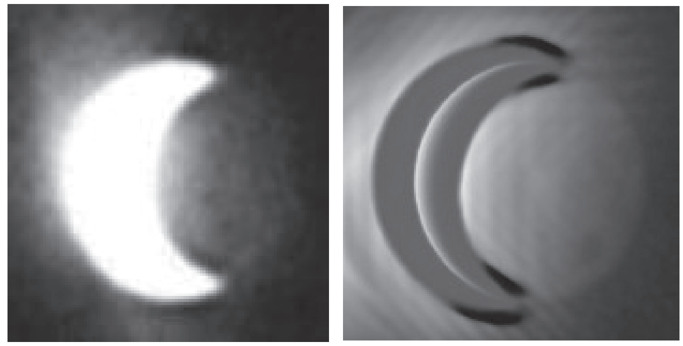

A B

Figure 1 — A: 2013 December 27 (22:10 UT) by F. Melillo, 0.25-m Schmidt-Cassegrain, 1 μm filter; B: 2012 May 20 (0:43 UT) by J. Boudreau, 0.28 m SC, 0.986-μm longpass filter for the dark side. The author would like to thank Frank Melillo and John Boudreau for their images, which are reproduced here.

report a rotational period of 243.023 ±0.002 days for Venus. Basilevsky et al. (2012) summarized results of images taken with the 1-μm channel of the Venus Monitoring Camera onboard *Venus Express*. They reported that the tessera terrain southwest of Beta Regio has a lower emissivity than the surrounding terrain. Frank Mellilo and John Boudreau also imaged albedo features on the dark side of Venus that may be the tessera terrain described by Basilevsky et al. (2012), see Figure 1. Mellilo used a 1-micron filter and Boudreau used a 0.986-μm longpass filter.

The middle and lower cloud layers on the night side of Venus are reported to have become up to 35 percent brighter over a 407-day period (McGouldrick, Momary, Baines & Grinspoon, 2012). This group based their results on measurements made at a wavelength near 1.74 μm. This is evidence that parts of the Venusian atmosphere underwent large brightness changes. Perhaps the dayside undergoes changes in near-infrared wavelengths. More recently, Taylor (2014) summarized our knowledge of Venus up to 2014. He reports that light, with a wavelength of 1.2 μm, penetrates that planet's atmosphere to an altitude of ~5 km whereas light, with a wavelength of 1.7 μm, penetrates to an altitude of ~20 km.

Mallama, Wang, & Howard (2006) reported phase curves for the B, V, R, and I filters of Venus. They reported geometric albedos of 0.64, 0.67, 0.69, and 0.57 for the B, V, R, and I filters, respectively.

There are at least four reasons for carrying out J and H filter brightness measurements of Venus. Firstly, there are no published brightness measurements of that planet in these filters. Such values may help us better understand its atmosphere and heat budget. Secondly, part of the J filter bandwidth penetrates near the surface. Therefore, it can serve as a probe into that planet's atmosphere near the surface. Thirdly, the day side of the Venusian atmosphere may also undergo brightness changes similar to that of the deeper layers on the night side. Finally, J and H filter measurements of Venus may help us to better understand exoplanets. Astronomers have begun making J and H filter magnitude measurements of hot exoplanets. Wagner et al. (2016) summarize a few J and H filter measurements of exoplanets.

Methods and Materials

All brightness measurements were made with an SSP-4 photometer and filters transformed to the Mauna Kea J and H system (Optec, 2005), (Simons & Tokunaga, 2002). Tokunaga, Simmons, & Vacca (2002) describe the transmission versus wavelengths for the J and H filters along with transformation corrections. Tokunaga and Vacca (2005) summarize flux densities for the J and H filters for the star Alpha Lyrae. A 0.09-m Maksutov telescope and a Celestron CG-5 mount were also used in making brightness measurements. The photometer field of view with this telescope was 6.9 arcminutes (Optec, 1997).

Henden (2002) presents a list of J and H magnitude values for 53 bright stars. This was the source of comparison and check-star magnitude values. The comparison star for Venus measurements was either Alpha Aurigae, Alpha Boötis, or Alpha Lyrae. In a few cases, check stars were used. Mean brightness values of comparison and check-star magnitudes in 2014 and 2016 were consistent to within 0.04 magnitudes.

Transformation coefficients were measured as $\varepsilon_J = 0.0443$ and $\varepsilon_H = 0.0151$ for 2014; $\varepsilon_J = 0.107$ and $\varepsilon_H = 0.056$ for 2015, and $\varepsilon_J = 0.057$ and $\varepsilon_H = 0.006$ for 2016. These values were measured using the star-pair method in Hall and Genet (1988). Transformation corrections were less than 0.10 magnitudes.

Extinction corrections were almost always measured for each day. The mean extinction coefficients, in magnitudes/air mass, for Barnesville, Georgia (elevation = 250 m) are $k_J = 0.103$ and $k_H = 0.082$. These mean values are for one year starting on 2014 April 26. The standard deviations, in magnitudes/air mass, are 0.05 and 0.06 for the J and H filters, respectively.

There are at least four sources of uncertainty for each Venus measurement. These are from 1) comparison-star magnitude values, 2) atmospheric extinction, 3) colour transformation, and 4) random changes. Each of these is described.

The stars in Henden (2002) are reported to have an accuracy of 0.01 magnitudes. He, however, points out that his list could be further refined for the specific filter set for the SSP-4. Schmude (2000), and references cited there, mention that Alpha Boötes is probably a micro-variable. The variability is believed to be below 0.02 magnitudes. Therefore, an uncertainty of $U_c = 0.02$ magnitudes is selected for the comparison-star magnitude values.

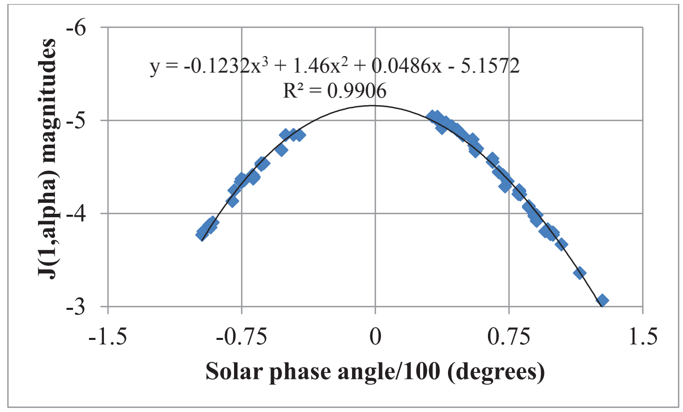

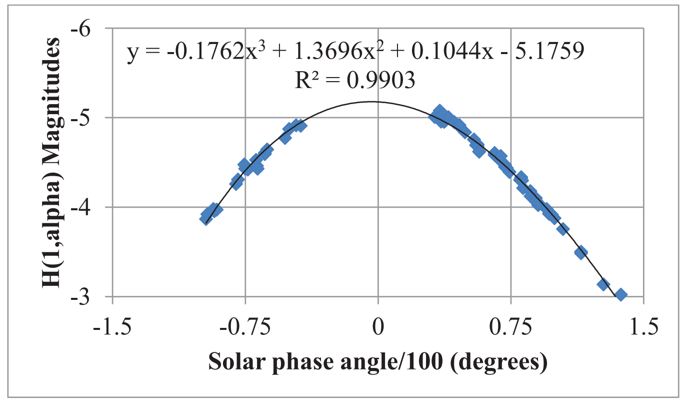

Figure 2 — J (top) and H filter (bottom) values are fitted to cubic equations according to Model 1 in Table 3. The solar phase angle, a, is the angle between the Sun and the observer measured from the centre of Venus. In the equations, y represents either J(1,a) or H(1,a) and x represents a/100.

A second source of uncertainty is atmospheric extinction (U_e). All-sky photometry was almost always used. As a result, extinction corrections of 0.2 to 0.3 magnitudes were the norm. In some cases, like late July 2015, extinction corrections were larger. The estimated mean uncertainty caused by extinction is 0.06 magnitudes for the J filter and 0.05 magnitudes for the H filter.

A third source of uncertainty is colour transformation (U_{tr}). Typical transformation corrections were 0.04 and 0.02 magnitudes for the J and H filters, respectively. Since the transformation coefficients fluctuated between 2014 and 2016, estimated mean uncertainties of 0.03 and 0.015 magnitudes are selected for the J and H filters, respectively.

A final source of uncertainty (U_r) is from random fluctuations in the signal. This may arise from detector noise, or from seeing, or some other random event. Mean random fluctuations in early 2016 were 0.016 and 0.006 magnitudes for the J and H filters, respectively. These values are selected for U_r.

The total uncertainty for each measurement (U) is the square root of the sum of the squares of each source of uncertainty which is:

$$U = (U_c^2 + U_e^2 + U_{tr}^2 + U_r^2)^{1/2} \quad (1)$$

The uncertainty of each J and H filter measurement is 0.08 and 0.06 magnitudes, respectively.

Brightness measurements are reported in magnitudes. The magnitude in the J and H filters are equivalent to light flux and may be determined from the list of standard stars in Henden (2002). Tokunaga and Vacca (2005) describe flux densities for the J and H filters.

Results

The J and H filter measurements are summarized in Tables 1 and 2. All measurements were corrected for atmospheric extinction and colour transformation. The solar phase angle of Venus along with both the Venus–Earth and Venus–Sun distances affect brightness. The normalized magnitude of Venus for the J filter, J(1,α), is the value that planet would have if it was 1.0 astronomical unit (au) from both the Earth and Sun at a solar phase angle α. To compute this quantity, equation 2 is used

$$J(1,\alpha) = J - 5\ \mathrm{Log}(r\ \Delta) \quad (2).$$

In this equation, J is the measured magnitude, r is the Venus–Sun distance and Δ is the Venus–Earth distance. Both r and Δ are in astronomical units. The H(1,α) values are computed in the same way. The advantage of computing J(1,α) and H(1,α) values is that brightness changes caused by changing distances are eliminated.

Both the J(1,α) and H(1,α) values depend on the value of a. This is the solar phase angle and is the angular distance between the observer and the Sun measured from the centre of Venus. It can range from 0° to 180°. To determine if there is change between waxing and waning phases for a given value of a, it was decided to follow initially a sign convention for the solar phase angle. Essentially, if the phase is waning (growing thinner) a is positive; otherwise it is negative. The values of J(1,α) were fit to a cubic equation of the form:

$$J(1,\alpha) = J(1,0) + a(\alpha/100) + b(\alpha/100)^2 + c(\alpha/100)^3 \quad (3)$$

Where J(1,0) is the normalized magnitude when a = 0°, and a, b, and c are coefficients to be determined through a least-squares routine. Figure 2 shows J(1,α) plotted against α. The fit is considered to be good with $R^2 = 0.9906$. A similar fit to equation 3 was carried out for H(1,α). The results are also presented in Figure 2.

One objective of this study is to determine if there is any brightness change based on whether the phase is waxing or waning. Accordingly, the difference between the model value for the J filter and each measured value was determined for α <0° and α >0°. The mean discrepancy (y) and standard deviation (s) were computed for all points with a <0. This was repeated for all points with a >0. The corresponding values for the J filter are listed in Table 3. This was also done for the H filter. A t-test was then carried out on the J- and H-filter data to see if there is any statistical difference between positive and negative phase angles. As it turns out, there is no statistical difference between the predicted minus observed values for positive and negative phase angles at the 90 percent confidence level for the two filters (Larson & Faber, 2006) for the standard deviations in Table 3. An experiment with lower standard deviations may yield a difference for brightness values between positive and negative phase angles.

Discussion

Preliminary photometric models for the J and H filter are presented for Venus covering phase angles between 32.0° and 137.2° (J filter) and 32.0° and 138.7° (H filter). A cubic equation may not work well at high phase angles. Mallama et al. (2006) report that Venus brightens, in the V filter, at phase angles above ~165°. This group attributes this to forward-scattered light from droplets of sulfuric acid. A similar brightening may take place for near-infrared wavelengths.

It was decided to fit the data to other mathematical models. These fits could yield an approximate uncertainty for the J(1,0) and H(1,0) values. These different models are described in Table 4. Model 1 has already been described. Model 2 is the same as Model 1 except that a quadratic equation is used for fitting. Cubic and quadratic equations are used for Models 3 and 4, respectively, to fit the data with all α values being positive regardless of Venus having a waxing or waning phase. In Models 5 and 6, a geometry term, –2.5 log(k) is added as described in equations (4) and (5):

$$J(1,\alpha)' = J - 5\mathrm{Log}(r\ \Delta) - 2.5\mathrm{Log}(k) \quad (4)$$

$$H(1,\alpha)' = J - 5\mathrm{Log}(r\ \Delta) - 2.5\mathrm{Log}(k) \quad (5)$$

where k is computed from:

$$k = \frac{\mathrm{Cosine}(\alpha) + 1}{2} \quad (6).$$

In equation 6, a is the solar phase angle. The J(1,α)′ and H(1,α)′ darken as a increases only because of phase darkening and not because of changes in geometry. In Model 5, the J(1,α)′ is plotted against a and a linear equation is computed. The H(1,α)′ values are treated in the same way. In Model 6, a quadratic fit is carried out instead of a linear one. The resulting equations, normalized magnitudes at α = 0º and standard errors of estimate (SE), are summarized in Table 5.

A close examination of the selected V, R, and I "polynomial fit coefficients" in Mallama et al. (2006) shows that Venus brightens by 0.24, 0.32, and 0.13 magnitudes as the solar phase angle drops from 32° to 0°. The mean difference is 0.23 magnitudes. If we assume that Venus brightens by 0.23 magnitudes as the solar phase angle drops from 32.0° to 0° and

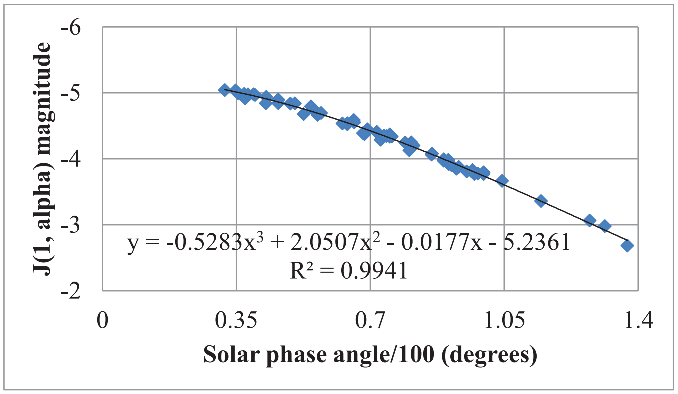

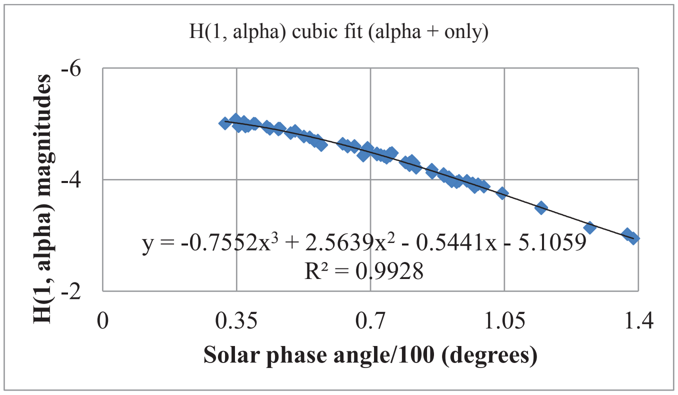

Figure 3 — Selected cubic equations for the J and H filter brightness of Venus. The absolute values of all phase angles are plotted in the graphs above. The quantity α is defined in Figure 2. In the equations, y represents either J(1,α) or H(1,α) and x represents α/100.

start with the measured J(1,32°) and H(1,32°) values in Tables 1 and 2, then J(1,0) = –5.27 and H(1,0) = –5.24.

The values of J(1,0) and H(1,0) are somewhat uncertain. They require extrapolation and are dependent on which model is used. An uncertainty of 0.14 magnitudes is selected. Essentially this is the standard deviation of the six values presented in Table 5.

Model 3 is selected for both filters because it has nearly the lowest standard error of estimate and because it yields values of J(1,0) and H(1,0) values near the mean values of the six models. Figure 3 illustrates the data and the selected cubic equations (Model 3)

Table 6 lists photometric constants for Venus for solar phase angles of 0°, 60°, and 120° based on Model 3. The uncertainties at a = 0° are larger because the values are extrapolated. ✶

Acknowledgements

The writer would like to thank Gordon State College for a Faculty Development Grant which enabled him to purchase the SSP-4 photometer. He is also grateful to the library staff at Gordon State College for their assistance.

References

Allen, D. A., & Crawford, J. W. (1984). Cloud structure on the dark side of Venus. *Nature, 307*, 222–224.

Basilevsky, A. T., Shalygin, E. V., Titov, D. V., Markiewicz, W. J., Scholten, F. Roatsch, T., Michalik, H. (2012). Geologic interpretation of the near-infrared images of the surface taken by the Venus Monitoring Camera, Venus Express. *Icarus, 217*, 434–450. doi: 10.1016/j.icarus.2011.11.003

Bézard, B., de Bergh, C., Crisp, D., & Mallard, J-P. (1990). The deep atmosphere of Venus revealed by high-resolution nightside spectra. *Nature, 345*, 508–511.

Carlson, R. W., Baines, K. H., Girard, M., Kamp, L. W., Drossart, P., Encrenaz, T., & Taylor, F. W. (1993). Galileo/NIMS near-infrared thermal imagery of the surface of Venus-[Abstract] 24th Lunar & Planetary Science Conference, Part 1: A-F p. 253, abstract retrieved from adsabs.harvard.edu/abs/1993LPI….24..253C

Hall, D. S., & Genet, R. M. (1988). Photoelectric Photometry of Variable Stars, 2nd ed. Richmond, VA: Willmann–Bell Inc., p. 200.

Harris, D. L. (1961). Photometry and Colorimetry of Planets and Satellites. In G. P. Kuiper and B. M. Middlehurst (eds.), Planets and Satellites (pp. 272 – 342). Chicago, IL: The University of Chicago Press.

Henden, A. A. (2002). JHK Standards for Small Telescopes. *Journal of the American Association of Variable Star Observers, 31*, 11–20.

Kuiper, G. P. (1952). The Atmospheres of the Earth and Planets, rev. ed., Chicago, IL: The University of Chicago Press, pp. 306-405.

Larson, R., & Farber, B. (2006). Elementary Statistics, 3rd ed., Upper Saddle River, NJ: Pearson Education, Inc., pp. 416-418.

Mallama, A., Wang, D., & Howard, R. A. (2006). Venus phase function and forward scattering from H_2SO_4. *Icarus, 182*, 10–22. doi: 10.1016/j.icarus.2005.12.014

McGouldrick, K., Momary, T. W., Baines, K. H., & Grinspoon, D. H. (2012). Quantification of middle and lower cloud variability and mesoscale dynamics from Venus Express/VIRTIS observations at 1.74 µm. *Icarus, 217,* 615-628. doi: 10.1016/j.icarus.2011.07.009

Mueller, N. T., Helbert, J., Erard, S., Piccioni, G., & Drossart, P. (2012). Rotation period of Venus estimated from Venus Express VIRTIS images and Magellan altimetry. *Icarus, 217*, 474–483. doi: 10.1016/j.icarus.2011.09.026

Optec, Inc. (1997). Model SSP-3 Solid-State Stellar Photometer Technical Manual for Theory of Operation and Operating Procedures, Lowell, MI, Appendix B.

Optec, Inc. (2005). Model SSP-4 Solid-State Infrared Photometer Technical Manual for Theory of Operation and Operating Procedures, Lowell, MI.

Pollack, J. B., Erickson, E. F., Witteborn, F. C., Chuckerian, C. Jr., Summers, A. L., Van Camp, W., Caroff, L. J. (1974). Aircraft Observations of Venus' Near-Infrared Reflection Spectrum:Implications for Cloud Composition. *Icarus, 23*, 8–26.

Roddier, F., Roddier, C., Brahic, A., Dumas, C., Graves, J. E., Northcott, M. J., & Owen, T. (2000). Adaptive Optics Observations of Saturn's Ring Plane Crossing in August 1995. *Icarus, 143,* 299-307. doi: 10.1006/icar.1999.6251

Schmude, R. W. Jr. (2000). Photoelectric Magnitude Measurements of Mars Made During the 1998–2000 Apparition, *JRASC, 94*, 241–245.

Simons, D. A., & Tokunaga, A. (2002). The Mauna Kea Observatories Near-Infrared Filter Set. I. Defining Optimal 1–5 Micron Bandpasses. *Publications of the Astronomical Society of the Pacific, 114*, 169–179.

Taylor, F. W. (2014). *The Scientific Exploration of Venus*, Cambridge: Cambridge University Press.

Tokunaga, A. T., Simons, D. A., & Vacca, W. D. (2002). The Mauna Kea Observatories Near-Infrared Filter Set. II. Specifications for a New JHKL′M′ Filter Set for Infrared Astronomy. *Publications of the Astronomical Society of the Pacific, 114*, 180–186.

Tokunaga, A. T., & Vacca, W. D. (2005). The Mauna Kea Observatories Near-Infrared Filter Set. III. Isophotal Wavelengths and Absolute Calibration. *Publications of the Astronomical Society of the Pacific, 117*, 421–426.

Wagner, K., Apai, D., Kasper, M., Kratter, K., McClure, M., Robberto, M., & Beuzit, J.-L. (2016). Direct imaging discovery of a Jovian exoplanet within a triple-star system. *Science, 353*, 673–678.

Table 1 — J filter measurements of Venus during 2014 to early 2016

Date	α (deg.)	Magnitude Meas.	Magnitude J(1,α)	Date	α (deg.)	Magnitude Meas.	Magnitude J(1,α)
May 5.403, 2014	−68.5	5.03	4.37	Jun. 5.075, 2015	89.2	5.39	3.98
May 6.409	−68.1	5.04	4.39	Jun. 5.108	89.2	5.38	3.97
Jan. 28.990, 2015	32.0	4.82	5.04	Jun. 7.056	90.4	5.44	3.98
Feb. 5.995	34.8	4.87	5.04	Jun. 7.093	90.5	5.38	3.92
Feb. 8.008	35.5	4.83	4.99	Jun. 14.063	95.2	5.45	3.81
Feb. 12.008	37.0	4.85	4.98	Jun. 16.058	96.6	5.51	3.82
Feb. 13.008	37.3	4.79	4.92	Jun. 16.093	96.7	5.52	3.83
Feb. 15.008	38.0	4.87	4.98	Jun. 18.078	98.1	5.52	3.78
Feb. 19.015	39.5	4.90	4.98	Jun. 20.056	99.6	5.57	3.77
Feb. 20.017	39.9	4.90	4.97	Jun. 20.090	99.6	5.60	3.80
Feb. 28.006	42.8	4.93	4.94	Jun. 26.056	104.4	5.65	3.67
Mar. 8.019	45.9	4.95	4.89	Jul. 7.067	114.6	5.70	3.36
Mar. 8.029	45.9	4.96	4.90	Jul. 18.077	127.3	5.78	3.07
Mar. 16.024	49.1	4.97	4.84	Jul. 21.051	131.3	5.79[a]	2.98
Mar. 29.034	54.5	5.07	4.80	Jul. 25.059	137.2	5.64[a]	2.69
Mar. 31.070	55.4	5.03	4.73	Oct. 14.427	−97.2	5.57	3.77
Apr. 2.017	56.2	4.99	4.67	Oct. 15.426	−96.5	5.59	3.81
Apr. 2.048	56.2	5.01	4.69	Oct. 20.407	−93.1	5.53	3.88
Apr. 4.030	57.1	5.04	4.70	Oct. 21.406	−92.5	5.48	3.85
Apr. 23.032	65.7	5.18	4.59	Oct. 23.429	−91.2	5.48	3.90
Apr. 23.060	65.8	5.15	4.55	Nov. 11.419	−80.2	5.30	4.13
Apr. 30.057	69.2	5.15	4.44	Nov. 13.450	−79.1	5.37	4.25
Apr. 30.095	69.2	5.15	4.45	Nov. 20.448	−75.6	5.33	4.34
May 5.086	71.7	5.20	4.41	Nov. 21.437	−75.1	5.35	4.37
May 5.107	71.7	5.19	4.41	Nov. 21.467	−75.1	5.31	4.33
May 7.092	72.7	5.11	4.29	Nov. 24.445	−73.6	5.28	4.36
May 10.070	74.2	5.22	4.35	Dec. 4.454	−68.9	5.17	4.41
May 21.046	80.2	5.29	4.21	Dec. 15.453	−64.0	5.12	4.52
May 22.063	80.7	5.35	4.25	Dec. 15.470	−64.0	5.13	4.54
May 22.095	80.8	5.34	4.24	Dec. 19.453	−62.7	5.09	4.54
May 23.063	81.3	5.32	4.20	Jan. 12.483, 2016	−52.6	4.93	4.68
May 31.051	86.0	5.36	4.07	Jan. 18.487	−50.3	5.02	4.84
May 31.085	86.1	5.37	4.08	Jan. 30.461	−45.9	4.91	4.84
Jun. 5.068	89.2	5.41	3.99	Feb. 8.466	−42.7	4.83	4.84

Note. The angle between the Sun and observer measured from the centre of Venus is designated as α. It is negative for waxing phases and positive for waning phases. [a]Only two measurements made; clouds prevented the third measurement.

Table 2 — H filter measurements of Venus during 2014 to early 2016

Date	α (deg.)	Magnitude Meas.	Magnitude J(1,α)	Date	α (deg.)	Magnitude Meas.	Magnitude J(1,α)
May 5.415, 2014	−68.5	5.12	4.46	Jun. 5.058, 2015	89.1	5.51	4.10
May 6.426	−68.1	5.07	4.43	Jun. 5.085	89.2	5.48	4.06
Jan. 29.004, 2015	32.0	4.79	5.01	Jun. 5.096	89.2	5.49	4.07
Feb. 6.011	34.8	4.91	5.08	Jun. 7.071	90.4	5.48	4.02
Feb. 7.994	35.5	4.80	4.96	Jun. 7.081	90.5	5.50	4.05
Feb. 11.994	36.9	4.91	5.04	Jun. 14.074	95.2	5.62[b]	3.98
Feb. 12.994	37.3	4.83	4.95	Jun. 16.073	96.6	5.62	3.93
Feb. 14.994	38.0	4.86	4.97	Jun. 16.111	96.7	5.62	3.93
Feb. 18.997	39.5	4.93	5.01	Jun. 18.059	98.1	5.66	3.92
Feb. 19.999	39.9	4.93	5.00	Jun. 20.072	99.6	5.68	3.88
Feb. 28.022	42.9	4.94	4.95	Jun. 26.069	104.4	5.74[b]	3.76
Mar. 8.006	45.9	4.96	4.90	Jul. 7.078	114.6	5.84	3.50
Mar. 8.042	45.9	4.98	4.92	Jul. 7.090	114.6	5.82	3.49
Mar. 16.009	49.1	4.97	4.84	Jul. 18.066	127.3	5.85	3.14
Mar. 28.038	54.1	5.02	4.76	Jul. 25.049	137.1	5.97	3.02
Mar. 31.058	55.4	4.99	4.69	Jul. 26.051	138.7	5.93[a]	2.95
Apr. 2.031	56.2	5.02	4.70	Oct. 14.412	−97.2	5.67	3.87
Apr. 2.060	56.2	5.00	4.68	Oct. 15.412	−96.5	5.70	3.92
Apr. 4.018	57.1	4.97	4.62	Oct. 20.422	−93.1	5.63	3.98
Apr. 4.047	57.1	4.96	4.62	Oct. 21.422	−92.5	5.58	3.96
Apr. 23.044	65.8	5.18	4.59	Oct. 23.419	−91.2	5.55	3.97
Apr. 23.072	65.8	5.20	4.61	Nov. 11.440	−80.2	5.42	4.26
Apr. 30.067	69.2	5.22	4.52	Nov. 13.421	−79.1	5.43	4.31
Apr. 30.106	69.2	5.28	4.57	Nov. 20.417	−75.6	5.47	4.48
May 5.074	71.7	5.24	4.45	Nov. 21.426	−75.1	5.44	4.47
May 5.097	71.7	5.26	4.47	Nov. 21.450	−75.1	5.41	4.43
May 7.102	72.7	5.26	4.44	Nov. 24.433	−73.6	5.35	4.42
May 10.080	74.2	5.27	4.40	Dec. 4.440	−68.9	5.29	4.53
May 21.057	80.2	5.39	4.31	Dec. 15.431	−64.0	5.20	4.61
May 22.049	80.7	5.42	4.32	Dec. 15.481	−64.0	5.19	4.59
May 22.078	80.8	5.44	4.34	Dec. 19.438	−62.7	5.20	4.65
May 23.047	81.3	5.42	4.30	Jan. 12.471, 2016	−52.6	5.02	4.78
May 24.051	81.9	5.36[a]	4.21	Jan. 18.472	−50.3	5.06	4.88
May 31.065	86.0	5.47	4.18	Jan. 29.469	−46.3	4.99	4.92
May 31.106	86.1	5.42	4.13	Feb. 5.469	−43.7	4.92	4.91

Note. α *is defined in Table 1.* [a]*Thin clouds present.* [b]*Only two measurements made; clouds prevented a third set from being made.*

Table 3 — Statistical information for the equations plotted in Figure 2

J filter		H filter	
α > 0	α < 0	α > 0	α < 0
y = 0.002155	y = –0.00825	y = 0.002662	y = –0.00653
s = 0.049824	s = 0.050587	s = 0.046746	s = 0.050625
n = 48	n = 21	n = 48	n = 21

Note. The mean discrepancy between each point and the equation in Figure 2 has the symbol y; the standard deviation and number of data points are s and n.

Table 4 — Description of the six photometric models used for Venus

Model	Description
1	Solar phase angles are positive for waning phases and negative for waxing phases. The J(1,α) versus α and H(1,α) versus α values are fitted to a cubic equation.
2	Solar phase angles are positive for waning phases and negative for waxing phases. The J(1,α) versus α and H(1,α) versus α values are fitted to a quadratic equation.
3	All solar phase angles are positive. The J(1,α) versus α and H(1,α) versus α values are fitted to a cubic equation.
4	All solar phase angles are positive. The J(1,α) versus α and H(1,α) versus α values are fitted to a quadratic equation.
5	The J(1,α)′ versus α and H(1,α)′ versus α values are fitted to a linear equation.
6	The J(1,α)′ versus α and H(1,α)′ versus α values are fitted to a quadratic equation.

Note. J(1,α) = J – 5Log(r Δ), H(1,α) = H – 5Log(r Δ), J(1,α)′ = J – 5Log(r Δ) – 2.5Log(k) and H(1,α)′ = H – 5Log(r Δ) – 2.5Log(k). In these equations J and H are the measured J and H filter magnitudes, r equals the Venus–Sun distance in astronomical units (au), Δ equals the Venus–Earth distance in au and k is the fraction of Venus's disk which is illuminated by the Sun as seen from the Earth.

Table 5 — The values of J(1,0) and H(1,0) predicted from the six models.

J filter

Model	J(1,0)	SE	Equation
1	–5.16	0.050	$J(1,\alpha) = -5.157 + 0.0486(\alpha/100) + 1.46(\alpha/100)^2 - 0.1232(\alpha/100)^3$
2	–5.1	0.050	$J(1,\alpha) = -5.112 - 0.0379(\alpha/100) + 1.3723(\alpha/100)^2$
3	–5.24	0.040	$J(1,\alpha) = -5.236 - 0.0177(\alpha/100) + 2.0507(\alpha/100)^2 - 0.5283(\alpha/100)^3$
4	–5.46	0.042	$J(1,\alpha) = -5.464 + 0.9784(\alpha/100) + 0.7398(\alpha/100)^2$
5	–5.38	0.039	$J(1,\alpha)' = -5.379 + 0.7395(\alpha/100)$
6	–5.34	0.039	$J(1,\alpha)' = -5.343 + 0.6127(\alpha/100) + 0.1002(\alpha/100)^2$

H filter

Model	H(1,0)	SE	Equation
1	–5.18	0.048	$H(1,\alpha) = -5.176 + 0.1044(\alpha/100) + 1.3696(\alpha/100)2 - 0.1762(\alpha/100)^3$
2	–5.11	0.062	$H(1,\alpha) = -5.107 - 0.0192(\alpha/100) + 1.2358(\alpha/100)^2$
3	–5.11	0.041	$H(1,\alpha) = -5.106 - 0.5441(\alpha/100) + 2.5639(\alpha/100)^2 - 0.7552(\alpha/100)^3$
4	–5.44	0.045	$H(1,\alpha) = -5.443 + 0.9149(\alpha/100) + 0.6647(\alpha/100)^2$
5	–5.32	0.042	$H(1,\alpha)' = -5.323 + 0.5669(\alpha/100)$
6	–5.30	0.042	$H(1,\alpha)' = -5.299 + 0.4868(\alpha/100) + 0.0632(\alpha/100)^2$

Note. J(1,α), H(1,α), J(1,α)′ and H(1,α)′ are defined in Table 4 while α is defined in Table 1. In models 3–x6 α is always positive.
The J(1,0) and H(1,0) and SE values are in stellar magnitudes.

Table 6 — Photometric constants of Venus

Parameter	Solar phase angle – α (degrees)		
	α = 0°	α = 60°	α = 120°
J(1,α)	–5.24 ± 0.14	–4.62± 0.05	–3.22 ± 0.05
H(1,α)	–5.11 ± 0.14	–4.67 ± 0.05	–3.37 ± 0.05
V – J	0.85 ± 0.15	1.01 ± 0.07	–1.01 ±0.07
J – H	–0.13 ± 0.2	0.05 ± 0.07	0.15 ± 0.07
Geometric albedo, J	0.54 ± 0.07[a]	– – –	– – –
Geometric albedo, H	0.36 ± 0.05[a]	– – –	– – –

Note. J(1,α) and H(1,α) are defined in Table 4 and α is defined in Table 1. The V – J values are computed by subtracting the J magnitude from the V magnitude. The J – H value is computed in a similar way. The J(1,α), H(1,α), V – J and J – H values are in units of stellar magnitudes.

[a]Geometric albedos are computed in the same way as in Mallama et al. (2006); the normalized magnitudes for the Sun were assumed to equal J(1,0) = –27.86 and H(1,0) = –28.17 (F. Roddier et al., 2000).

A Precise Measurement of a Perseid Meteor

by Michael Boschat and Andy Hasler, Halifax Centre (andromed@dal.ca; andyhasler@hotmail.com) and Jeremy B. Tatum, University of Victoria, (jtatum@uvic.ca)

Abstract

Two simultaneous photographs of a perseid meteor were obtained by separated observers in Nova Scotia in 2016. Measurement of these photographs enabled the beginning (100.1 km) and end (83.6 km) heights of the visible passage of the meteor to be determined.

Résumé

Deux photographies d'un météore provenant des perséïdes ont été obtenues simultanément par deux observateurs eloignés, en Nouvelle-Écosse en 2016. Des analyses de ces images ont permit de déterminer son altitude au début (100,1 km) et à la fin (83,6 km) de son passage visible.

Introduction

In November 2002, the first author, MB, and another member of the RASC Halifax Centre, Barry Burgess, initially unaware of each other's observations, successfully photographed a leonid meteor from separated locations. This led Bishop (2003) and later Tatum and Bishop (2005) to determine the height of the meteor.

History was repeated in June 2016 when MB and AH, again unaware of each other's observations, photographed a perseid meteor from separated locations. Only after they had posted their photographs on Facebook did they realize that they had photographed the same meteor. The images were also seen by Roy Bishop, who contacted JBT to see whether he might be interested in measuring the photographs and doing the necessary calculations. By some miracle, JBT found his detailed notes from 2002 on how to do the calculation, so he jumped at the chance. The only substantial difference between the 2002 and the 2016 observations is that the former were made on photographic film and were measured with a measuring microscope, whereas by 2016, time had moved on and the images were digital and were measured by computer.

In both cases, the two observers, while they had set out to photograph meteors, had not planned to photograph a single individual together. To that extent their success in doing so was fortuitous. In a later section of this article ("Future observations"), we point out that advance planning by two separated observers could substantially increase the chance of simultaneous photographs of an individual meteor.

The Observations

MB has been doing meteor observations for 41 years, sending data to amateurs in Canada, the U.S.A., and to Russia. He also monitors meteors by radio methods. Data from these observations are sent to Belgium and are put on the "Meteorobs" online group. AH has become interested in astronomy relatively recently (last six years) when he moved from Australia to Canada with his 12-year-old daughter Elli. They have been able to image some really special treats such as the Andromeda Galaxy, the Milky Way, Comet Lovejoy, transits of Jupiter's satellites, and watching Venus and Jupiter sink below the horizon while less than four arcminutes apart.

MB's observations were made from a stationary camera set up on a tripod in the parking lot of his apartment building, trying to avoid the security lights. He aimed towards the radiant for a better chance of recording a meteor, since the 50-mm lens is limited in sky coverage. The camera was a Canon 450D, with a 50-mm $f/1.8$ lens (not stopped down), ISO 400. An ISO of 800 made the sky too bright, and he had to stay within a 15-second exposure time.

AH, too, had to cope with light pollution. He and Elli set up their Canon T5I with a 50-mm lens on their Ioptron Smart equatorial mount, though the tracking was not turned on. Like MB, they set the ISO to 400, and used a 15-second unguided exposure.

The two images are shown here as Figures 1 and 2. The brightest star in each is b Andromedae, and readers will recognize the "fuzzy" object near the upper left of each photograph as the Andromeda Galaxy, M31. The meteor is moving from left to right. It is easy to see the different positions of the meteor with respect to the background stars on the two photographs. One cannot tell from a casual glance at the photographs, of course, whether the meteor is moving away from or toward the observer or more-or-less broadside on, but the subsequent measurement and analysis shows that it is in fact moving more-or-less towards the observer, the angle between the path of the meteor and the line of sight to the beginning (left-hand end) of the streak being very close to 30 degrees.

The Measurements

On each image (Boschat and Hasler), the x- and y-coordinates of 20 comparison stars surrounding the meteor path were measured. Twelve points along the meteor path were also measured on each image and a least-squares linear regression was computed for the path. Equatorial coordinates for the comparison stars were obtained from the *Sky Catalogue 2000.0* (Hirshfield and Sinnott 1982) and were precessed to refer them to the equinox and equator of date. The attainable precision of measurement did not warrant corrections for stellar proper motions or aberration of light. The equatorial coordinates were transferred to alt-azimuth coordinates by solution of the triangle PZX. Entirely necessary corrections for atmospheric refraction were made to the computed zenith distances. Standard coordinates for the comparison stars (i.e. their positions by gnonomic projection on to the tangential plane of the sky) were calculated in the usual fashion for astrometric plate reduction, except that altazimuth coordinates

Figure 1 — Michael Boschat's photograph of the meteor

Figure 2 — Andy Hasler's photograph of the meteor

rather than equatorial coordinates were used. To allow for possible barrel/pincushion distortion, a quadratic (rather than linear) relation was assumed between measured and standard coordinates in computing the plate constants.

The Computation

The foregoing completes the description of the measurement and reduction of the images. At this stage, the alt-azimuth coordinates of points along the path of the meteor were known. Two coordinate systems were used, which we refer to as boschatocentric B*xyz* and haslerocentric H*x′y′z′* systems, as illustrated schematically in Figure 3.

For each observer, the directions to two points on the meteor path define a plane containing the meteor and the observer. The eq uation to this plane for one observer (Boschat) is

$$\begin{vmatrix} x & y & z & 1 \\ \sin\theta_1\cos\phi_1 & \sin\theta_1\sin\phi_1 & \cos\theta_1 & 1 \\ \sin\theta_2\cos\phi_2 & \sin\theta_2\sin\phi_2 & \cos\theta_2 & 1 \\ 0 & 0 & 0 & 1 \end{vmatrix} = 0 \qquad (1)$$

with a similar equation with primed symbols for the second observer (Hasler). Here θ_1 and θ_2 are the zenith distances of two points along the track, and ϕ_1 and ϕ_2 are the corresponding azimuths counterclockwise from east.

We now erect a third, double-primed, system of coordinates, which are haslerocentric, but whose axes are parallel to the Boschat coordinate system. They are related by

$$\begin{pmatrix} x'' \\ y'' \\ z'' \end{pmatrix} = \begin{pmatrix} \cos\Phi & -\sin\Theta\sin\Phi & \cos\Theta\sin\Phi \\ 0 & \cos\Theta & \sin\Theta \\ -\sin\Phi & -\sin\Theta\cos\Phi & \cos\Theta\sin\Phi \end{pmatrix} \begin{pmatrix} x' \\ y' \\ z' \end{pmatrix} \qquad (2)$$

where Q = North latitude of Hasler *minus* north latitude of Boschat, and F = West longitude of Hasler *minus* west longitude of Boschat.

Finally, we need to express the equation to the Hasler plane in boschatocentric coordinates by replacing χ'' with $\chi - \Delta\chi$ and γ'' with $\gamma - \Delta\gamma$, where $\Delta\chi$ is $R\phi\cos\beta$ and $\Delta\gamma$ is $R\phi$. Here b is Boschat's north latitude, and *R* is the distance between the centre and the surface of Earth at latitude b. If we take the figure of the Earth to be an oblate spheroid of semi major and semi minor axes *a* and *b*, this is given by

$$R = \left(\frac{\cos^2\beta}{a^2} + \frac{\sin^2\beta}{b^2}\right)^{-1/2} = 6367.6 \text{ km}. \qquad (3)$$

I took Δz, estimated to be about 20 m, to be negligible for the purpose of this analysis.

The equations to the two planes, in Boschatocentric coordinates, were computed to be

$$0.687\,0679x + 0.119\,8658y - 0.716\,6379z = 0 \qquad (4)$$

and

$$0.674\,8127x + 0.139\,2132y - 0.724\,7396z + 1.721\,0870 = 0. \qquad (5)$$

These equations are normalized so that the coefficients are equal to the direction cosines of the normals to the planes, and the constant term is such that *x*, *y*, and *z* are to be expressed in km. The equations were tested for mistakes by ensuring that they satisfy the original coordinates, and the orthogonal sums of the coefficients are each unity.

These two equations between them represent the line of intersection of the two planes, and hence the path of the meteor. The distance between the two observers was just 2.6 km, and it will be observed, unsurprisingly, that these two equations are somewhat similar, the angle between the planes being only 1.4°. This somewhat limits the precision with which a final result can be attained, and it directs the subsequent computational strategy.

While it is possible in principle (Tatum 2007) to determine the apparent geocentric radiant (hereafter simply "the radiant") of a single meteor observed by separated observers, to do so with an acceptable degree of precision requires that the angle between the planes should be reasonably large. Trigo-Rodríguez et al. 2002 recommended at least 20° Numerical experiments with this meteor showed that making an error of one pixel in the measurement at each end of the meteor trail resulted in moving the computed radiant by a few degrees, while hardly affecting the computed height of the meteor. (To illustrate how very sensitive the line of intersection is to small changes in the planes, it might be remarked that, if two planes are inclined to each other at a very small angle, and if this angle be reduced, the special theory of relativity places no restriction on the speed at which the line of intersection can recede!)

That being so, it was decided that these observations should not be used in a doomed attempt to determine the radiant, but to use the known radiant as a fixed point in the computation (i.e. to assume as known the direction of travel of the meteor), and to use the observations to determine the height of the meteor at the beginning and end of its path. The position of the radiant moves slightly with time as Earth moves around the Sun in its orbit, and, from data supplied by Campbell-Brown and Brown (2016) and Mason (2016), the radiant was taken to be, at the time of the appearance of the meteor, RA (J2000.0) = $3^h\ 13^h$, Dec (J2000.0) = +37.9°. This necessitated artificially changing the measured position of each end of the meteor trail by 0.0005 rad = 1.7 arcmin = 1.5 pixels, which is within the variation (±2 pixels) of pixel number found from repeated measurements.

The distance r to a point in the direction (θ,ϕ) on the meteor trail can be found by substituting $(r \sin\theta \cos\phi, r \sin\theta \sin\phi, r \cos\theta)$ for (x, y, z) in equation (5), and the values of the (x, y, z) coordinates in km immediately follow.

An interesting check on the correctness of the arithmetic is to measure the positions of four points A, B, C, D along the track of the meteor in the sky and then to inspect the corresponding points in (x, y, z) coordinate system. By a well-known theorem from projective geometry, the cross-ratio

$$\frac{AC.BD}{BC.AD} \text{ is invariant.}$$

The z- coordinate is the height of the meteor above the tangent plane to Earth at Boschat's station B. The height h above the surface of Earth is a little greater. Figure 4 (in which ZD is the zenith distance of a point on the track) shows the geometry, from which h can readily be calculated

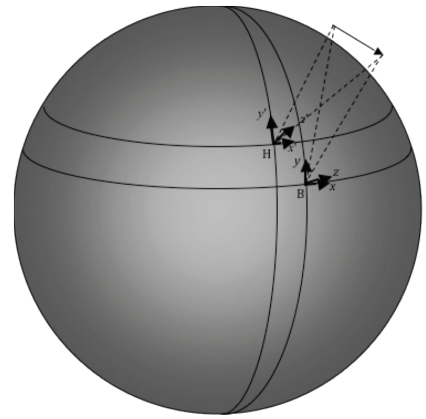

Figure 3 — Illustrating the coordinate systems used.

Uncertainties

The largest potential source of uncertainties results from the closeness (2.6 km) of the observers to each other. As described in the previous section, this makes it impossible to obtain a reliable position of the radiant, and therefore the position of the radiant, corrected for its hourly motion, was obtained from the two cited sources and was used as a fixed point in the calculations. The closeness of the observers, however, did not at all prevent a reliable calculation of the height of the meteor. Another source of uncertainty is the uncertainty in knowing the exact time of the event, which is thought to be known within an uncertainty of ±10 s. And, of course, there is also uncertainty in the measurements of the positions of the meteor and comparison stars on the image. Repeated settings on the star images suggested an uncertainty of not more than ±1 pixel (±1.1 arcmin), and ±2 pixels for settings on the meteor.

The effect of these uncertainties on the final computed position of the meteor was not difficult to estimate, because the entire calculation was, of course, completely coded for computer, and the possible range of times of the event and errors in the pixel settings were varied within plausible limits.

The estimated uncertainties are mainly as a result of the small distance between the observers rather than the uncertainty in the time. In the case of the Boschat–Burgess observation of a leonid meteor in 2002 (Tatum and Bishop 2005), the observers were separated by 49 km, and the uncertainty in the time was 30 s. In the present case, the observers were separated by 2.6 km, and the uncertainty in the time was about 10 s. The tracks in the two photographs are almost parallel, and are separated by a lateral displacement of about 21 arcmin. Thus a measurement error of one pixel (1.1 arcmin) introduces an appreciable error in the final result.

Results

The following table shows the results for two points on the meteor track, one point near the beginning, and one near the end.

x, y, z are the rectangular coordinates (east, north, and zenithal) in km from Boschat's station.

Continued on page 116

Pen & Pixel

Figure 1 —Ron Brecher imaged globular cluster M12 from his SkyShed in Guelph, Ontario, in 2014 using an SBIG STL-11000M camera, Baader LRGB filters, and a 10" ƒ/6.8 ASA astrograph on a Paramount MX. The final image is a stack of 8x10m R, 7x10m G, 7x10m B, 22x15m Luminance for a total of 8 hours and 40 minutes.

Figure 2 — Michael Gatto of the Halifax Centre painted this view of the"supermoon" rising over the town of Wolfville, Nova Scotia on 2016 November 13. Oil paint on board, 14 x 11", from an original photograph.

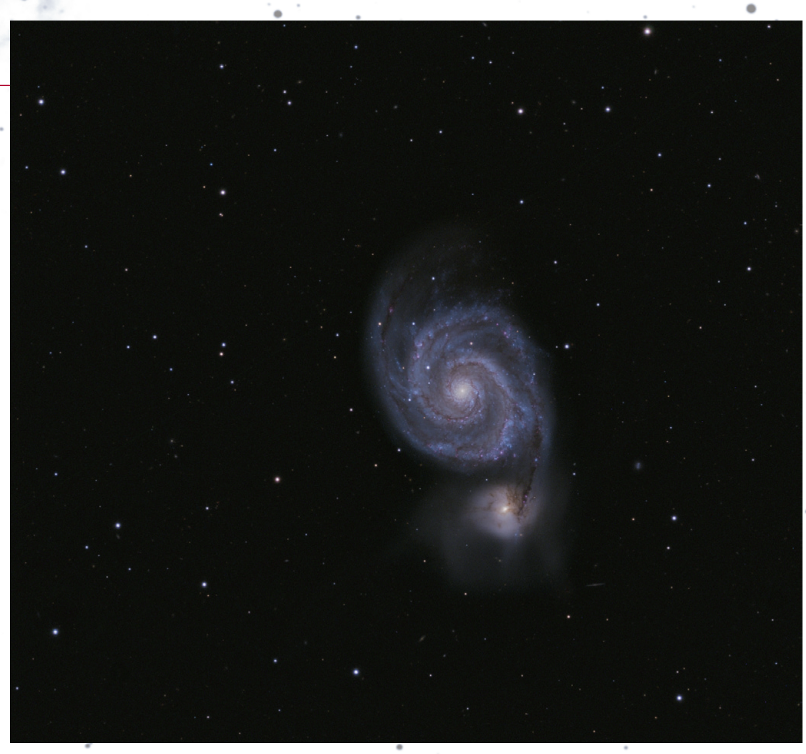

Figure 3 — Andre Paquette imaged beautiful M51 at the Barred Owl Observatory in Ottawa, Ontario. Paquette used an Apogee U16M camera on a Celestron Edge HD 14, mounted on a CGE Pro.

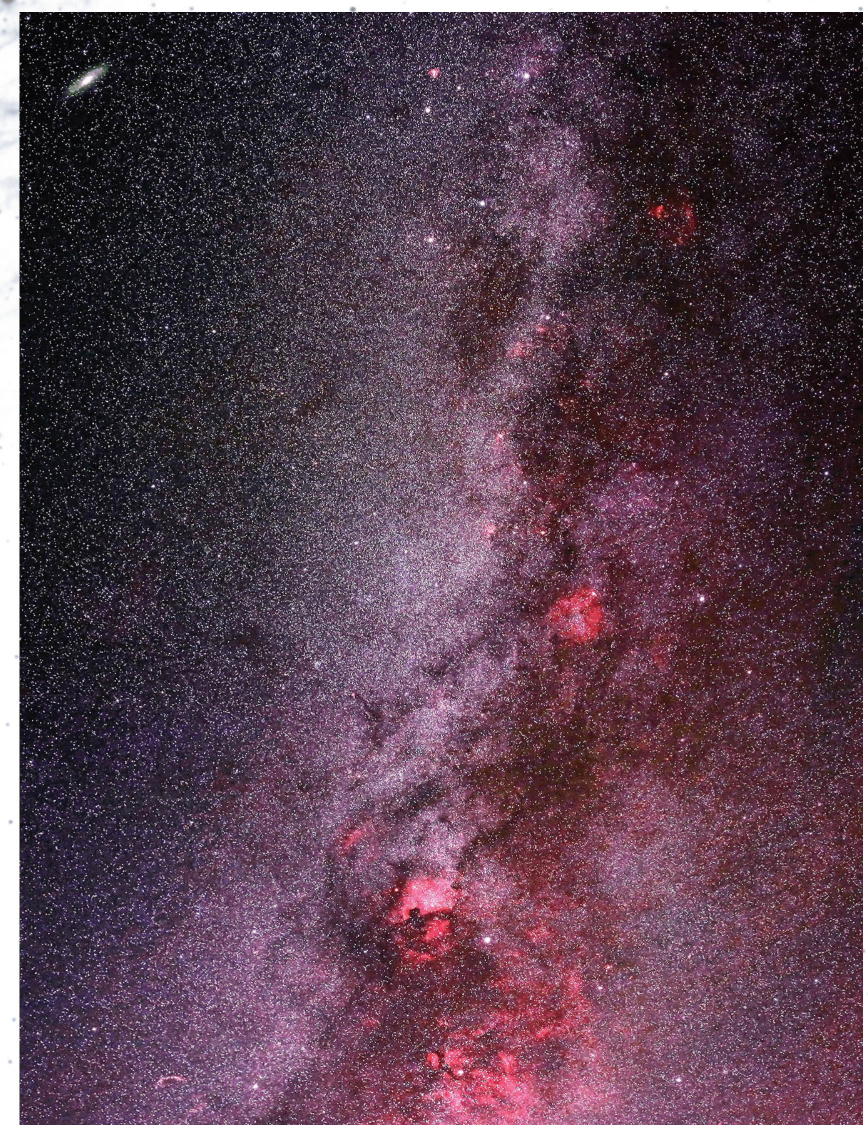

Figure 4 — Who doesn't love the Milky Way when we can see it? This image is a mosaic of several two-minute ISO 6400 exposures of the Milky Way from Cygnus to Cassiopeia, shot with a Canon 40-mm lens and Astronomik clip-in filter from one of our favourite dark sites near Wupatki National Monument near Flagstaff, Arizona, taken by Klaus Brasch. The Andromeda Galaxy can be seen at the top left.

Continued from page 113

long and lat are the west longitude and north latitude of the sub-meteor point, and ht is the height in km.

The estimated uncertainties in the distances (x, y, z) are about ±2.5 km. The estimated uncertainty in the longitudes is about 20 arcmin in longitude, and in latitude it is about 1.5 arcmin.

	x km	y km	z km
Beginning	100.7	16.4	99.3
End	86.5	0.6	83.0

	x km	y km	z km
Beginning	62° 28′.8	44° 46′.4	100.1
End	62° 39′.0	44° 39′.0	83.6

These figures refer to two points near the ends of the path that could be easily measured. In fact, the path of the meteor could be traced (but not accurately measured) slightly beyond these points. It was first detected at a height of about 106.1 km and last detected at a height of about 82.5 km.

The United Kingdom Meteor Observation Network reports 343 multi-station observations of perseid meteors in 2013 (UKMON 2013), showing a mean beginning height of 105.7 km and a mean end height of 92.7 km. While standard deviations are not given, an interesting graph on their website shows that the beginning and end heights of our meteor are well within the ranges given by UKMON.

We also show, in Figure 5, the projection of the track on the (x, y) plane, relative to the two observers (Boschat at the origin. Hasler is the dot to the left of the origin). The meteor is moving from right to left.

Comparison with the Boschat-Burgess 2002 leonid.

It is of interest to compare the beginning and end heights, in kilometres, of this perseid meteor with those of the 2002 Boschat-Burgess leonid (Bishop (2003), Tatum and Bishop (2005)).

	2016 perseid	2002 leonid
First detected	123	106.1
First measurement	112.16	100.1
Last measurement	80.77	83.6
Last detected	80.77	82.5

With just one meteor from each shower, there is little of statistical significance that can be gleaned from these two events. However, the perseid and leonid showers are both fast meteors (60 km s^{-1} and 71 km s^{-1} respectively (Campbell-Brown and Brown (2015)), since they are both meeting Earth more-or-less head on, and it is no surprise that their beginning and end heights are not greatly dissimilar.

Future observations

In the present case, and for the 2002 leonid, the two simultaneous photographs from separated locations were not planned and to some extent, therefore, were fortuitous. This does not mean that it was "luck"—the two skilled and experienced observers had each planned to photograph meteors, and did so successfully. However, the chances of two separated observers simultaneously photographing a single meteor could be substantially increased by consciously planning in advance to do so. For example, the observers could agree in advance to start each photograph at the same instants of time—for example at the beginning of each even-numbered minute. And the plan could also include agreeing to point their cameras in the same direction for each photograph pair. The UKMON website cited shows that, with suitable deliberate planning, hundreds of multi-station observations of a single shower can be obtained every year.

It is important to know the time of the meteor accurately. This is needed because the computer (by which we mean the person who does the calculations—in the present case JBT, certainly with the help of an electronic computer) needs to know the local sidereal time in order to convert equatorial coordinates to alt-azimuth coordinates. It should be not too difficult for each observer to record accurately (to the nearest second) the time when the shutter was opened, and the duration, in seconds, of the exposure. Recording the time of the actual meteor may be more challenging, but not impossible.

It is also important for the observers to supply the computer with the completely uncropped photograph, as they did in the present case. This is because the computer has to make a gnomonic projection of positions on the inside of the celestial sphere onto the tangent plane of the sky, and for this he or she has to know the position of the point where the celestial sphere osculates the tangent plane, i.e. the coordinates of the centre of the photograph.

While two observers are most likely to set up their cameras from where they live, it would nevertheless be desirable, as will be understood from the section on uncertainties, if the observers were a few tens of km apart.

It would be interesting if observers could obtain a pair of geminid meteors in December. Unlike the perseids and leonids, the geminids are overtaking Earth and are slow (35 km s^{-1}, Campbell-Brown and Brown (2015)). According to a graph cited on page 128 of McKinley (1961), beginning and end heights in the range 85 to 65 km are to be expected for bright meteors at this speed. McDonald and Dunkley (2015)

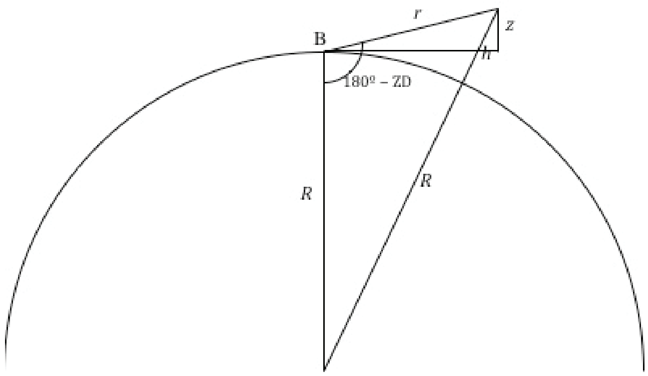

Figure 4 — Illustrating the coordinate systems used.

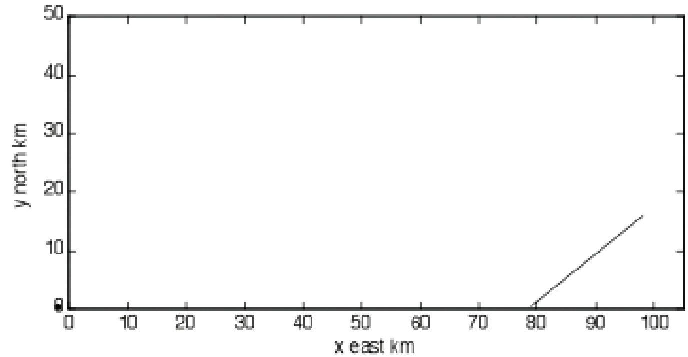

Figure 5 — Projection of the meteor trail on the x-y plane.

quote more recent data specifically for the geminid shower. Thus the UKMON site (UKMON 2013) gives average beginning and end heights for 436 multi-station Geminid observations in 2013 of 91.3 and 87.8 km, and Toth (2011) gives 96.4 and 84.2 km. A further difference between the geminids on the one hand, and the perseids and leonids on the other, is that the latter two are associated with comets (Swift–Tuttle and Tempel–Tuttle respectively), whereas the geminids are associated with an asteroid (3200 Phaethon, which admittedly may be an inactive comet), and the meteoric particles may have a different chemical composition, physical structure, or mass. A further factor that may influence the height of burnup of a meteor is the angle at which the meteoric particle enters the atmosphere. In the case of the perseid meteor of this investigation, the path of the meteor made an angle of 37.5° to the horizontal.

The paper describing the Boschat–Burgess leonid meteor (Bishop and Tatum, 2005) was titled *A Precise Measurement of a Leonid Meteor*. The present paper is *A Precise Measurement of a Perseid Meteor*. Observers, can we look forward soon to *A Precise Measurement of a Geminid Meteor*?

Final random and trivial thoughts

While writing this article, an idle thought occurred to one of the writers (JBT). The investigation described in this article is very much "old-fashioned" astronomy, and may appear to have little connection to modern-day "cutting-edge" research. And yet, maybe there is a connection. In "adaptive optics" we create an "artificial star" by directing a laser beam into the sky. This excites sodium atoms that are in a layer about 5 km thick at a height of about 90 km. So, where do these sodium atoms come from? We leave the reader to ponder.

The astute reader may have noticed that the words "perseid," "leonid" and "geminid" in this article have been written (by JBT!) with lower case initial letters. JBT writes that this follows the convention in biology. For example, it is conventional in biology that a moth in the family Noctuidae (with a capital N) is called a noctuid moth (with a small n).

There seems to be no compelling reason to use a different convention in another science, so, by analogy, it seems natural to refer to a meteor that radiates from the constellation Perseus (with a capital P) as a perseid meteor (with a small p).

Acknowledgments

The authors would like to thank Dr. Roy Bishop for his interest in this work, and for encouraging us to get together in our various roles to obtain the results here presented.

We also thank Matthias Le Dall for the French-language résumé.

References

Bishop, R.L. (2003), A Leonid Meteor. *JRASC, 97*, 128–131.
Campbell-Brown, M. & Brown, P. (2015), In *Observer's Handbook* of the RASC 2015.
Hirshfield, A. & Sinnott, R.W. (1982), *Sky Catalogue 2000.0 Volume 1*. Cambridge University Press.
Mason, J., (2016), In *Handbook of the British Astronomical Association 2016*.
McDonald, W.J. & Dunkley, R. (2015) Time-sequence Study of a Persistent Meteor Train, JRASC, 109: 101-107.
McKinley, D.W.R. (1961). *Meteor Science and Engineering*. McGraw-Hill.
Tatum, J.B. & Bishop, R.L. (2005). A Precise Measurement of a Leonid Meteor. *JRASC, 99*, 61-64.
Tatum, J.B. (2007), Where is the Radiant? *JRASC, 101*, 14 - 24.
Toth, I, *et al.* (2011), Video Observations of Geminids 2010 and Quadrantids by SVMN and CEmeNt. *WGN, the Journal of the IMO 39*,2.
Trigo-Rodríguez, J.M., Llorca, J., and Fabregat, J. (2002), On the Origin of the 1999 Leonid Storm as Deduced from Photographic Observations. *Earth, Moon and Planets, 91*, 107–119.
UK Meteor Observing Network Annual Report for 2013. www.ukmeteornetwork.co.uk/2014/05/ukmon-annual-report-2013

CFHT Chronicles

Venus, Student Scientists, and a New Addition

by Mary Beth Laychak, Outreach Program Manager, Canada-France-Hawaii Telescope.

Our very first column in this *Journal* chronicled a day in the life of a Sun watcher at CFHT. At the time, CFHT staff had just completed a series of observations for Thomas Widemann and Pedro Machado of Venus using Espadons. As we described in that first column, daytime Venus observations are scheduled very carefully; usually they occur when Venus is at its maximum elongation from the Sun. Those 2015 observations occurred in conjunction with another set of daytime Venus observations on the summit. The second observations were in the infrared and occurred at the Infrared Telescope Facility (IRTF). The opportunity to obtain simultaneous spectra in multiple wavelengths was too perfect an opportunity to pass up, even though Venus was closer to the Sun than ideal.

The 2015 observing run was not the first nor the last for Thomas, Pedro, and the team. On 2017 March 15, the team released a paper with some fascinating insights into the winds of Venus. The paper provides the first scientific evidence on Venus of wind between the equator and the poles. This wind, known as a meridonial wind, was discovered using data from Espadons and ESA's *Venus Express* spacecraft.

The team analyzed reflected sunlight off the cloud tops on Venus. They identified wind travelling perpendicular to the equator. This wind, with an average velocity of 81 km/h, is similar to the Hadley cells on Earth. Solar heating is greater at the equator than the poles, resulting in the circulation of warmer air away from the equator. This wind reduces the temperature difference between the equator and poles. On Earth, the Hadley cells exist on either side of the equator. The cells span the Earth between the equator and 30th latitude. As the air moves poleward in the tropopause, the Coriolis effect turns the air eastward, creating the subtropical jet streams. At the surface, the Coriolis effect turns the winds westward, creating the trade winds, winds well known and beloved in Hawaii for keeping the islands a pleasant temperature year round.

According to Mechado, "this detection is crucial to understand the transfer of energy between the equatorial region and the high latitudes, shedding light on a phenomenon that for decades has remained unexplained and which is the super-rotation of the Venus atmosphere." Astronomers are searching for a physical model to explain the super-rotation on Venus. The newly released data adds to the model by studying the wind parallel to the equator and how these winds change with time and latitude.

Figure 1 — Thomas, Pedro, and team observing Venus at summit

The team's success comes in part from a method they designed using visible light to measure the instantaneous speed of the wind on another planet from Earth-based telescopes. The method is based on the Doppler effect that the clouds cause on the reflected sunlight.

Understanding the weather of different planets is challenging, but important work. As astronomers learn more about other planets, we gain a greater understanding of Earth.

Student Scientists

In 2016, CFHT and Gemini piloted the Maunakea Scholars program for Hawaii high-school students. Students from two schools, Kapolei on Oahu and Waiakea on the Big Island, researched and wrote proposals for submission to CFHT to receive observing time for their own independent research. The students worked with mentors from the University of Hawaii's Institute for Astronomy and Gemini Observatory to refine their topics. Post submission, CFHT staff reviewed the proposals and selected three.

We expected proposals requesting time to take pretty pictures but received quite the opposite. Students requested time on all four of CFHT's instruments—Megacam, Wircam, Espadons, and Sitelle—and for deep topics ranging from comets to white holes and everything in between.

We selected the following proposals the first year:

"Exploring Star-Formation in the hosts of Radio Quiet Quasars" by Ana Bitter, Hannah Blue, Kylan Sakata, and Ramsey Hayashi using Megacam.

"Quasars and What They are Made of" by Jamie Valdez and David Zerba on Espadons

"Validating or Redefining Mischaracterized Unconfirmed Exoplanets" by Ashley Cobbs and Nevyn Tyau on Espadons.

Figure 2 — Kalani high school students outside EAO

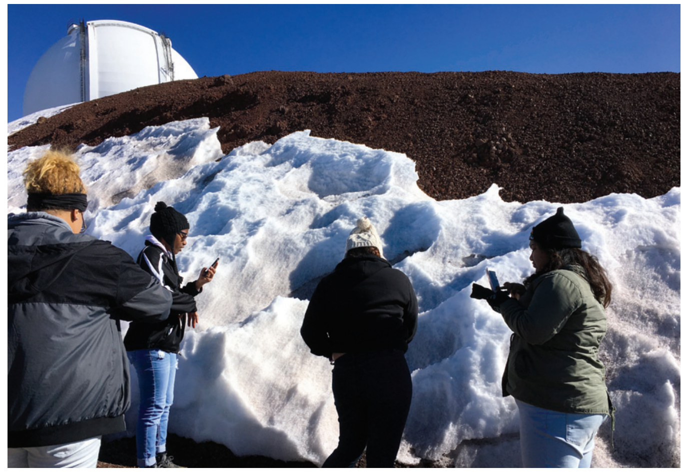

Figure 3 — Nanakuli students playing in the snow at the summit. It was the first time they've ever seen snow.

All of the students whose programs were selected operated the cameras themselves to take their observations from CFHT's remote observing room. All of the students in the class, program selected or not, had an opportunity to tour the summit. They visited CFHT and Gemini.

The impact of the program on the students was enormous. Jamie said she felt like she won a Grammy when her name was announced as one of the selected programs. She explained having her proposal reviewed and selected by professional astronomers boosted her confidence and made her believe she was capable of more than she previously thought.

After the success of the pilot year, the program expanded to five schools and seven telescopes in 2017. Three of the schools are located on Oahu—Kapolei, Kalani, and Nanakuli, along with two Big Island schools—Waiakea and Honokaa. Along with CFHT, Gemini, the East Asian Observatory (EAO), NASA's Infrared Telescope Facility (IRTF), Subaru Telescope, Robo-AO, and the Los Cumbres Observatory Global Telescope Network, all offered telescope time to the students. We also increased the number of mentors involved in the program, reaching out to seven UH graduate students.

The addition of the new schools brought new challenges. We created a few guidelines for ourselves as we expanded the program: the teacher/school decides how to fit the program into their curriculum, the project ideas are student driven and to balance the addition of Oahu schools with Big Island schools.

Leaving the placement of the program within the schools up to the teachers and administration resulted in several unexpected scenarios. Nanakuli and Honokaa both started astronomy clubs where the members worked on their proposals after school. Working with the clubs meant the students self-selected for an interest in astronomy and had more initial passion for the program. However, without the pressure of a grade or teacher-imposed deadlines, the number of students waxed and waned over the course of the year based on other commitments. In the end, we received high-quality, well-researched proposals from both groups. Interestingly, both clubs were comprised exclusively of female students, a trend that may warrant additional investigation.

At Waiakea high school, we worked with our largest group of students to date, two classes of roughly 20 each. The students were the opposite of those in the astronomy club; they took the science class because they needed it to graduate, not because of an interest in science, let alone astronomy. Over the course of the year, the students became very invested in their projects. The teachers noticed a change in their students because of the program. One of the teachers swelled with pride when the students started arguing over rain in space using science terms and rationalizations for their arguments. The proposals from these students were not as sophisticated as their counterparts at other schools, but they were creative, and concerned topics that deeply interested the students. When we announced the selected programs, the students were ecstatic. For many, it was the first time their academic work was recognized and rewarded.

When the CFHT review committee looks at the proposals, we look for three things: 1) feasibility. Can we do this proposal and in a reasonable amount of time? 2) creativity. Is this something interesting? and 3) is it student driven? Does the proposal read as though the student or students wrote it? Feasibility eliminates many of the proposals. Students have wildly creative ideas, which often are more complicated or time consuming than they anticipate. Several students proposed dark-matter surveys, programs that take years to do correctly. Several more students wanted to count supernovae. CFHT's supernova survey, which at its essence did the same, was a five-year survey. Last year, a team of students proposed using SITELLE to take the spectra/image of a globular cluster to look for stars within the globular containing different ratios of iron. A student this year wanted to measure the amount

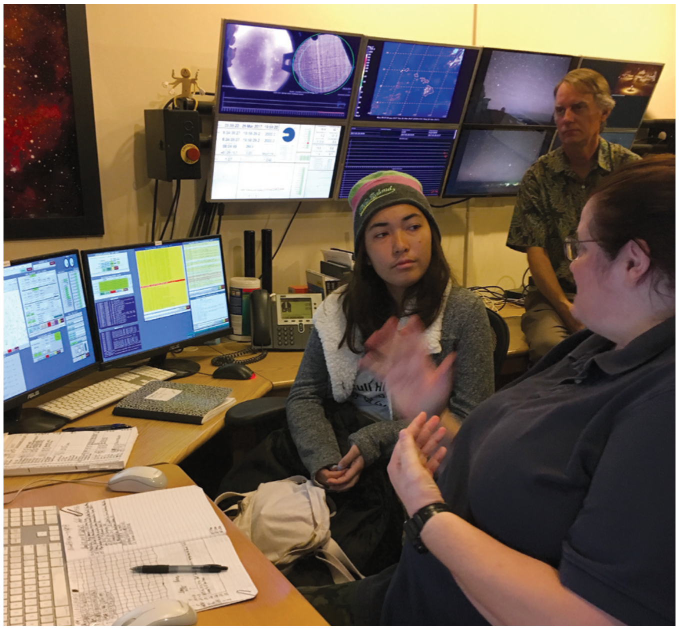

Figure 4 — Amber, her project is observing a binary black hole with Espadons, operating Megacam.

Figure 5 — CFHT's new resident Canadian astronomer—Laurie Rousseau-Nepton

of gold in a supernova remnant to estimate the number of supernovae needed to account for the Earth's gold. Both these proposals stretch the limits of what SITELLE can currently do.

This year's selected proposals run the gamut of astronomical research topics. Take a look for yourself:

"Eclipsing X-Ray Binary System" by Amber Nakata, Nanakuli. Amber will use Espadons at CFHT to observe the binary at three points over the next 6-9 months.

"Rogue Planets" by Jasmine Atcherson, Nanakuli. Jasmine received spectra from GNIRS at Gemini to observe an object that some astronomers classify as a brown dwarf, others as a rogue planet.

"Spectroscopy of Hydrogen Rich Exoplanet Atmsopheres" by Chantelle Lopez, Kapolei. Chantelle is also using GNIRS at Gemini. She will observe an exoplanet and compare its spectra with a previous observation looking for changes or weather.

"The Source of the Earth's Water" by Emily Little, Kapolei. Emily used Espadons at CFHT to observe Comet 45P in February to look for the make-up of the comet, particularly the D/H ratio.

"Comparing Elements in Different Supernova Remnants" by Ashlyn Takamiya and Justin Fernando, Kapolei. Ashlyn and Justin will use FOCAS at Subaru to compare the spectra of Type Ia and Type II supernova remnants.

"Orion Nebula" by Mason Mihkel and Marc Agpawa at Waiakea. Mason and Marc plan a multi-wavelength survey of the Orion Nebula using Megacam at CFHT. Their narrow-band filter selection will give the highest resolution images of Orion in H-alpha.

"Nebulas" by Thomas Pakani and Rylan Salvador, Waiakea. Thomas and Rylan will observe the nebula Sh2-261. It will be one of the potential 2018 CFHT calendar images.

"Exploring the Asteroid Belt" by Cicily Pa and Georgia Carter, Waiakea. Cicily and Georgia will use the Las Cumbres Observatory Global Telescope Network to observe an asteroid in an attempt to calculate its rotation rate.

"Globular Clusters" by Jordaynelexi Drasal, Kalani. Jordaynelexi used Megacam on CFHT to observe M92. She wants to use a colour-magnitude diagram to determine the age of the cluster.

"The Creation of the Moon" by David Higashi, Kalani. David used Espadons at CFHT to observe the surface of the Moon. David selected both maria and highlands to compare the composition of the two regions. His program advanced to the Hawaii State Science Fair.

"Star Forming Regions and how they retain their shapes" by Spence Young, Kalani. Spencer used POL2 at the East Asian Observatory to measure the magnetic field of the Orion Nebula in an attempt to determine the origin of the nebula's shape. A professional astronomer studying the same region used Spencer's data and Spencer will be acknowledged in all her publications on the subject. Spencer also has access to her data.

"Dark Nebulae and Their Connection to Star Formation" by Hokunani Sanchez and Keilani Steele, Honokaa. Hoku and

Keilani will use Megacam and Wircam at CFHT to study the Great Rift Nebula in the center of the Milky Way. They hope to determine if there is a difference between the difference patches in the nebula.

"Possible Life in Other Places in Our Solar System" by Anika Wiley, Marie-Claire Ely and Kaitlin Villafuerte, Honokaa. Anika, Marie-Claire and Kaitlin plan to use NASA's IRTF to study the infrared spectra of Titan over the course of a few months.

We aim to expand the program for the 2017-2018 school year. The W.M. Keck Observatory will offer two hours of telescope time for students next year. We plan to add schools on Maui and perhaps Molokai along with an additional Big Island High School. We are partnering with the Hawaii State Department of Education to develop curriculums for our participating teachers. Stay tuned for more updates!

New Addition

CFHT is pleased to introduce our newest Canadian Resident Astronomer, Laurie Rousseau-Nepton. Freshly graduated from Université Laval in Québec where she perfected her expertise in instrumentation and on galaxies' evolution she is now sharing her knowledge on SITELLE, the CFHT's Imaging Fourrier Transform Spectrograph, with the whole scientific community. In the past years, while in charge of the observing runs with SITELLE's prototype called SpIOMM at the Observatoire du Mont Mégantic, Laurie worked on improving the observing procedures, the data reduction and the analysis of the large amount of data produced by these instruments. She also taught to a generation of students the basics of astronomical observations using different instruments and was dedicated to science outreach activities in schools and astronomy clubs. Excited by star-forming regions in galaxies, her work is now focused on understanding how the environment affects the generations of new born stars.

Laurie Rousseau-Nepton's father was fascinated by the stars and regularly organized observation sessions of eclipses or shooting stars in their home on the outskirts of Quebec City. Last year, she was the first Aboriginal woman to earn a doctorate in astrophysics at Université Laval. Her family comes from the Pointe-Bleue (Mashteuiatsh) reserve in Lac-Saint-Jean. "My father told me that I would be an astronaut so much that I loved stars and planets, but I do not like risk."

We are happy that Laurie decided to stay on Earth! ✶

Mary Beth Laychak has loved astronomy and space since following the missions of the Star Trek Enterprise. She is the CanadaFrance-Hawaii Telescope Outreach Coordinator; the CFHT is located on the summit of Maunakea on the Big Island of Hawaii.

Skyward

Of Shadows, Eclipses and Comets

by David Levy, Montreal and Kingston Centres

On the evening of 2017 February 10, I saw the shadow of the Earth extend all the way to the Moon as night fell.

Nightfall happens every evening. The Sun sets and towards the east a dark shadow appears, darkening the sky as it strengthens. After an hour, the "shadow" has spread itself across the whole sky, and it is night. But on February 10, the start of that night was different. Just as Wendee and I saw the first indications of the Earthshadow in the east, the full Moon rose.

Only it didn't look full. There appeared to be a shading on the Moon's upper left portion. What we were seeing was the Earth shadow actually project all the way to the Moon. It was a lunar eclipse.

Figure 1 — Just after sunset, the Moon rises in a penumbral eclipse.

There are several kinds of eclipses of the Moon and of the Sun. Lunar eclipses can be penumbral, in which the partial shadow of the Earth falls on a portion of the Moon. They can be partial, where the full dark shadow of the Earth falls on a portion of the Moon. If the full Earth shadow covers the whole Moon, the eclipse is total. Eclipses of the Sun, which involve the shadow of the Moon reaching a portion of the Earth, are different. If the Moon covers a portion of the Sun, then it is a partial eclipse. The full shadow of the Moon tracks along a narrow band, no larger than about 257 kilometres, across a portion of Earth, and along that band there can be a total eclipse of the Sun.

That February eclipse was the ninetieth eclipse I have seen. These eclipses range from tiny penumbral lunar eclipses like the one last February, to the grand spectacles of total eclipses of the Sun, of which I have seen ten so far, and I hope to see my eleventh this coming August.

But there is more. The night before the lunar eclipse, while I was out in my observatory, I recalled missing one just like this one, decades ago. On 1963 January 9, I was a 14-year-old patient at the Jewish National Home for Asthmatic Children in Denver, Colorado. I watched the Moon rise that night during observing session No. 99E, never knowing that a soft penumbral eclipse was actually underway. That early eclipse was a member of a Saros (Greek for cycle), Saros 114.

It turns out that, unbeknownst to me, I saw that same eclipse (Saros 114) on 1981 January 19. That eclipse, also a penumbral lunar eclipse, was a repeat of the one I didn't recognize in 1963. The Saros cycle lasts 18 years, 11 days, and 8 hours; and this was the very next repetition of that eclipse. Because of the eight hours (or a third of a day), the eclipse took place at a different time. Eighteen years after that, I missed the next one, because the third of a day meant that the eclipse was visible only in the predawn hours, and I was under a deck of clouds.

Figure 2 — A little later, and a little darker, here is an image of the later stage of the February 10 penumbral eclipse.

That brings us to February 10. We were now pretty much back to the same time of day, and the eclipse was much like the one from 1963. This third repetition is called an *exeligmos*. It is Greek for a period of 54 years and 33 days. Thus, on February 10, I saw the 1963 eclipse, but 54 years later. It will be total along a narrow path that extends from Oregon to South Carolina. From our home in Vail, it will be a deep partial eclipse.

The existence of the Saros cycle, and the related exeligmos, make these wonderful events even more remarkable. This coming August 21, some of us witnessing the solar eclipse might recall seeing the *exeligmos* one, under similar conditions, 54 years ago.

Of a comet and history

Last week I got a good visual observation of Comet Tuttle-Giacobini-Kresak, (41P) one of the earliest known periodic comets. It was a fat little "faint fuzzy" spot of light projected against a background of faint stars—nothing to write home about, but for me it was fun just because it was a comet. This comet was only the 41st that was determined to be periodic when it was rediscovered in 1907, which means that it returns to our part of the Solar System again and again. This comet returns every five years or so. However, this comet was actually discovered three times before the details of its periodic past were finally figured out, and the stories of its findings take us through a good portion of modern history.

This comet was first spotted by the famous comet discoverer Horace W. Tuttle on 1853 May 3, in the little constellation of Leo Minor. It was part of a streak of comets he discovered between then and the first half of the 1860s. Within a few years of this discovery, Tuttle joined the Union army fighting the Civil War. After the end of the war, in 1869 whilst serving as paymaster aboard the monitor ship *Guard*, he somehow "lost" the considerable sum of $8800 (a very large sum of money at that time) from the accounts of his ship. He was arrested and charged with defrauding the U.S. Navy. At his court martial Tuttle was convicted, but later his sentence was reduced, on approval by President Grant, to a dishonorable discharge from the Navy. One wonders if this semi-pardon had anything to do with his illustrious record as a comet discoverer.

Fast forward through time, to the dawn of the 20th century when Michel Giacobini was observing from the Observatoire de Nice in France. On 1907 June 1, Giacobini discovered what turned out to be a return of Tuttle's comet. Moving forward again, we arrive at 1951 April 24. I was almost four years old when Lubor Kresak of Czechoslovakia discovered this comet a third time.

Now we know that this comet orbits the Sun in a period of precisely 5.419 years. This spring it happened to pass pretty close to Earth, at about a tenth of an astronomical unit (distance between Earth and Sun). As we look back at the numerous times this comet was found and found again, we can see how, in 1858, the United States was about to fall into the abyss of its civil war. In 1907, Lord Baden-Powell was starting the Boy Scout movement. And in 1951, the Korean War was about to begin. Drifting through the sky, we have the opportunity to see not just a comet sailing through space, but also to take a dip into the ocean of history. ✶

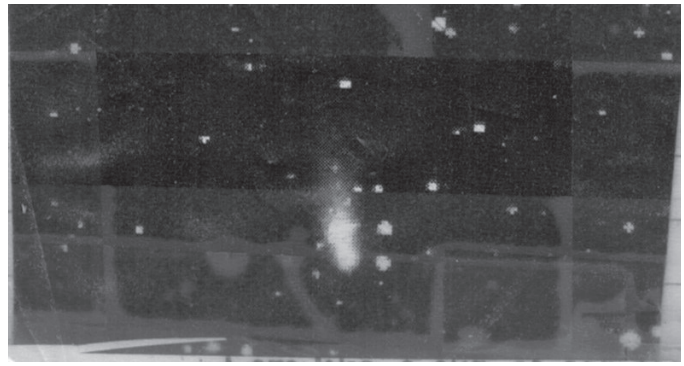

Figure 3 — Comet Kresak–Peltier, in June 1954; one of Kresak's comet discoveries.

David H. Levy is arguably one of the most enthusiastic and famous amateur astronomers of our time. Although he has never taken a class in astronomy, he has written over three dozen books, has written for three astronomy magazines, and has appeared on television programs featured on the Discovery *and the* Science Channels. *Among David's accomplishments are 23 comet discoveries, the most famous being Shoemaker-Levy 9 that collided with Jupiter in 1994, a few hundred shared asteroid discoveries, an Emmy for the documentary* Three Minutes to Impact, *five honorary doctorates in science, and a Ph.D. that combines astronomy and English Literature. Currently, he is the editor of the web magazine* Sky's Up!, *has a monthly column, Skyward, in the local* Vail Voice *paper and in other publications. David continues to hunt for comets and asteroids, and he lectures worldwide. David is also President of the National Sharing the Sky Foundation, which tries to inspire people young and old to enjoy the night sky.*

Astronomical Art & Artifact

Earliest RASC Star Party Antecedents?

by R.A. Rosenfeld, RASC Archivist
(randall.rosenfeld@utoronto.ca)

Abstract

This article seeks to establish how far back star parties can be found in the RASC.

The thing antedates the name[1]

By the time this number of the *Journal* arrives in your virtual inbox, or through your very-real letter box, the serious annual spring-to-autumn star-party season will have commenced. At those locales, amateur astronomers gather to observe, commune, and learn, in observing environments vastly superior to the urban skies to which they are habituated. There are star parties, of course, that run in urban or semi-urban settings where amateur astronomers—and some professional astronomy educators—offer celestial vistas to thepublic in a regular or semi-regular cadence throughout the year.

Most of us think we know what a star party is, but there are surprisingly few formal definitions one could cite, if the need arose. Surprisingly, standard works decline to define "star party." The latest edition of the *Oxford English Dictionary*, which responsibly cites usage on both sides of the pond, offers no entry (*lema*) for the term; indeed, "star party" doesn't even appear in quotations illustrating the lexical practice for other words (OED). Nor are there entries for "star party" in either the most recent edition of the *Collins Dictionary of Astronomy* (Daintith & Gould 2006—aimed at advanced amateurs, and those embarking on first degrees), or the *Oxford Dictionary of Astronomy* (Ridpath 2012—intellectually downmarket in comparison to the *Collins*).

A simple, serviceable, and serious definition could be "a star party is an occasion for mainly recreational observing involving more than one person." Or, in Biercian pastiche, "a star party is the peculiar practice of congregating under the stars with intent to waylay passersby with celestial enticements." If one wished to construct a typology of star parties, various organizing principles could be employed. Categories could be established according to location (urban/semi-rural/rural), quality of the sky (Bortle class), number of attendees, annual duration (a single night/a week), closed or open invitation (intrinsic/extrinsic star party), types of astronomers (visual observers and astrosketchers/mixed visual observers and astrophotographers), types of object observed (any object observable/or with the emphasis placed on an eclipse/comet/meteor shower/the deep sky/a single class of DSO/planets/a single planet/an occultation/variable stars/a class of variables/satellites and probes, etc.), style of observing (pure recreation/education and training/useful data acquisition), or sponsor (an association, educational or cultural institution/a commercial vendor). Add demographic factors and one might embark on a meaningful analysis of this aspect of the culture of astronomy. Intriguing though it may be, the sociology of star parties will not be pursued here; rather, the earliest traces of "star parties" within the RASC are sought.

The term "star party" is probably of North American origin. Its occurrence is scarce in British astronomical literature before the mid to late 1980s.[2] The earliest printed citations uncovered in the course of the present investigation date from 1939–1940. Brief articles in *The Sky* (a constituent of what would become *Sky & Telescope*), and *Popular Astronomy*[3] (the outstanding North American amateur magazine of the first half of the 20th century), report on what would now be called urban star parties, held in parks in downtown Cleveland, and, in imitation, in Evanston, Illinois (Fisher 1939; Russell 1940a; 1940 b; 1941). The occasions were advertised to the populace at large in the media, the telescopes and expertise were mostly provided by amateur astronomers, the locations were accessible to urbanites, and the objects chosen were those that might appeal at first blush to non-astronomers. There are signs in the reporting that indicate the organizers thought they were engaged in a novel activity: "star party" appears in quotation marks, signalling that the use is unusual (Russell 1940 a; 1940b; 1941); the organizers are said to have "conceived the idea of putting on a 'Star Party' for the public," a report echoing "the tremendous response to the series of summer star parties amply demonstrated to the originators of the idea, that there is a wide-spread interest in astronomy among lay peoples" (Russell 1940 b, 566; Fisher 1939); and the Evanston imitator, impressed by Cleveland's effort, was "determined to put on a 'Star Party' that would sweep the town…as this stunt had never before been attempted in Evanston," and it is reported by one of the Cleveland initiators "with a hope that it will stimulate interest…to such an extent that other people will take up the idea in other cities" (Russell 1941, 55-56).

The use of the term, then, appears to be just under eight decades old. The practice in some form is demonstrably older than the term.

Observing together under the stars

What was the nature of star parties, before the term "star party" was coined? Are their characteristics identical to those of our day, or are there differences?

Before the Cleveland and Evanston star parties of 1939–1940, occasions for planned, recreational group observing not tied to dramatic celestial events seem to have been "intrinsic," chiefly reserved for a closed, invited group, such as family, friends, or

Figure 1 — One of the earliest photographs of an "RASC" "star party," ca. 1900-1901. This was an intrinsic star party, only open to members, held on the property of D.J. Howell, Lambton Mills, Ontario. Reproduced courtesy of the RASC Archives.

learned Society members, rather than the public. The earliest RASC (i.e. Toronto Astronomical Society) images of "star parties" from ca. 1900–1901 show such "intrinsic" gatherings (Figure 1; www.rasc.ca/early-star-party; www.rasc.ca/early-star-party-2; www.rasc.ca/early-star-party-3; Howell 1931, 235). These were part of the tradition of Georgian and Victorian convivial, and frequently non-trivial, group observing, such as the evenings when William Herschel, "Astronomer to his Majesty," would conduct observing parties for his patron, his family, and guests, or when Dr. Lee, Captain Smyth, and friends observed at Hartwell House, or when William Lassell viewed the heavens with other Liverpudlian amateurs (Herschel 1912, xxxv; Hoskin 2011, 71-72; Smyth 1851, 293; Chapman 1996, XVII, 344-346).

Dramatic celestial events could cause star parties, either of the planned sort (by intrinsic, or extrinsic invitation), or of the unplanned, and seemingly spontaneous sort; people just showed up where the action was—around the astronomers. At the last of the 19th-century transits of Venus, on 1882 December 6, both the Minister and Deputy Minister of Marine and Fisheries witnessed the event at the Nepean Point Observatory in Ottawa, along with "quite a number of persons" (Broughton & Rosenfeld—one could characterize this instance as having both an intrinsic and an extrinsic list of participants). Solar eclipses, and great naked-eye comets, could have the same effect, the latter well illustrated by Jan Luyken's engraving of the Great Comet of 1681 (C/1680 V1, also known as Kirch's Comet; Figure 2). Such grand celestial shows could equally command the involvement of grand crowds, or more intimate groups (e.g. the Wordsworths' "comet party" of 1814; Gaull 2015, 609).

Several types of pre-1939–1940 star party seem at first to have an economic feature not found today. The lectures in natural philosophy, which were part of the popular intellectual landscape of the 18th century, sometimes offered group observing sessions (e.g. Carpenter 2011, 30-31). Not unrelated, but certainly socially downscale and intellectually less ambitious, were the occasions when itinerant astronomers offered views of celestial "scenery" through their telescopes in public places in Europe and North America, for a monetary consideration. This sort of street hawking is immortalized in Wordsworth's "Star Gazers," and was an outreach activity perpetrated by the first president of the Toronto Astronomical Club (i.e. the RASC), Daniel Knode Winder, when he returned to live in Detroit (Wordsworth 1807, 87-89; Broughton 2008, 241). The practice does exist today in its partly lineal descendants, the star-gazing inn, hotel, and guest house (Treadwell 2017).

Most early examples of group observing for education and public outreach (EPO) conducted by the RASC and its members were not of a mercenary nature, and it is to these we now turn.

"Star party" activity in the early RASC

How far back can traces of EPO activity, recognizable in large part as belonging to star-party practices, be found in the records of the Society?

At the eighth meeting of the Society on 1890 June 3:

> *"An animated discussion arose with respect to the desirability of having, in popular parlance, "A Night with Saturn," such of the public as might be interested to be invited. Ultimately, several of the members expressed their willingness to place their telescopes at the disposal of any persons desirous of seeing Saturn and other celestial objects;" TAPST 1891, 8.*

Clearly not all members at the time thought that it was either a good use of the Society's resources to engage in "star-party" style EPO, or that it was appropriate. They may have wanted to keep the Society's group observing intrinsic—if anyone wanted to observe with the group, or use its instruments, then they ought to apply for membership. This attitude was not foreign to a main trend of early "star parties" in amateur practice (see above). It could also reflect the desire to engage in serious astronomical observing, the sort that gathered data and advanced science, rather than a type of observing seen as frivolous, i.e. mere stargazing.

The case for serious observing over EPO was memorably stated by RASC honorary member and *Observer's Handbook* contributor W.F. Denning, FRAS, in his *Telescopic Work for Starlight Evenings*, an influential work dating from this period. The passage is worth quoting:

> *"Every man whose astronomical predilections are known; and who has a telescope of any size, is pestered with applications from friends and others who wish to view some of the wonders of the heavens. Of course it is the duty of all of us to encourage a laudable interest in the science, especially when evinced by neighbours or acquaintances; but the utility of an observer constituting himself a showman, and sacrificing many valuable hours which might be spent in useful observations, may be seriously questioned…Is it therefore desirable to satisfy the idle curiosity of people who have no deep-seated regard for astronomy, and will certainly never exhibit their professed interest in a substantial manner? Assuredly not. The time of our observers is altogether too valuable to be employed in this fashion. Yet it is an undisputed fact that some self-denying amateurs are unwearying in their efforts to accommodate their friends in the respect alluded to. My own impression is that, except in special cases, the observer will best consult the interests of astronomy, as well as his own convenience and pleasure, by declining the character of showman;" Denning 1891, 74-75.*

Denning was an important amateur observer, and his opinion ought not to be dismissed as that of a pre-modern ogre (on Denning, see Beech 1998). Not all astronomers, amateur or professional, were, or are cut out for EPO. Denning's time probably was best turned toward research. The trend now among most amateur organizations in the English-speaking world is to devote more attention and resources toward EPO, than toward skilled and disciplined data collection (including initiation and training in the latter). There is merit is pursuing both activities, of course. A healthy astronomical culture, indeed, is one that encourages both.

What was the result of that discussion among the members at the meeting on 1890 June 3 as to whether they should hold what we would now recognize as a public (extrinsic) "star party"? The account of the meeting in the manuscript minute book of the Society is much less detailed than the printed version(!), and offers even less detail on the tenor of the discussion, and none as to its outcome: "A suggestion was made by the vice-president as to an open meeting which could be held in the Normal School Grounds;" A&PST 1890, 30. This assumes, of course, that a "star party" is what is referred to by "an open meeting…on the Normal School Grounds."[4]

The printed minutes for the year have nothing further to say on the matter (TAPST 1891), but in this case, the manuscript minute book is a little more informative. At the meeting of 1890 June 17: "The proposal to hold an open meeting in the Normal School Grounds or a more suitable place was dropped for the present;;" A&PST 1890, 33. It seems that, for whatever reason, the proposal for the Society to hold its first public (extrinsic) "star party" was allowed to lapse in the year in which it was made!

Solid evidence of the Society making it possible for others to look through telescopes survives from four years later. A transit of Mercury was predicted for November 10, and:

> *"Arrangements had been made to send telescopes to some of the public schools of the city, that the pupils might have an opportunity to observe the phenomenon. Mr. G.H. Meldrum and Mr. A. Elvins had placed 3-inch refractors at Wellesley School, and under the management of Miss A.A. Gray, very satisfactory observations had been made of the planet on the disc. Messrs. Michael Bros. had placed one of their 3-inch*

Figure 2 — Great Comet of 1680 (C/1680 V1), from Jan Luyken, Beschouwinge der wereld*, 1725. Some celestial events are so impressive they can call forth spontaneous, extrinsic star parties, involving every and anyone. Reproduced courtesy of the Specula astronomica minima.*

> *telescopes by Vion Frères, of Paris, at the York Street School[5]; two others of these refractors were successfully used, one by Dr. A.D. Watson, and one by Mr. C.T. Gilbert, who had taken charge of the arrangements at the Jesse Ketchum School. Messrs. Michael Bros. had announced their willingness to place their telescopes at the service of the School Board on any special occasions. A Gregorian reflector had been sent to the Ryerson School by Dr. Watson, and also a small refractor;" TAPST 1895, 103.*

Fortunately this initiative was not left to wither; the following year, at a Society meeting of 1895 May 28, it was recorded that:

> *"Miss A.A. Gray reported having spent an evening at the telescope with the pupils of Wellesley School, who were much interested in observations of Jupiter and Saturn. With the assistance of another member, she had arranged to give the senior classes of the public schools as many opportunities as possible to engage in practical telescopic work. The general interest taken and the order that prevailed during the observations had been very encouraging. Several members repeated their desire to assist Miss Gray in this work, which was directly in line with the Society's objects;" TAPST 1896, 46.*

Would that it were as apparently easy to get volunteers and instruments into schools now as it was then! It is notable that this sort of EPO was described in 1895 as being "directly in line with the Society's objects." That is broadly true of the RASC's EPO objectives today.

School observing parties are certainly a variety of star party, but they are not identical to the extrinsic star parties, to which any member of the public is invited.

At a Society meeting of 1898 May 31, it appears that the next step to realizing open-invitation (extrinsic) star parties is initiated, with civic support:

> *"The President read a brief account of an interview had with a committee of the City Council since the previous meeting and in reference to a money grant to the Society. The sum of $100 had been voted, it having been asked for the purpose of providing opportunities for the general public to view celestial objects with the telescope;" TAPST 1899, 26.*

This may have borne fruit, as noted at the 12th meeting of the Society, 1899 June 27:

> *"…this was an open meeting held in the Toronto Observatory, at the invitation of the Director…The meeting then adjourned and a pleasant hour was spent in observation with the large telescope of the observatory, and with smaller instruments brought by members and placed on the lawn;" TAPST 1899, 37–38.*

By 1900, "star parties" not too dissimilar from current practice, and attitudes of enthusiasm for such events, mark the Society's activities. At the 16th meeting of 1900 September 5:

> *"A series of reports of successful out-of-door meetings for telescopic work were received… the President and other members had willingly set up telescopes for the evening on public and private lawns in various parts of the city in order that the public might be enabled to observe celestial phenomena and had themselves attended and had presided at their instruments or had given practical instruction in Constellation study. Some of these meetings had been held under the auspices of churches and of public and private schools, and one of them on the grounds of the Harbord Collegiate Institute at the instance of the Froebel Society; another on the grounds of the Normal School when the teachers attending the school were present, and a third on the grounds of St. Andrew's Boys' College. These meetings had been attended by large and appreciative gatherings, and the Society had been thanked for what it had done. The President*

> *added that during a holiday in Muskoka he had placed a telescope on the lawn every clear evening, and had welcomed any one who chose to use it. Sometimes as many as fifty guests and others were present. The Muskoka air was admirably adapted for observation. During August, Venus was a beautiful daylight object being easily visible to the naked-eye in bright sunshine. In the telescope she was, of course, still more attractive. To many people, ability to see a star in the daytime was a pleasing novelty;" TTAS 1901, 29.*

The star-party activity that seems an integral part of the modern RASC's EPO was developed during the 1890s, and was largely established by 1900. We have been doing this for nearly 120 years. We had, in fact, employed star parties as a tool of outreach four decades before the term "star party" was coined. The RASC was probably not unique in this, although it would be interesting to identify any differences between the experience of the RASC and comparable organizations. Are there discernible "dialects" in star parties across the RASC, that is, regional differences, and if so, what is their history? ✶

Acknowledgements

This research has made use of NASA's Astrophysics Data System.

References

Manuscripts, Books, and Articles

A&PST (1890). Astronomical and Physical Society of Toronto. Minute Book. Feb. 25, 1890-March 7, 1893

Beech, M. (1998). W.F. Denning—The Doyen of Amateur Astronomers. *WGN, Journal of the International Meteor Organization 26, 1*, 19-24

Broughton, P. (2008). Daniel Knode Winder (1828-97). *JRASC 102, 6*, 238-241

Carpenter, A.T. (2011). *John Theophilus Desaguliers: A Natural Philosopher, Engineer and Freemason in Newtonian England*. London: Continuum

Chapman, A. (1996). *Astronomical Instruments and Their Users: Tycho Brahe to William Lassell*. Aldershot–Brookfield VT: VARIORUM Ashgate

Daintith, J. & Gould, W. (Eds.) (2006). *Collins Dictionary of Astronomy*, 5th edition. Glasgow: HarperCollins Publishers

Denning, W.F. (1891). *Telescopic Work for Starlight Evenings*. London: Taylor and Francis

Fisher, C. (1939). Reports of Amateur Groups Throughout the Country: Cleveland Star Party. *The Sky 4, 1* (November), 22

Gaull, M. (2015). Wordsworth and Science. In (Ed.) R. Gravil & D. Robinson, *The Oxford Handbook of William Wordsworth* (pp. 599-613). Oxford : Oxford University Press

Gillespie, C.C. (2016). *The Edge of Objectivity: An Essay in the History of Scientific Ideas*. Princeton NJ: Princeton University Press

Herschel, William (1912). *The Scientific Papers of Sir William Herschel*. J.L.E. Dreyer (Ed.), 1. London: The Royal Society and the Royal Astronomical Society

Hoskin, M. (2011). *Discoverers of the Universe: William and Caroline Herschel*. Princeton & Oxford: Princeton University Press

Howard-Duff, I. (1987). Ordinary Meeting 1987 April 29… *JBAA 97, 5*, 304-306

Howell, D.J. (1931). Recollections of the Early Days of the Astronomical Society. *JRASC 25, 6*, 233-236

Might, J.M. (1894). The Toronto City Directory 1894, vol. XVIII. Toronto: The Might Directory Company

Ridpath, I. (Ed.) (2012). *Oxford Dictionary of Astronomy*, 2nd edition rev. Oxford: Oxford University Press

Russell, J.L. (1940 a). The Cleveland "Star Party." *Popular Astronomy 48, 4* (April), 195-197

Russell, J.L. (1940 b). The Cleveland Star Party, August 8, 12, and 15, 1940. *Popular Astronomy 48, 10* (December), 566-568

Russell, J.L. (1941). The Star Party, Evanston, Illinois, July 30, 1940. *Popular Astronomy 49, 1* (January), 55-56

Smyth, W.H. (1851). *Ædes Hartwellianæ*. London: John Bowyer Nichols and Son

TAPST (1891). *Transactions of the Astronomical and Physical Society of Toronto for the Year 1890-91*. Toronto: Brough & Caswell

TAPST (1892). *Transactions of the Astronomical and Physical Society of Toronto for the Year 1891*. Toronto: Brough & Caswell

TAPST (1895). *Transactions of the Astronomical and Physical Society of Toronto for the Year 1894*. Toronto: Rowsell & Hutchison

TAPST (1896). *Transactions of the Astronomical and Physical Society of Toronto for the Year 1895*. Toronto: Rowsell & Hutchison

TAPST (1898). *Transactions of the Astronomical and Physical Society of Toronto for the Year 1898*. Toronto: Rowsell & Hutchison

TAPST (1899). *Transactions of the Astronomical and Physical Society of Toronto for the Year 1899*. Toronto: The Carswell Company, Limited

TTAS (1901). *Transactions of the Toronto Astronomical Society for the Year 1900*. Toronto: The Carswell Company, Limited

Treadwell, T. (2017). *Astronomy Adventures and Vacations: How to Get the Most Out of Astronomy in Your Leisure Time*. Cham: Springer

Wordsworth, W. (1807). *Poems, in Two Volumes*, vol. 1. London: Longman, Hurst, Rees, and Orme

Websites

OED: Oxford English Dictionary
www.oed.com.myaccess.library.utoronto.ca
(consulted 2017 April 8)

R.P. Broughton & R.A. Rosenfeld, Transit History—the Canadian Experience: 1882 Science
www.rasc.ca/1882-science
(consulted 2017 April 11)

Endnotes

1 Gillespie 2016, 153—not a reference to star parties, of course.

2 A rare occurrence is in Lynch, C. (1964).The Preston and District Astronomical Society. In *1965 Yearbook of Astronomy* (p. 198). (Ed.) P. Moore. London: Eyre & Spottiswoode. Howard-Duff 1987 writes as if it were a rare occurrence in England.

3 *Popular Astronomy* ran from 1893–1951, and arguably remains the high mark that all subsequent periodicals for the amateur market fail to reach.

4 An entry from later that year suggests that an "open meeting" might not involve any public observing at all. At the 14th meeting of the Society in 1891 September 8, two members: "advised the holding of a public meeting, with an exhibition of lantern slides, illustrating astronomical subjects. A committee was appointed to consider the proposition." TAPST 1892, 28.

5 These were the commercial opticians Solomon and Henry Michael, 57 King St. East; Might 1894, 1108

Imager's Corner

Mask Basics

by Blair MacDonald, Halifax Centre
(b.macdonald@ns.sympatico.ca)

The next few editions of Imager's Corner will cover masks and some of their uses in processing astrophotos. Once you make it past basic stretching, most people quickly find out that masks are essential in improving their processing. Masks allow you to tailor and constrain your processing. You can limit sharpening to the bright edges and limit noise reduction to the dark background. Over the next few editions, we will look at things like luminance masks, noise-reduction masks, star masks, and edge masks to control processing and limit some of the nastier side effects that can occur while we attempt to improve our images.

Mask Basics

At its simplest, a mask is a monochrome image that allows us to control where processing is applied. One of my favourite ways to think about how a mask works is to think of a stack of two images. On the bottom of the stack is the original image; on top is a copy that has had some processing applied, let's assume a simple stretch in this example. The mask is a simple monochrome image that sits on top of the top image. Where the mask is white, the top image shows through. Where the mask is black, the top image is hidden and the bottom image shows through. Where the mask is a shade of grey, it blends both layers together based on its brightness. You can readily see the effect in the following example. It is made from a stack of two layers: the bottom is filled with red and the top filled with green, a simple linear brightening layer is placed on top as shown in the Paint Shop Pro image stack at right. Where the mask is white, the green shows through, and where the mask is black, the green is hidden and the red is revealed. A brightening layer is placed on top to make the colours brighter.

This stack produces the image shown below, a green circle on a red background.

This is a very simple application of a mask in producing an image from multiple layers. Now let's take a look at something other than simply revealing a layer where the mask is white. Remember that when the mask is a shade of grey, the layers are blended together based on the brightness of the mask. If we simply blur the mask used in the above example, then it will be white at the centre and fade to black at the edges, as shown in the next image.

Since the two layers are red and green, where the mask is a grey shade near the edges, the result will be a shade of yellow.

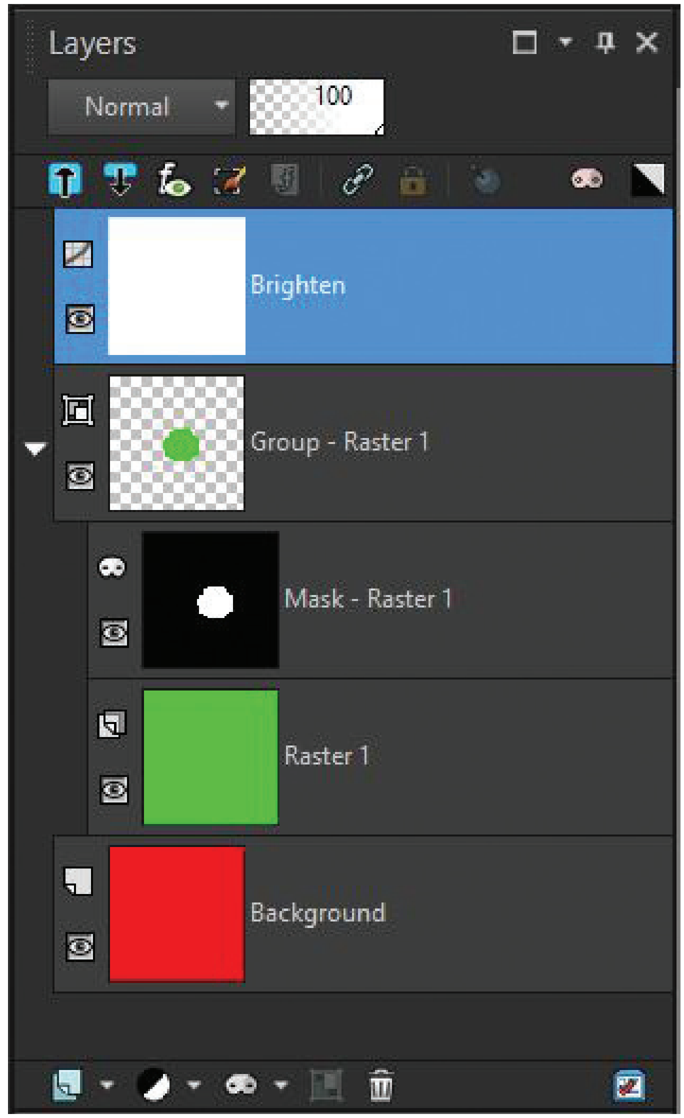

Figure 1 — Simple masked image stack

So that's it, the basics of masks. Some of the things you will want to consider when using masks are what is it you want to emphasize, whether to blur the mask or not, and what type of mask to use for a given situation. Over the next several columns we will look at how to create masks for a particular purpose. We will cover how to make star masks, edge masks, sharpening masks, and noise reduction masks. For the rest of this edition we will look at the humble luminance mask and some of its uses.

When stretching an image, quite often we want to limit the effect to the bright object so as not to increase noise in the background. Take the image below as an example, M27 is rather dark and we want to brighten it up without affecting the dark background. Here the straightforward approach results in bloated stars and a bright, noisy background.

Duplicating the layer and applying a simple curve to the top layer is shown in Figure 6, with the resulting stack shown in Figure 7.

Figure 2 — Image produced from the image stack in Figure 1

Figure 3 — Blurred mask

Figure 4 — Stack combined with blurred mask

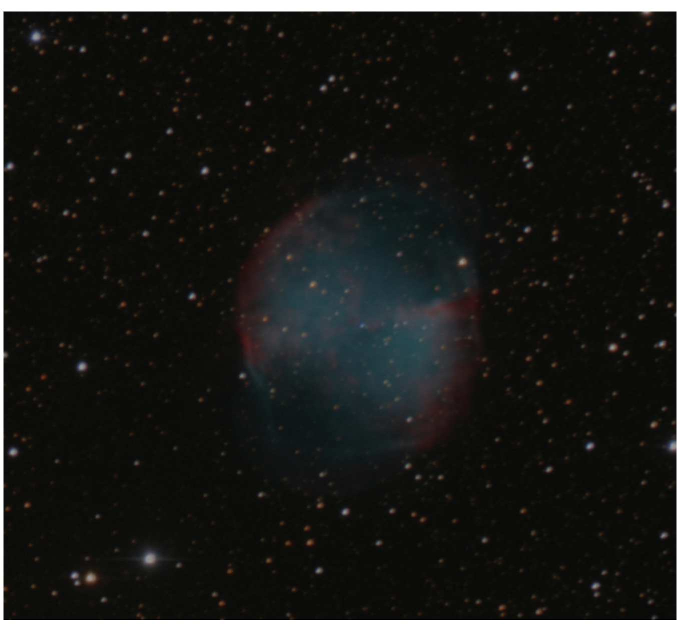

Figure 5 — Original M27 Image

The problem with this simple approach is that the background becomes noisy as it is brightened substantially and the stars become bloated producing a rather poor image. The bottom end of the curve could be lowered, but this tends to produce a high-contrast image that looks a little unnatural.

A simple luminance mask can take care of both problems by limiting the stretch in the dim areas of the image. A luminance mask is simply a greyscale copy of the stretched layer that is used to blend the two layers together.

Using the luminance mask, we have the following stack of two images with the mask on the top, stretched layer.

The result of this stack is an image with a nice smooth, dark background and most of the bright detail from the simple stretch. In addition, the core of M27 in the masked stretched image shows more detail and contrast.

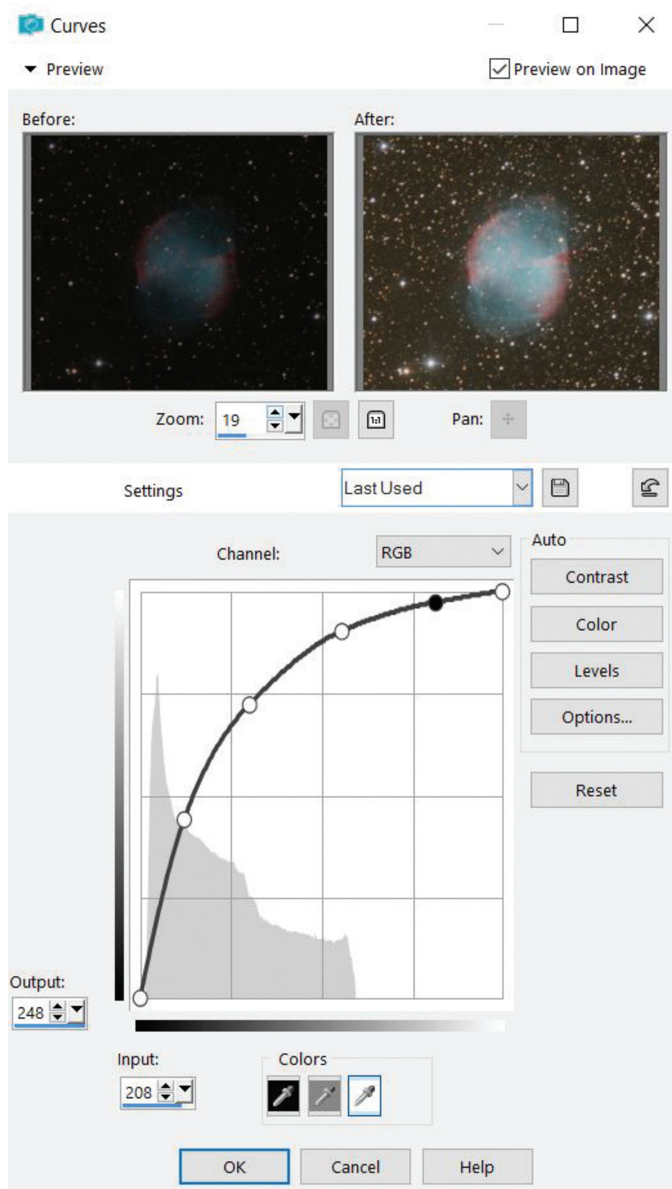

Figure 6 — Curve adjustment applied to top layer of stack

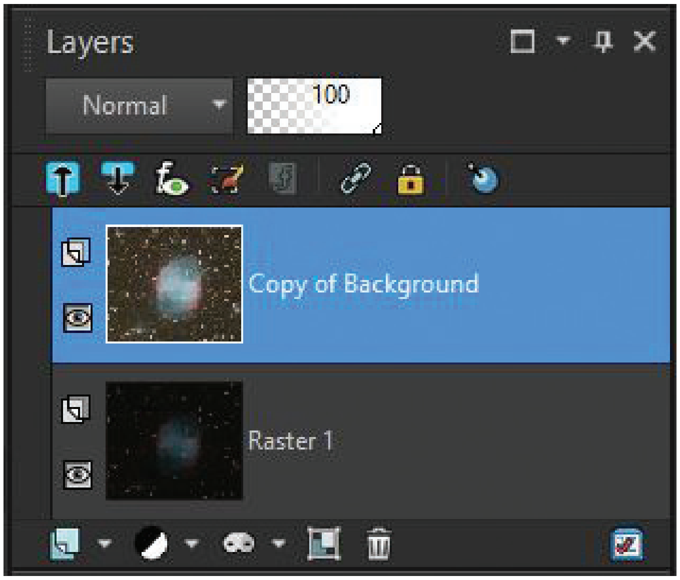

Figure 7 — Paint Shop Pro image stack

Figure 8 — Simple stretch produces bloated stars and bright background

Figure 9 — Luminance mask

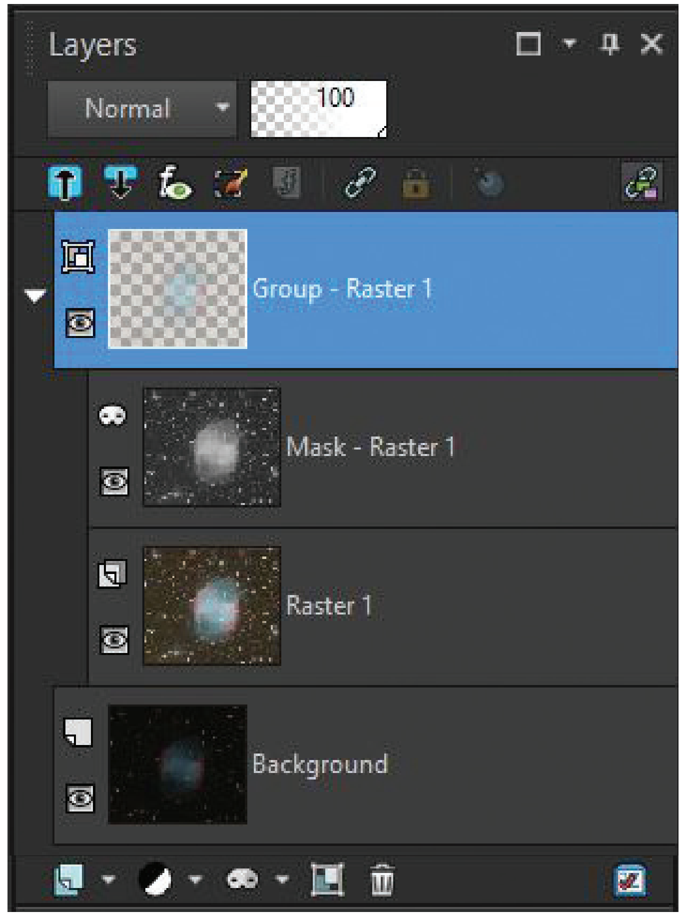

Figure 10 — Stack using luminance mask

Figure 11 — Masked versus unmasked image

Tune in for the next installment where we look at making a mask to select just the stars in an image and then use it to make a starless mask to stretch images while avoiding star bloat.

Remember, this column will be based on your questions so keep them coming. You can send them to the list at hfxrasc@lists.rasc.ca or you can send them directly to me at b.macdonald@ns.sympatico.ca. Please put "IC" as the first two letters in the topic so my email filters will sort the questions. ✶

Blair MacDonald is an electrical technologist running a research group at an Atlantic Canadian company specializing in digital signal processing and electrical design. He's been an RASC member for 20 years and has been interested in astrophotography and image processing for about 15 years.

Dish on the Cosmos

Hearts of Darkness

by Erik Rosolowsky, University of Alberta (rosolowsky@ualberta.ca)

Astronomers are using radio telescopes to make the sharpest images of astrophysical objects. Even though the images made by a single radio telescope have low resolution, connecting several telescopes together into an interferometer leads to dramatically improved resolution. The latest push in radio interferometry is to use networks of telescopes to directly observe the size of the supermassive black holes at the centres of our galaxy and others. This black-hole size is a direct test of the theory of relativity, but it also provides a key measurement for understanding how black holes are fed.

Telescopes of all types can be broadly characterized by their resolution and their light-gathering power. The resolution is defined as the angular separation between objects that a telescope can recognize as distinct. Smaller values of resolution correspond to sharper images. The light-gathering power is the amount of light that a telescope can catch, essentially the size of the bucket that is being used to gather the light. Because of the limitations of atmospheric seeing, most optical telescopes are optimized for light-gathering power, leading to a bigger-is-better approach for telescopes. The turbulence in the Earth's atmosphere limits optical telescope resolution to 0.5 to 1.0 arcseconds under most circumstances.

The resolution of a telescope also depends on the wavelength of light, with shorter (bluer) wavelengths having better resolution, but in the optical these colours also suffer most from atmospheric blurring. Long-wavelength radio telescopes do not seem like the best choice to attain superior resolution, but linking several radio telescopes into an interferometer

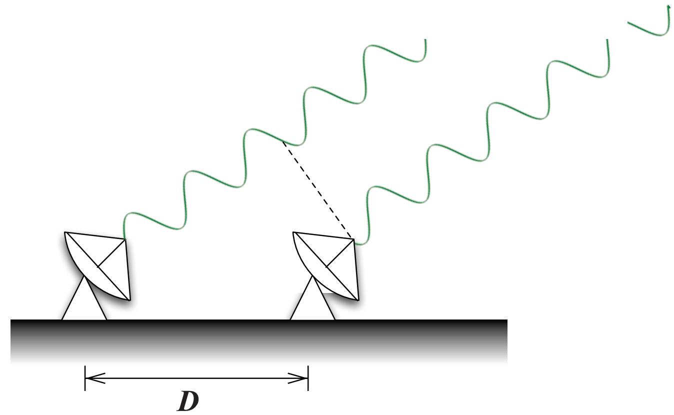

Figure 1 — A schematic representation of an interferometer. Radio waves arrive in phase from distant astronomical objects. The time difference between when a given part of the wave (dashed line) arrives at the different antennae allows the distance between the telescopes (D) to be carefully measured. Precise knowledge of the baseline distance D and how it changes over time can be used to make high-resolution images of the radio sky.

can dramatically improve the resolution. The techniques of aperture synthesis yield a telescope where the angular resolution of the telescope is controlled by the separation between the instruments (the distance *D* in Figure 1, called a *baseline*). Most arrays of telescopes stretch over a few kilometres, but in Very Long Baseline Interferometry (VLBI), the array of telescopes is spread over thousands of kilometres. Ordinary interferometers combine their signals by sending information over data cables to a single *correlator*. With VLBI, the data are recorded separately with precise measurements of time and then shipped to a common location using more mundane means (Canada Post!). The data are then combined to form the astronomical measurements. In 1967, Canadian radio astronomers made the first VLBI measurements, linking data between the 46-m antenna in Algonquin Provincial Park in Ontario and the 26-m antenna in Penticton, British Columbia.

With baselines of 10,000 km, telescopes can routinely image the sky at milliarcsecond resolutions (1 milliarcsecond = 1 mas = 0.001 arcseconds), with the most ambitious approaches reaching 0.02 mas. With these resolutions, several areas of astronomy are exclusively accessible to radio interferometers. First, for the technique to work, the distances between the telescopes must be known to the accuracy of a fraction of the wavelength being observed. This corresponds to knowing the baseline to 0.05 mm over 10,000 km. Shorter wavelength observations require even higher accuracy, which is why interferometry is largely restricted to radio observatories rather than the much shorter wavelength optical light. At these high levels of accuracy, the drift of the tectonic plates as well as the small fluctuations in the rotation of the Earth begin to affect the calibration of the observations. Fortunately, these effects can be calibrated by observing distant radio galaxies. The light from these galaxies arrives as a synchronized wave front across the Earth (Figure 1) and timing the wave arrivals (dashed line) allows the distance to be measured to the required accuracy using trigonometry. The careful measurement of the changing baseline lengths reveals the changing distances between telescopes, often as a consequence of plate tectonics. Interferometers easily measure the millimetres per year of drift between plates. The radio galaxies form an absolute frame of reference against which we can judge plate movements. This field of geodesy also uses VLBI to measure the wobbling of the Earth's axis and changes in the length of the day. These wobbles are caused by effects like the seasonal movement of water around the Earth through the hydrologic cycle.

This astounding accuracy makes for amazing opportunities in precision measurement of the changing Earth, but VLBI has major applications in high-resolution observations of astronomical targets. One of the major applications of VLBI has been in making careful measurements of parallax. By observing the apparent change in the positions of objects created by the Earth's motion around the Sun, we can directly measure distances to objects. While this works at all wavelengths, the high-resolution VLBI observations can see this apparent motion at much larger distances than other approaches, enabling mapping of the structure of our galaxy in good detail. Mapping the Milky Way is often hampered by our limited perspective from within the disk of the galaxy. These VLBI data provide benchmarks for surveying, making VLBI the best method for understanding the geography of our galaxy.

Looking to the future, VLBI promises to make direct observations of the event horizon of the supermassive black hole at the centre of the Milky Way. Black holes are the most compact known objects in space. An event horizon defines the separation between the inside and outside of the black hole. Formally, anything at a point within the black hole must have its future converge to the singularity at the centre of the black hole. This supermassive black hole at the galactic centre has a mass 4 million times that of the Sun, but the size of the event horizon is only ~20 times the radius of the Sun. This corresponds to an angular resolution of 0.01 mass. This is currently just beyond the resolution of our current VLBI. One option to improve the resolution would be to use longer baselines, but we are at the limit of the size of the planet. We could launch antennae on satellites (and have done so), but their relatively small sizes mean the interferometer is not sensitive. The other option is to work at shorter wavelengths. The maximum baseline we can use that can observe the centre of the galaxy is about 9000 km long and is limited by the geography of the planet—telescopes are more easily built on land! Using this baseline, we must observe at the shortest wavelengths available to interferometers: 0.6 mm. This is the challenge: can astronomers create a VLBI system that is stable at short wavelengths and high baseline precisions? Slowly, the technology is improving, building the Event Horizon Telescope (EHT).

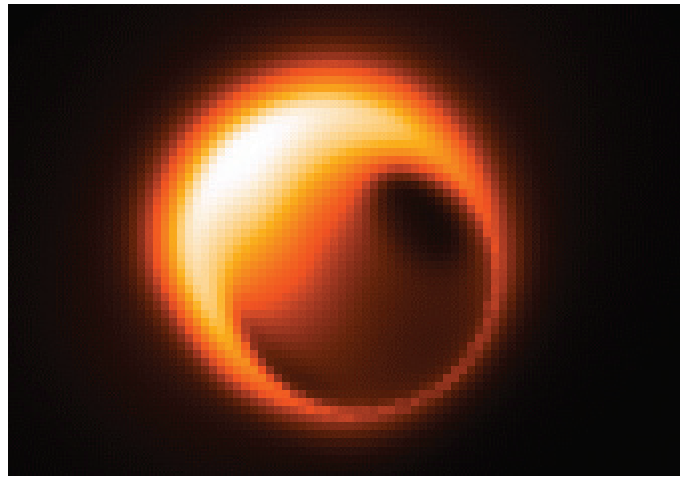

Figure 2 — A simulated image of the shadow cast by the supermassive black hole at the centre of our galaxy. The light in the image comes from gas that is accreting onto the black hole. The exact shape of the shadow will answer important questions about the nature of gravity as well as how black holes at the centres of galaxies are fed. This image is much higher resolution than the expected observations, but the Event Horizon Telescope will be able to distinguish this image from similar predictions made by other models. Image credit: Avery Broderick.

At first glance, the goal of imaging a black hole may seem foolish. After all, these objects emit no light by definition, so how can we see them? Instead, astronomers aim to see the particular shadow cast by the black hole as the intense gravity distorts the light coming from behind the black hole. An example of such an image is shown in Figure 2, which was created by Avery Broderick, who works at the Perimeter Institute and the University of Waterloo. One of Dr. Broderick's main lines of work is to develop different models for images that will be seen by the EHT. The theory of relativity and other theories of gravity make predictions for what this shadow should look like. The shape of the shadow also depends on the black hole's spin, which would provide a method to determine how the black hole is twisting the spacetime around it. Finally, the image will show how the black hole is actually fed through material accreting onto it. How this black hole feeding process occurs is largely unknown at these small scales, and the exact process is central to understanding the evolution of how black holes increase in mass over the lifetime of the Universe. The EHT is being improved so that the first successful observations could come as early at this year. Radio telescopes are unveiling the hearts of darkness at the centres of galaxies. ✶

Erik Rosolowsky is a professor of physics at the University of Alberta where he researches how star formation influences nearby galaxies. He completes this work using radio and millimetre-wave telescopes, computer simulations, and dangerous amounts of coffee.

Cosmic debris spotting

by Blake Nancarrow, Toronto Centre
(blaken@computer-ease.com)

The Earth constantly tumbles through meteoroid streams. When we tumble into summer in Canada, people plan out their fair-weather weekends. Some consider where they want to be on August 12, for that's the perennial predicted peak of the Perseids. Happily, that falls on a Saturday this year. However, unfortunately, the Moon will be nearly full. Boo, Moon!

While the peak date is important and normally yields the best show of meteors (Perseids are around 80 per hour), it is not the only night worth considering. Immediately before and after the peak can still make for a satisfying display. The Perseids are in fact active from mid-July through late-August. If the meteorologists say you will be clouded out on the peak, maybe early Sunday morning will be the best time to spot some streaks.

Many think July and August the "high season" for meteor watching. In addition to the Perseids, we may witness other showers including the delta Aquarids (30), Pisces Australids (14), alpha Capricornids (10), iota Aquarids (13), and kappa Cygnids (10). There are many more but I've only noted some with high zenithal hourly rate (ZHR) values. On any given clear summer night, outside a polluted light dome, you'll see many meteors over a short time.

Late-fall-early-winter is arguably better as there are more major events and two of them yield the highest yearly ZHR counts. The Quarantids in December can produce 100 meteors an hour, while the Geminids in January top out at 120! It is ironic few Canadians are aware of winter meteors.

A tool to remind us of upcoming events or the best night might encourage us to strap on the winter boots or grab a warm blanket.

I recently found Meteor Shower Calendar (MSC) by Christopher Wilcox. I installed (free, ad-supported) version 2.3.5 to my Android tablet; onto an iPad, version 1.3.1. The app works in portrait and landscape orientations.

The main screen (Figure 1 for iOS) shows the current sunrise and sunset times and Moon phase. The Android app (Figure 2) adds local weather. There is a table of current and upcoming showers, noting when each starts, culminates, and concludes, sorted by peak date (this can be changed). The app covers many known showers, some with just two sightings per hour. The developer incorporates data from a variety of sources in addition to the International Meteor Organisation. The rating, out of four stars, draws your attention to the best showers.

When you tap on an event, you get the shower details. On Android, the right side of the screen updates; on iOS, a new screen slides into view. The top image, sometimes a star chart or photograph, actually links to a small gallery with related

Figure 1 — The Meteor Shower Calendar main screen from iOS

Figure 2 — The Android main screen with list panel and selected event.

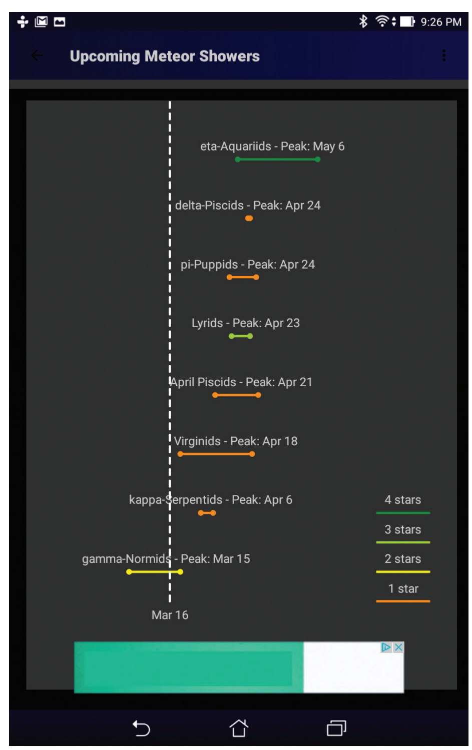

Figure 3 — Timeline chart view showing upcoming events.

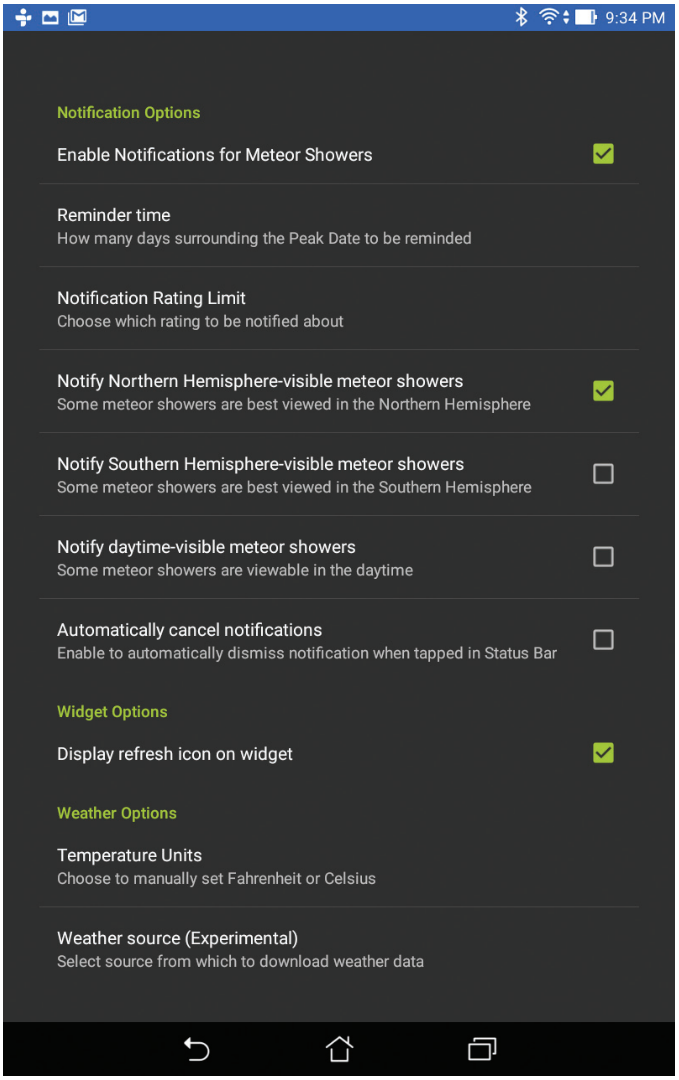

Figure 4 — Settings screen on Android showing Notifications controls

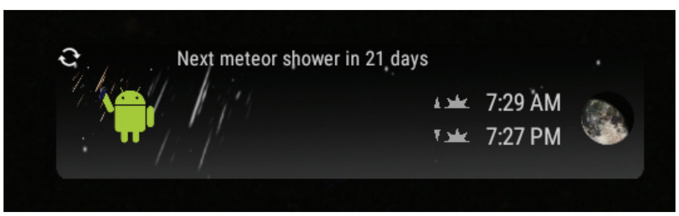

Figure 5 — Widget on Android home screen.

images. A toolbar provides buttons for conducting a web search, activating a planetarium view centred on the radiant, and showing your current five-day weather forecast. A very helpful element then appears: the predicted lunar phase during the meteor shower apex. Below the globe are ZHR and average velocity numbers.

On the Android, from the menu, use View Next Event to quickly see what's coming up.

The screen has a blue background. During the day, it is quite bright; but it automatically darkens in the evening. Unfortunately, there is no red-light mode.

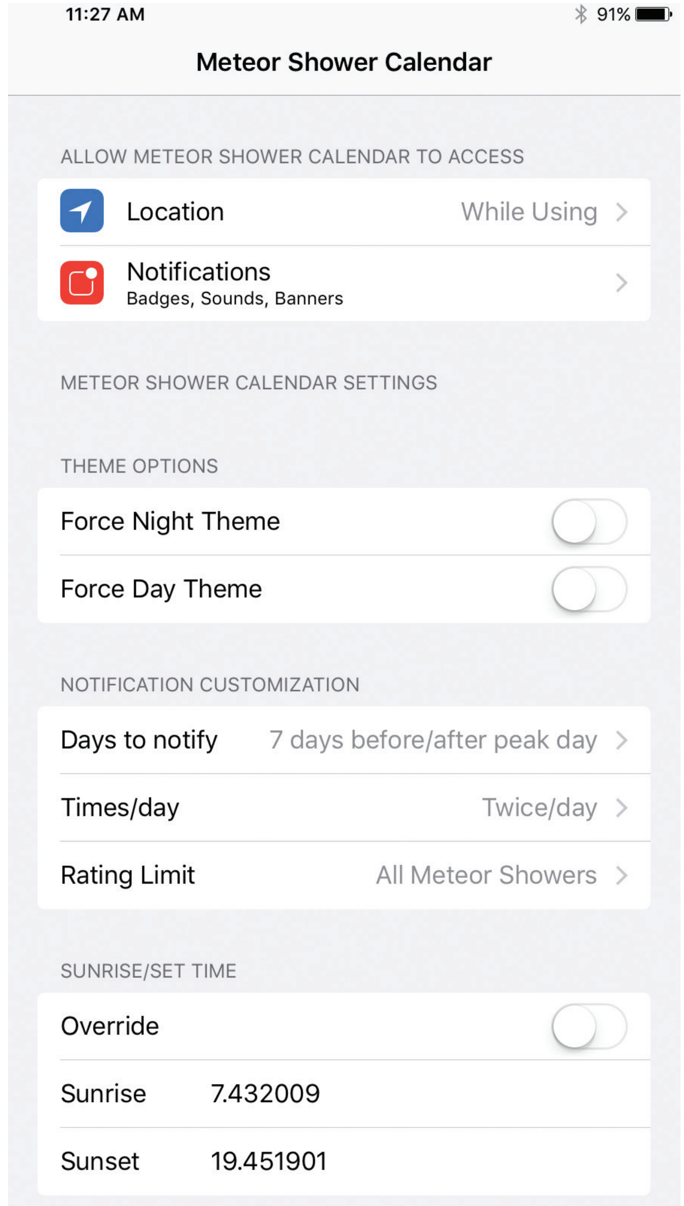

Figure 6 — Settings screen on iOS.

The app includes an interesting timeline chart (Figure 3) showcasing upcoming events with colourful horizontal lines. The length of the line alludes to the shower run. It would be nice if there were another bullet, in addition to the endpoints, for the peak. The colour reflects the rating: dark green is good. The time now is represented by the vertical white line.

The main and chart displays are useful when browsing but automated reminders help us avoid missing events. MSC has very good notification controls, revealed in Settings. One can adjust the lead time up to seven days ahead of the peak. There is a filter for highly rated events. On Android (Figure 4), you can filter for the hemisphere and day-time meteors; on iOS (Figure 6), you can ask for two daily notifications. When a flurry of meteors is near, a notification pops up.

Android MSC also provides widgets. There is a one-by-one that simply counts down. The three-by-one widgets show the Sun times with a countdown and then the current Moon (Figure 5) or local weather.

As noted, it is possible to display the sky in a planetarium app. Through the Settings on Android you can indicate whether this should be Google Sky Map or SkEye. I did not try this feature but believe it is a good idea, pointing to the relevant constellation, for new astronomers. You may already use software (like *Stellarium* or *SkySafari*) to show the radiant. Oddly, on iOS, the button did nothing.

Learning the app is easy. There are embedded usage notes and definitions found in the Help (Android) or About (iOS) screen and there is a brief video on the developer's website (www.ccwilcox.com/blog/meteor-shower-calendar/). From Wilcox's site you'll find links to Google Play and the App Store. Alternately, you can access the store on your device and search for "Meteor Shower Calendar."

I used and tested the free editions of MSC. I had a hard time finding out what would be different with the paid version. On iTunes, a note indicated the app was fully functional implying the fee would merely strip the ads. But there are dimmed options in the Android Settings that suggest one might get more features. Regardless, the paid versions are inexpensive: Android, $1; iOS, $1.39.

I reached out to Mr. Wilcox regarding some questions but never heard back. I wanted to ask, for example, why I wasn't seeing Leonids, Geminids, or Quadrantids in the main list. I suspect it is simply that the list only goes so far into the future and they will appear over time.

Hopefully you'll spot many meteors, perhaps even an elusive storm, in the future. Meteor Shower Calendar with its timely notifications can remind you when to get outdoors.

Update Bits

Days after the big exoplanet news in February 2017, I fired up the NASA Eyes software. Happily, *Eyes on Exoplanets* was already updated for the seven worlds of the TRAPPIST-1 system.

I would enjoy hearing from members regarding apps and software they use and think others might benefit from. Similarly, if you run into a new app and want to spread the word, let me know. ✶

Blake's interest in astronomy waxed and waned for a number of years but joining the RASC in 2007 changed all that. He volunteers in education and public outreach, supervises at the Carr Astronomical Observatory, and is a councillor for the Toronto Centre. In daylight, Blake works in the IT industry.

John Percy's Universe

Later-Life Learners, Revisited

by John R. Percy
(john.percy@utoronto.ca)

In 2015, Canada marked an important demographic milestone: for the first time in its history, seniors—of which there were 5,780,900—outnumbered children under 15. Canada invests significant amounts of money in school education, and in post-secondary education, and encourages and supports our students to become lifelong learners, prepared to adapt to changing careers. But what about the growing demographic of *seniors*, most of whom are retired? Are they beyond education? Some years ago, Mirjan Krstovic and I pointed out that later-life learners were a significant and receptive audience for introductory astronomy (Percy and Krstovic 2001). Since we published that article, its message is even more true: there are now more older people in Canada than younger ones.

The Benefits of Later-Life Learning

School education and post-secondary education are important because they help to produce an educated workforce to advance our economy, and a populace that can think critically about societal issues. We also promote continuing education, because young people will most likely follow multiple careers during their working life, and these careers will be constantly changing with technology and society.

Seniors, even if retired, are still voters and taxpayers. Most of them still serve society, as volunteers, philanthropists, caregivers, informal educators, role models, and/or other ways. On average, they can expect two more decades of active life. They should therefore keep informed about the world (and Universe) around them. Later-life learning is one way to do that.

There's another reason. We are constantly reminded that the "silver tsunami" may be bringing an epidemic of Alzheimer's disease and other dementias. One way to stave off the epidemic is through lifestyle factors, such as diet, regular physical activity, management of cardiovascular risk factors (diabetes, obesity, smoking, hypertension), and *intellectual and social activity*. Baumgart et al. (2015) have summarized the evidence that these modifiable risk factors fend off cognitive

*Figure 1 — *Living and Learning in Retirement* presents a cheque for $25,000 to Glendon College, York University, through its charitable arm *Friends of Glendon College*, to provide scholarships at the College. Source: Living and Learning in Retirement.*

*Figure 2 — At the inaugural lecture of *Lifelong Learning Markham* in October 2016, the author introduced 230 members to "The Amazing Universe." Source: Lifelong Learning Markham.*

decline and dementia. In fact, lifestyle modifications seem to be even more effective than medications, which have not shown much success in treating dementias (Shurkin 2015). It's interesting to note that this conclusion is not much different than the one quoted by Percy and Krstovic (2001). So "use it or lose it." And remember that, by participating in RASC lectures and other activities, *you* are probably doing *your* brain a favour.

How to Proceed?

Why add later-life learners to your outreach audience? Because they are a *receptive* audience. They appreciate lectures, and lecturers' expertise and enthusiasm. They have longer attention spans than younger students (though it's always wise to break any lecture up into shorter segments). You are serving society by educating this audience. A few people in the audience might even support or join your Centre. And almost every later-life learners group either provides an honorarium, or makes a donation to your favourite charity (the RASC?) in your name.

So, let's assume that you or your Centre wants to reach this audience. How do you make contact with them (assuming that they have not approached you)? In Ontario, one strategy is to investigate the Third Age Network (www.thirdagenetwork.ca), which is an umbrella organization of 29 clubs, with over 9,000 members, including many of the groups mentioned below. Its website includes a list of clubs across Canada, including their contact information. Note that some of the university-based groups may prefer to have professional astronomers as presenters, but ultimately it's your willingness and ability that counts.

Many universities have programs for later-life learners. They may be directly administered by the university, or through a closely or loosely affiliated group. At Ryerson University, for instance, they are administered through the Chang School of Continuing Studies. Here at the University of Toronto, I've given courses/lectures for: Innis College (course size 250) and Knox College Summer Program (60). I've given lectures for several alumni groups, including my own University College Alumni.

Glendon College, York University has a well-established Living and Learning in Retirement (LLIR) group (up to 200), which was the first such group in Canada—maybe the world. It was an outgrowth of a New Horizons grant program of the federal Department of Health and Welfare, to encourage retired people to undertake projects that would benefit them and their community. Initially, its courses focused on Canadian Studies. Now, they cover a wide range of topics, including astronomy. This group, and some of the other groups, raises significant funds to support scholarships at the host universities or colleges (Figure 1).

There are also community groups, such as Learning Unlimited (180) in Etobicoke, and its new spinoff group in Mississauga (up to 150). I recently gave the inaugural lecture for a large (250) new group, Lifelong Learning Markham (Figure 2). The Ulyssean Society was founded in 1977 by Dr. John McLeish, one of the pioneers of third-age education.

My experience is that these stand-alone community groups run a very competent operation, with capable volunteers to run the programming, the website, the audio-visual, the registration, etc. This, along with the large course sizes, helps to keep the tuition low, and therefore accessible. It also enables the group to give a generous honorarium! These groups are well-organized, and often plan their programs over a year in advance.

I've also given lectures for several Probus Clubs (www.probus.org/canada.htm), in Toronto, Mississauga, and Oakville.

Probus is loosely affiliated with Rotary. There are 237 clubs in Canada, with 33,800 members. Lectures are only one part of their programs, which include a variety of ways for retirees to keep their minds active, develop new interests, stay healthy, and enjoy fellowship. Their website includes a place where organizations (such as RASC Centres) could advertise their willingness to give presentations.

Last year, I gave three presentations at retirement homes. That was a first for me. The audience was not much different from that of a later-life learners group, but that was probably a selection effect; only the healthier residents attended. This year, I gave my first presentation at a long-term care centre (nursing home). Even though I spend a lot of time at my mother's nursing home, this presentation was a challenge in the sense that many of the residents had limited communication skills. I could sense, though, that they understood the material, and had questions and comments to make. For this, the staff proved very helpful. And I had the sense that I was bringing something new and interesting to a group that was largely cut off from the world. One member of the small audience had clearly been an amateur astronomer, and genuinely appreciated this opportunity to reconnect with his old hobby.

When I give a course, it's sometimes a general introduction to astronomy, or to the frontiers of astronomy, or to the history of astronomy. During International Year of Astronomy, I used Galileo as a theme. Once or twice, I've let my colleagues give most of the lectures, but I find that this requires a lot of co-ordination on my part; the course "flows" better if I give most or all of the lectures myself. In any case, I make a policy of attending all the lectures. I've also invited colleagues from the RASC to contribute a lecture on astronomy as a hobby, and on the activities of amateur astronomers. Recently, I've been asked to give some shorter (four-lecture) courses, and I've put together a coherent "Astronomical Potpourri" of my favourite individual public lectures. Incidentally, I generally make a PDF version of my presentation available on-line, so that audience members can review it afterwards if they wish.

Percy and Krstovic (2001) described a survey of later-life learners' interests, including gender differences. The interests are very diverse; I can also tell this from the question periods after any lecture. Although there is a variety of lectures that I could give (they are all on my USB!), my most popular lectures are: "The Amazing Universe," an overview of exciting topics from modern astronomy; "Misconceptions in Astronomy: From Everyday Life to the Big Bang," which is a rather unusual "backward" introduction to astronomy; "Toronto's Astronomical Heritage," which is especially appropriate for this sesquicentennial year; "The Birth, Life, and Bizarre Deaths of Stars," which is closest to my research interests; and more recently "Archaeoastronomy: The Astronomy of Civilizations Past." No matter what the topic of the lecture, the question period ranges far and wide, from the highly technical to the very basic and personal. I make a special effort to encourage these basic questions, since I know that most audience members have the same questions, but may be too shy to ask. Though usually not. Many audience members arrive early and, if it's appropriate, I encourage them to start the question and discussion period then!

The survey also generated some advice about how to make the lectures more effective and enjoyable: (1) In the content, avoid unnecessary scientific jargon and concepts, equations, and graphs. The content doesn't have to be "dumbed down," just explained in everyday language, and with analogies, if possible; (2) Make the lecture audible, and the slides visible. Repeat audience questions, using a microphone.

What Still Needs to Be Done

As with most forms of astronomy outreach, later-life learner audiences are not very culturally diverse. However, there is a good balance between male and female and, especially in the community groups, the tuition is low enough to make the lectures accessible. But there are very few non-white people. Groups affiliated with universities tend to be made up of educated people, and members of underserved groups may feel out of place on a university campus. One advantage of library presentations (which I do a lot of) is that they happen in every corner of the community.

So please consider reaching out to this audience. As always, I would be happy to provide further advice or assistance.

Acknowledgements

I thank my wife Professor Maire Percy for keeping me updated on Alzheimer's disease research, and the benefits of a healthy lifestyle. She also organizes courses for later-life learners, on health and medicine, using eminent speakers from her vast network of contacts. I also thank later-life learners' groups in general for the wonderful work that they do, and the members of the groups mentioned above, for the privilege of working with them. ✶

John Percy FRASC is Professor Emeritus, Astronomy & Astrophysics and Science Education, University of Toronto, and Honorary President of the RASC.

References

Baumgart, M. et al. 2015, Summary of the evidence on modifiable risk factors for cognitive decline and dementia: A population-based perspective. *Alzheimers and Dementia, 11(6)*, 718-26.

Percy, J.R. and Krstovic, M. 2001, Later-life learners: A significant and receptive audience for introductory astronomy, *JRASC, 95*, 205-7.

Shurkin, 2015, *Inside Science*, www.insidescience.org/news/failure-upon-failure-alzheimers-drugs

Second Light

A Retrograde Trojan Asteroid of Jupiter

by Leslie J. Sage
(l.sage@us.nature.com)

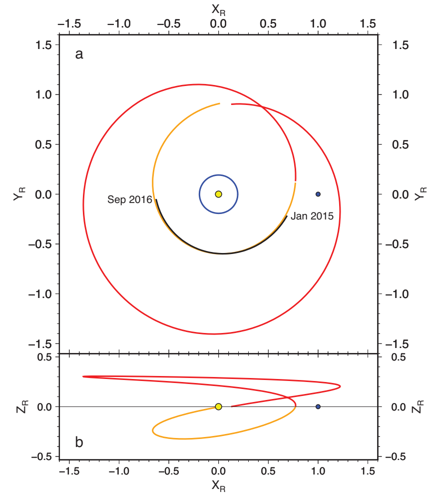

Figure 1 — The orbit of 2015 BZ_{509} from above the Solar System (top) and looking along the plane of the Solar System (bottom). For further information, see www.astro.uwo.ca/~wiegert/2015BZ509 Image courtesy of Paul Wiegert and Nature.

Jupiter is accompanied in its orbit by two groups of asteroids—one that leads it by an angle of 60 degrees, and one that trails it by 60 degrees. These are points where the gravitational influence of Jupiter equals that of the Sun. There are three other Lagrangian points—between the Sun and Jupiter, on the far side of Jupiter from the Sun, and on the far side of the Sun from Jupiter, though the last two are somewhat more complicated in their explanation. Today I will be talking about the L4 (leading by 60 degrees) and L5 (trailing by 60 degrees) points. Jupiter actually has a lot of Trojan asteroids, as they are called; by some estimates as many as there are in the main asteroid belt itself. To that group we can now one with a truly strange orbit. Paul Wiegert of the University of Western Ontario, Martin Connors of Athabasca University Observatories, and Christian Veillet of the Large Binocular Telescope in Arizona have determined that the orbit of the asteroid 2015 BZ_{509} is a retrograde Trojan, with a stable orbit (see the March 30 issue of Nature).

How can a retrograde co-orbital body be in a stable orbit? Theoretically, this was first explored back in 2012. Obviously, if the orbit lay in the plane of the Solar System, a retrograde co-orbital body would soon run into Jupiter. But this body is on a peculiar looping orbit (see Figure 1) that takes it out of the plane of the Solar System at all but just two points, when it crosses from above to below the plane, and then back again.

The asteroid was first discovered by the Pan-STARRS observatory (http://pswww.ifa.hawaii.edu/pswww) in Maui, but its orbit was very poorly constrained, though there were hints that it might be a retrograde co-orbital. Wiegert and his colleagues set out to determine the orbit, using the Large Binocular Telescope (www.lbto.org) on Mt Graham, in Arizona, along with the early observations reported to the Minor Planet Center (http://minorplanetcenter.net) at Harvard University. These new observations allowed the team to determine that 2015 BZ_{509} is in a resonant co-orbital orbit with Jupiter. A resonance is where a body makes an integral number of solar orbits in the same period as another body. 2015 BZ_{509} is in a retrograde 1:1 resonance, taking the same time to orbit the Sun as Jupiter. The asteroid passes Jupiter relatively closely twice each orbit around the Sun.

Then there is the question of its orbital stability. Wiegert and colleagues ran some simulations and found—somewhat surprisingly—that the orbit is stable on a million-year timescale. The perturbations it receives from Jupiter on the two passes per orbit cancel out, and they happen at the rather high speed of 26 km s^{-1}, meaning that Jupiter's influence is brief. Other kinds of co-orbital states, such as prograde "horsehoes" and "quasi-satellites," are unstable on much shorter timescales.

Wiegert tried to explore the origin of the asteroid, using simulations, but there was no clear-cut answer. An interaction with Saturn might have injected it into its current orbit, or it might have been a retrograde Oort cloud comet, or a Halley-like comet. It appears to be about 3 km in diameter, assuming an albedo of 7%, but it showed no comet-like activity at its recent perihelion of 3.1 au, though at 20.9 magnitude it was just above the Pan-STARRS limit of 22.7. The deeper LBT observations by Wiegert et al. also showed no sign of cometary activity. It is thought that there are many burned out comets floating around the Solar System. So, 2015 BZ_{509} could be either a dead comet, a comet that never gets close enough to the Sun to produce a tail, or an asteroid.

In early May, 2015 BZ_{509} will be in the constellation of Aquarius (morning sky), at a visual magnitude of about 23. In mid-August 2018, it will be in opposition in the constellation of Capricorn, but only reaches 22 magnitude. Given that the 1.8-m telescopes of Pan-STARRS could barely see at that magnitude from the very dark site of Haleakala, this is not a source that amateur astronomers could go after. But if you are up before dawn, look in the direction of Aquarius and think about the weird things we keep finding in astronomy, some of them inside our own Solar System. ✶

Leslie J. Sage is Senior Editor, Physical Sciences, for Nature Magazine and a senior visiting scientist in the Astronomy Department at the University of Maryland. He grew up in Burlington, Ontario, where even the bright lights of Toronto did not dim his enthusiasm for astronomy. Currently he studies molecular gas and star formation in galaxies, particularly interacting ones, but is not above looking at a humble planetary object.

Astrocryptic

by Curt Nason

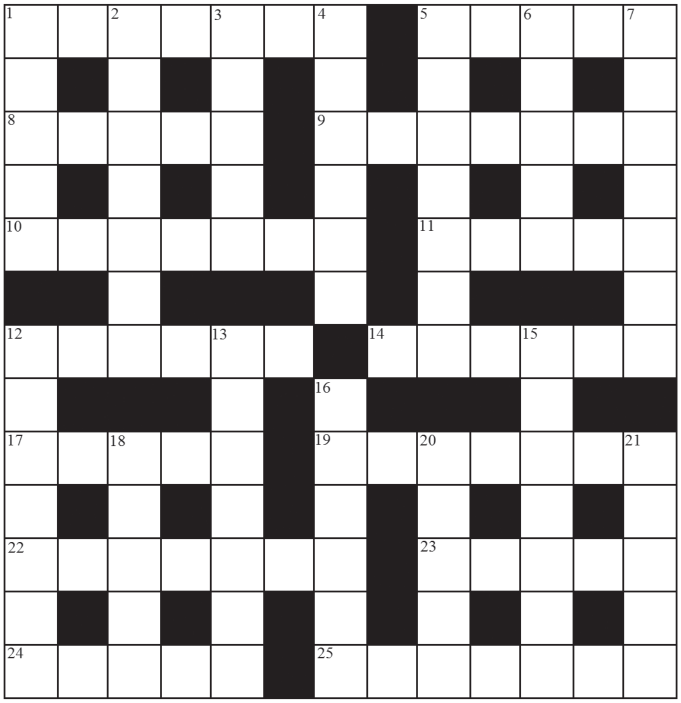

ACROSS

1. Round ratio of spliced music related to corded fish (7)
5. Sam I am, without a rotating satellite sculpting rings (5)
8. Trailing Sinbad's taxi he breaks up within this limit (5)
9. Feeling delighted about some copper on the planet (7)
10. Areal brightness of one adept at Internet browsing? (7)
11. Traces of KNO_3 seen in Cassini trends (5)
12. Comet lost across a complex elliptical orbit (6)
14. Subaru backs up, turning first back to north of the planet (6)
17. Stave off attack from an asteroid (5)
19. While rounding Saturn it plays around in an empty casino (7)
22. What you are reading when a little woman gives the runaround to Mr. Nagler (7)
23. Plato made AU much farther from the Sun (5)
24. Telescope mounted English style like oxen (5)
25. Relatively like the Hyades or Pleiades (7)

DOWN

1. Where Cassini's observatory is below par (5)
2. Cobalt X-rays scatter around Uranus (7)
3. One musical note leads to a great comet finder (5)
4. A RASC one like us spilt beer over the Messier Marathon (6)
5. Ancient rhymer first visited a planet (7)
6. Good observing with a scope on one, even better with them on one (5)
7. Magazine does well in risky new set-up (3,4)
12. Emotional comet hunter (7)
13. Reformed a lender like Whitman's astronomer (7)
15. Bad pun teen made beyond Uranus (7)
16. What Libra has in common with Serpens (6)
18. Grit made from Sputnik material with titanium removed (5)
20. Radio astronomers detected irregular pulse below Orion (5)
21. Rigel type in Oslo under construction receives what Aristarchus got on payday (5)

Answers to April's puzzle

ACROSS

1 RED DOT FINDERS (anag); **8** CLAVIUS (Cla(VI)us); **9** TITAN (2 def); **10** ERFLE (er(Fl)e); **11** OCULARS (an(Ar) ag); **12** TEAPOT (2 def); **15** SIGNAL (anag aliens, g=e); **18** SAGITTA (anag - e); **19** MUSIC (mus (Musca) + IC); **21** DIRAC (D(anag)C); **22** TURNOFF (2 def); **23** NEBULAR FILTER (anag)

DOWN

1 RICHEST (r(ich)est); **2** DWARF (2 def); **3** OXIDE (ox+I'd+E);**4** FUSION (fu(SiO)n); **5** NU TAURI (an(Au)ag); **6** ENTRAIN (2 def); **7** SINUS (2 def); **13** ALGORAB (hom); **14** OPTICAL (anag); **16** LUCIFER (anag); **17** CASTOR (anag); **18** SEDAN (anag); **19** MARDI (rev);**20** SHORT (shortstop)

It's Not All Sirius

by Ted Dunphy

Great Images

by James Edgar

On a cold, wintry evening in January 2007, Past President James Edgar tried out his newfound astrophotography hobby with his Canon 20D DSLR. The target, centred in the image, was Comet McNaught. Even though it didn't give the same show to northern viewers as it did for the south, it was a special comet—one that won't be back for another ~92,600 years! Image taken through a Canon 18–55 EF-S lens at 18 mm, ISO 400, ƒ/5.6 for 1/20 sec.

Journal

Great Images

Dan Meek took this beautiful image of Melotte 15, the "heart" of the Heart Nebula. This is a seven-hour narrowband image taken with an Celestron 11" Edge and a QSI583wsg camera.